YERSINIA PESTIS RESPONSE TO MACROPHAGE-INDUCED STRESS FROM HOSTS WITH HIGH AND LOW SUSCEPTIBILITY TO PLAGUE

By

DURAISAMY PONNUSAMY

Bachelor of Veterinary Science
Tamil Nadu Veterinary and Animal Sciences University
Tamil Nadu, India
2003

Master of Veterinary Science in Veterinary Pathology
Indian Veterinary Research Institute
Uttar Pradesh, India
2006

Submitted to the Faculty of the
Graduate College of the
Oklahoma State University
in partial fulfillment of
the requirements for
the Degree of
DOCTOR OF PHILOSOPHY
December, 2011

YERSINIA PESTIS RESPONSE TO MACROPHAGE-INDUCED STRESS FROM HOSTS WITH HIGH AND LOW SUSCEPTIBILITY TO PLAGUE

Dissertation Approved:

Dr. Kenneth D. Clinkenbeard

Dissertation Adviser

Dr. Susan E. Little

Committee Member

Dr. Timothy A. Snider

Committee Member

Dr. Sahlu Ayalew

Committee Member

Dr. Edward I. Shaw

Outside Committee Member

Dr. Sheryl A. Tucker

Dean of the Graduate College

TABLE OF CONTENTS

LIST OF TABLES

LIST OF FIGURES

CHAPTER I

INTRODUCTION

Yersinia pestis is a Gram-negative coccobacillary bacterium which causes the disease plague in a variety of animal species. Of these, rodents such as mouse, rat, guinea pig, and prairie dog are considered natural hosts for the infection. These natural host species experience high morbidity and mortality due to septicemia occurring within a few days of infection. Within these rodent populations, fleas act as biological vectors. In the rodent-plague cycle, rodent predators such as coyotes, ferrets, and occasionally domestic dogs and cats intrude and influence the dynamics of rodent plague epizootics. During this intrusion, rodent predators can also acquire the infection, primarily by ingestion of infected prey. However, in contrast to rodents, rodent predators vary in their susceptibility to infection; cats and ferrets suffer severe disease, while dogs and coyotes show mild to inapparent disease.

During the initial phase of flea bite transmitted plague, *Y. pestis* inoculated into subcutaneous tissues infects local macrophages where the bacterium multiplies intracellularly before causing septicemia and severe disease. Host macrophages employ a variety of antimicrobial activities to eliminate intracellular bacterial infections such as *Y. pestis* during the initial phase of infection. Therefore, the ability of *Y. pestis* to overcome the antimicrobial activities of host macrophages during the initial stage of infection may influence the subsequent disease outcomes (severe or mild disease). Limited information is available as it relates to the role of host macrophages in the severity of *Y. pestis* infections. In an effort to better understand the role of macrophages in disease severity, we observed *Y. pestis* intracellular infection dynamics in macrophages from hosts exhibiting severe disease such as mice and those exhibiting less severe disease such as dogs. Further, we conducted a proteomics study on intracellular *Y. pestis* to identify

possible virulence factors involved in the bacterial stress responses to macrophage parasitism.

CHAPTER II

LITERATURE REVIEW

Abstract

The Gram-negative bacterium *Yersinia pestis* is the etiologic agent of plague, causing disease in wide variety of animal species. *Y. pestis* is a systemic pathogen recently evolved from its close relative, *Yersinia pseudotuberculosis*, an enteric pathogen. Comparative genomics of these bacteria reveals that *Y. pestis* emerged by acquiring two new plasmids (pPCP and pMT) while preserving the common plasmid, pCD, and by reducing and rearranging its genome. *Y. pestis* is naturally transmitted by flea bites, causing high morbidity and mortality in natural rodent hosts. Epizootics can lead to extinction of entire local rodent populations. Similarly, rodent predators such as cats, dogs, coyotes and ferrets, which intrude into the rodent-flea-rodent plague infection cycle can also acquire the infection, but the severity of these infections in different predator species varies. Dogs and coyotes exhibit mild or inapparent disease, whereas cats and ferrets suffer severe disease with high mortality. In rodents, *Y. pestis* acquired through infected flea bites causes inflammatory swelling and necrosis of local lymph nodes within few days of infection. Subsequently, the bacterium disseminates to various internal organs, leading to septicemia and death of the infected rodents. During the progression of the infection in rodent hosts, various virulence factors of *Y. pestis* play an indispensable role in overcoming host immune defenses. At the early stage of infection, *Y. pestis* inoculated subcutaneously by infected flea bites into the susceptible host are phagocytized by local macrophages in which *Y. pestis* survives and multiplies for a short period before being released into the extracellular space. During this intracellular infection stage, expression of specific virulence genes, primarily encoded on its plasmids, is induced by host phagolysosomal stimuli. These virulence factors prepare *Y. pestis* to

adapt to the macrophage niche as well as the subsequent systemic infection. Therefore, it is likely that the pathogenic events at the macrophage stage of *Y. pestis* infection play a critical role in the subsequent progress and outcome of the infection. An improved understanding of *Y. pestis* infection dynamics in macrophages from high and low susceptibility hosts, the factors expressed by *Y. p*estis to adapt to macrophage infections, and mechanisms of these *Y. pestis* factors in adaptation to intracellular stress regulation are pivotal to understanding the early stages of *Y. pestis* pathogenesis.

Introduction

The Gram-negative coccobacillus *Yersinia pestis* causes severe disease in natural rodent hosts (81). The extent to which *Y. pestis* shares DNA homology with other bacteria indicates that *Y. pestis* is a mutant clone of *Y. pseudotuberculosis* serotype O:1b, having diverged 1,500 to 20,000 years ago (2). During this evolution, *Y. pestis* acquired two new plasmids, namely pPCP and pMT, while maintaining the common plasmid, pCD, intact. In addition, *Y. pestis* has completely or partially eliminated many chromosomal encoded genes which are either redundant or a disadvantage for its current pathogenic life cycle as a flea borne, acute systemic pathogen (24, 80, 84).

This recent evolution of *Y. pestis* from a facultative enteric pathogen to a systemic pathogen is associated with an increased range of animal species that are susceptible to infection (81). Rodents are considered a natural host for *Y. pestis* infection and suffer high morbidity and mortality. Under natural circumstances, fleas associated with rodents serve as biological vectors for transmission of the agent from animal to animal (7, 81). In

contrast to plague transmission in rodents, rodent predators such as dogs and coyotes most commonly acquire infection by ingestion of *Y. pestis* infected prey or occasionally by flea bite. Canine rodent predators normally develop only mild or inapparent clinical disease (78, 94). The mechanism(s) underlying the relative resistance of canine rodent predators to infection by *Y. pestis* is not known. The different routes of infection, flea-bite for rodents and ingestion for canines, may be attributed to the difference in disease severity between them; however, feline rodent predators are highly susceptible to plague by ingestion of infected rodents (94, 96). Another alternative hypothesis that is proposed herein is that the macrophages of canine rodent predators interact with *Y. pestis* in a different way than do rodent macrophages, the former limiting infection, whereas the latter facilitating infection. Under this circumstance, as an effort to gather more information about the role of host macrophages in *Y. pestis* infection severity and *Y. pestis* virulence factors involved during intracellular infection, various relevant scientific papers have been reviewed in the following sections.

A. *Y. pestis* general description

A1. Morphology, staining properties and growth characteristics

Y. pestis grows slowly on agar plates yielding grey-white circular, umbonate colonies measuring 1-2 mm. The colonies are γ-hemolytic on blood agar plates, and a majority of the virulence strains produce pigment on Congo-red nutrient agar (115). Failure to synthesize O-antigen of lipopolysaccharide gives an uneven or rough colony

morphology to *Y. pestis* on agar plates (106). The bacterium is a non-spore forming coccobacillus measuring 0.5-0.8 x 1-2.5 µm under light microscopy. It has a bipolar rod appearance when stained by Wright-Giemsa stain for clinical samples but not for laboratory cultures (19, 86). Distinguishing features of *Y. pestis* from other related bacterial species are its non-motility and production of a prominent capsule at higher growth temperature (86). The bacterium grows optimally at 28^{o}C with 5% CO_2 concentration in a nutrient rich neutral pH media (7.0-7.5) containing essential amino acids including methionine, phenylalanine, isoleucine, valine, glycine and threonine. In addition to these amino acids, at higher growth temperature *Y. pestis* requires vitamin B components such as thiamine (B1), pantothenic acid (B5) and biotin (B7) and the amino acid aspartate for optimal growth (20, 81). Irrespective of growth temperature, adequate concentrations of calcium, iron, and magnesium are important for *Y. pestis* to maintain virulence under laboratory conditions (81).

A2. Biochemical properties

Y. pestis carries mutational changes in many genes associated with varying metabolic pathways that are functional in other *Yersinia* species and *Enterobacteriaceae* members. Except for a positive catalase reactivity, *Y. pestis* colonies are negative for most routine diagnostic biochemical tests such as oxidase, urease and ornithine decarboxylase and are also unable to ferment lactose and reduce tryptophan to indole (56). In addition, *Y. pestis* lacks glucose-6-phosphate dehydrogenase, and therefore, cannot use the pentose phosphate pathway for the synthesis of ribose sugars. This deficiency is compensated by an increased activity of transketolase and transaldolase

enzymes. Similarly, absence of α-ketoglutarate dehydrogenase involved in the tricarboxylic acid (TCA) cycle is balanced by isocitrate lyase, which diverts TCA intermediates to the glyoxylate pathway. When compared with *Y. pseudotuberculosis*, *Y. pestis* varies in the catalytic activities of enzymes involved in amino acid metabolism such as γ-glutamyltransferase, aspartase, glutamase and serine deaminase (threonine dehydratase) (18-20, 51). Unlike many other bacterial species including *Y. pseudotuberculosis* and *Y. enterocolitica*, *Y. pestis* lacks a methionine salvage pathway that recycles sulfur ions from metabolic waste products (93).

A3. Classification

Y. pestis is classified under the family *Enterobacteriaceae* in genus *Yersinia*, which has 14 species in total. Of those, *Y. pestis*, *Y. pseudotuberculosis* and *Y. enterocolitica* are pathogenic to various animal species and human beings. Recently, *Y. ruckeri*, which exhibits high 16s rDNA sequence homology with *Y. pestis*, has been reported to cause disease in certain fish (113). *Y. pestis* is subdivided into four biovars; namely antiqua, mediaevalis, orientalis and microtus, based on the differential ability of these biovars to reduce nitrate and utilize the nutrients glycerol and arabinose. Biovars antiqua and microtus are likely sub-clones of a common ancestral *Y. pestis* strain which metabolized nitrate, glycerol and arabinose. During this subspeciation, biovar antiqua has maintained the genomic content for all these pathways intact, but microtus has lost the capability to reduce nitrate and ferment glycerol (129, 130). The biovars mediaevalis and orientalis are considered to have evolved from biovar antiqua with mutations in genes encoding nitrate reductase catalytic subunit (NapA) and aerobic glycerol-3-phosphate

dehydrogenase (GlpD), respectively (23, 74, 129, 130). Within each biovar, different strains of *Y. pestis* are further identified by employing rare metabolic profiles such as fermentation of rhamnose, mellbiose and melezitose; sensitivity to pesticin; requirement of different amino acids for optimal growth; infectivity to laboratory rodents; or combinations of these traits (4). However, nucleic acid based classification such as ribotyping, variable-number tandem repeats (VNTR), multilocus sequence typing (MLST) and restriction fragment length polymorphism (RFLP) are more definitive for *Y. pestis* classification, especially to identify strains of different geographic origin (27, 28, 48, 61).

B. *Y. pestis* genome and evolution

B1. Chromosome

The rich knowledge about the *Y. pestis* genome obtained through sequencing of different isolates representing four biovars allows us to better understand the molecular nature of *Y. pestis* evolution and the acquisition of various virulence factors involved in pathogenesis. The various biovars of *Y. pestis* have a single circular chromosome of 4.5 to 5.1Mbp with a 47.64% G+C content. *Y. pestis* biovar antiqua strain angloa, likely an immediate divergent of *Y. pseudotuberculosis*, and *Y. pestis* biovar orientalis strain IP275, a recent isolate of human plague from Madagascar, have shorter and longer chromosomes, respectively (34). Irrespective of biovars, all *Y. pestis* strains have functional genes encoded on both leading and lagging strands of the chromosome. The

chromosome has been extensively remodelled by insertion sequences and pseudogenes (23, 31, 34, 80). From *Y. pestis* genome sequence information, an average of 4,000 open reading frames (ORFs) have been identified as possible coding sequences, which represents 80 to 85% of the total genome (31, 80). These ORFs are present more often on the leading strand of DNA replication than on the lagging strand. Apart from these ORFs, 150 small non-coding RNA (sRNA) have also recently been identified through *in silico* analysis (59). These sRNAs may play an essential role in regulation of transcriptional, translational or post-translational activities of various genes (123). Depending on the strain, *Y. pestis* has 6 or 7 copies of rDNA sequences located very close to the origin of replication (31, 80). *Y. pestis* and *Escherichia coli* strain K-12 genomes share approximately 53.7% genes between them, and these shared genes form the back bone of the *Y. pestis* chromosome. When comparing these shared core genes, *Y. pestis* specific genes differ noticeably in their codon usage, indicating different level of translation between the back bone and specific genes of *Y. pestis* (31). A notable feature observed in the *Y. pestis* genome is that the bacterial chromosome has numerous insertion sequences and pro-phages, which have led to many pseudogenes and extensive segmental rearrangement of the *Y. pestis* genome among various strains (23).

B2. Plasmids

Y. pestis has three plasmids important for pathogenesis: pCD, pPCP and pMT. Of these, the pCD plasmid is highly conserved among *Y. pestis*, *Y. pseudotuberculosis* and *Y. enterocolitica*, but the pPCP and pMT plasmids are specific to *Y. pestis*. However, *Y. pestis* strain angola carries a fusion pMT-pPCP plasmid with a separate pPCP plasmid

(Table 1) (34). Similarly, *Y. pestis* strain pestoides-F lacks the pPCP plasmid altogether but has a larger pMT plasmid containing 137kbp in place of the 100kbp pMT plasmid presents in other strains (http://www.ncbi.nlm.nih.gov/nuccore/NC_009381). *Y. pestis* biovar microtus strain 91001, an isolate from China, has a fourth 21.7kbp pCRY plasmid encoding genes likely involved in DNA homologous recombination and type-IV secretion systems (108). Various *KIM* (*Kurdistan Iran man*) strains belong to biovar mediaevalis lack as natural isolates or have been cured of one or more of the above noted plasmids as well as pigmentation locus (*pgm*) from chromosomal insertion sequence *IS*100 (Table 1). These KIM strains are commonly being used for various *in vitro* studies related with *Y. pestis* infections (14, 45, 81).

The pCD plasmid is approximately 70kbp in size and encodes 60 ORFs involved in the formation of the various structural and functional components of type-III secretion system (TTSS). These ORFs are tightly regulated by environmental temperature and calcium concentration; 37^{o}C and low calcium favor the active expression of these genes (84). The plasmid has an *incFIIA* based origin of replication and a *sopABC* partitioning system. The plasmid copy number is controlled by RNA-RNA interaction between genes *repA* and *copA* in *incFIIA* replication locus. In *sopABC* partitioning system, *sopC* acts like a centromere for plasmid sharing between the daughter cells. It has three intact and many partial insertion sequences throughout the plasmid (84). The 9.6kbp pPCP plasmid is the smallest of the three *Y. pestis* plasmids and encodes three virulence genes; plasminogen activator-coagulase (*pla*), pesticin (*pst*) and pesticin immunity (*pim*). This plasmid was likely acquired by *Y. pestis* from *Salmonella enterica* serovar Typhi at the later stage of evolution, prior to *Y. pestis* becoming a systemic pathogen (80, 101). In

spite of its proposed late acquisition, *pla* gene expression is regulated by a chromosomally encoded cAMP receptor protein (Crp) (57). pMT is a low copy number 100kbp plasmid that has integrated into the chromosome of some strains. The plasmid carries genes for F1-antigen, murine toxin and numerous other hypothetical proteins (67, 89).

B3. *Y. pestis* evolution

Analysis of 16S rDNA sequences among 14 species of *Yersinia* reveals that *Y. pestis* is more closely related to *Y. pseudotuberculosis* than to any other *Yersinia* species, sharing 100% homology (109). In contrast to the rDNA sequence homology, *Y. pestis* varies drastically from *Y. pseudotuberculosis* with respect to the nature of disease produced in and the mode of infection transmitted to susceptible hosts. In natural rodent and incidental human hosts, *Y. pestis* causes severe acute systemic disease as a flea borne infection, but *Y. pseudotuberculosis* causes only mild gastroenteritis in human beings through an oral route of acquisition (81). (81, 119). Comparative analysis of DNA homology of six housekeeping genes involved in various metabolic pathways and LPS biosynthesis for *Y. pestis, Y. pseudotuberculosis* and *Y. enterocolitica* indicates that *Y. pestis* is a descendant of *Y. pseudotuberculosis* serotype O:1b. This divergence is thought to have occurred between 1,500 to 20,000 years ago (2). During early stages of this pathogenic speciation, it is likely that a free living non-pathogenic *Yersinia* species acquired plasmid pVY (homolog of pCD plasmid) and the chromosomal pigmentation locus through horizontal gene transfer and became *Y. pseudotuberculosis*. Subsequently, *Y. pestis* arose from *Y. pseudotuberculosis* through sequential genomic changes including

reductive evolution and the acquisition of plasmids pPCP and pMT (33). However, the transition from *Y. pseudotuberculosis* to *Y. pestis* is expected to have happened through an intermediate pro-*Y. pestis* species which is thought to have caused systemic infections less frequently and lacked the plasmid pPCP altogether. In accordance with this speculation, *Y. pestis* pestoides-F is considered the oldest *Y. pestis* strain. It is less virulent, lacks the pPCP plasmid and has intermediary metabolic profiles between modern *Y. pestis* and *Y. pseudotuberculosis* strains. Later, this pestoides-F or pro-*Y. pestis* species became virulence *Y. pestis* by obtaining the pPCP plasmid and a few new genes in the chromosome, as well as by losing many chromosomal genes as pseudogenes (24, 53, 80, 129). *Y. pestis* genome based DNA-microarray analysis of all *Yersinia* species reveals that approximately 292 genes are *Yersinia* genus-specific, and beyond these, *Y. pestis* has only 16 new genes in its chromosome (122). Comparative analysis of genomes of *Y. pestis* strains KIM10 and CO92 with *Y. pseudotuberculosis* strain IP32953 shows that the *Y. pestis* chromosome has 32 unique genes and 149 pseudogenes. *Y. pestis* also lacks 317 genes which are present in *Y. pseudotuberculosis* (24). Particularly, *Y. pestis* markedly varies from *Y. pseudotuberculosis* in relation with the genes encoding surface antigens such as adhesins, invasins, flagella and LPS components. Beyond these variations, *Y. pestis* also has some novel insect toxin encoding genes in the chromosome (52).

C. Plague in rodents and rodent predators–nature of infection and epidemiology

During the Modern plague outbreak in 1894, Alexander Yersin, a French bacteriologist and physician who successfully isolated the organism, suggested the involvement of rats in the plague infection cycle. Later, Paul Louis Simond successor of Alexander Yersin determined that the Oriental rat flea (*Xenopsylla cheopis*) could serve as the biological vector for transmission of *Y. pestis* among rodent populations and also to humans (81, 105). Thereafter, Guthier and Raybaud in 1903 and A.W. Bacot and C.J. Martin in 1914 repeated and extended Simond's work using experimental studies (81, 105). Since then, various epidemiological surveys and experimental approaches have been undertaken to understand the dynamics of the plague infection cycle in various rodent populations, specifically among mice, rats, guinea pigs, prairie dogs and squirrels.

C1. Epidemiology of plague in rodents

Within rodent populations the disease is still wide spread, and epizootics occur periodically, particularly where the rodent populations are high such as in the tropical steppes (81). Enzootic plague foci that maintain an infective reservoir are likely to support epidemiologically distinctive epizootic and enzootic rodent populations. The epizootic populations such as rat, mouse, guinea pig and prairie dog are highly susceptible to the infection and experience high mortality from the disease (7, 29). A few infected individuals within this group may occasionally survive the outbreak and develop partial immunity to plague (7, 95). Subsequently, those partially protected individuals may serve as reservoir hosts for the extension of plague to newly colonizing naïve rodent colonies, but the conclusive evidence supporting this conjecture is lacking. The enzootic

populations, for example gerbils, voles, chipmunks, squirrels and grasshopper mice, are relatively resistant to the infection and can harbor the infective agent for extended periods of time, especially during the inter-epizootic period (12, 73). When these two populations overlap, spread of the disease from the enzootic to epizootic populations can occur with subsequent outbreaks in the latter population (7). A recent study carried out to understand the relationship between prairie dog and grasshopper mouse population dynamics and plague outbreaks in the former group explicitly explains this assumption. Among prairie dog populations, grasshopper mice, which prey on dead prairie dog carcasses and are moderately resistant to *Y. pestis* infection, can transport the disease from colony to colony through either mechanically carrying *Y. pestis* infected prairie dog fleas on them or maintaining the agent as a subclinical infection and thus transmitting it to susceptible prairie dogs. Increasing the population size of grasshopper mice and the resultant increased frequency of contacts with prairie dogs positively influence the occurrence of outbreaks in prairie dog colonies (97).

After acquisition of the disease, subsequent spread within the epizootic populations is influenced by many factors. Primarily, density of the flea vectors influences the course of epizootic; a higher flea load causes more widespread occurrence of the disease within a short time frame. Progression of the infection in flea vectors causes *Y. pestis* to form a biofilm that causes occlusion of the flea's mouthpart, leading to a sharp increase in the number of rodents being bitten by infected fleas. Apart from this remarkable transmission capability, fleas infected with *Y. pestis* can also maintain the bacteria through the inter-epizootic period in a dormant stage, and later, when suitable rodent hosts become available, these fleas can successfully transmit the disease (9).

Occasionally, under heavy infestation, ingestion of infected fleas can also cause gastrointestinal plague in rats and mice (22, 95). In this flea mediated plague infection cycle, intervention by other infectious agents changes the disease transmission dynamics. For example, concurrent infection of a rodent population with *Y. pestis* and either *Salmonella typhimurium* or *Listeria monocytogenes* can negatively influence the efficiency of flea-mediated plague transmission (35, 128).

Apart from fleas, other factors such as rodents' social behavior, cannibalism, and habitat can also influence the dynamics of the plague outbreak within a given epizootic population. Social rodents have a higher risk of acquiring the infection from their colony-mates. This can occur either directly through contact with infected individuals or carcasses, or indirectly through exposure to *Y. pestis* contaminated soil (8, 60). In particular, high moisture content, richness of soil iron and calcium, and the presence of soil protozoans such as *Tetrahymena pyriformis* and cysts of soil amoeba may positively influence *Y. pestis* survival in soil and its related outbreaks in rodent populations (17, 76).

C2. Epidemiology of plague in rodent predators

In the rodent-flea-rodent plague infection cycle, rodent predators such as dogs, coyotes, cats and ferrets occasionally intrude and extend the radius of plague epizootic foci by mechanically carrying infected rodent fleas on their bodies or by transporting the infected carcasses from place to place (117). These predators typically acquire the infection through ingestion of infected rodents but occasionally through the bite of infected rodent fleas. In the United States, dogs and cats typically acquire the disease from *Y. pestis* infected prairie dogs, ground squirrels or rabbits (77, 78). These *Y. pestis*

infected rodents and rabbits are less active and more vulnerable to predation, resulting in significantly increased probability of *Y. pestis* transmission to the predator hosts. In cats and ferrets, the disease is similar to that of rodents or human beings, causing high mortality. In an experimental infection, 42% of cats infected through an oral route and 50% of cats injected subcutaneously with virulence *Y. pestis* succumb to the disease (78, 94). In cats, shortly after ingestion of *Y. pestis* infected rodents, enlargement of oro-pharyngeal lymph nodes is evident which on necropsy reveals multiple foci of necrosis (77, 78, 94). Subsequently, the disease progresses into septicemic form with a poor prognosis, similar to plague progression in human beings. Occasionally, the systemic infection in cats leads to the pneumonic form of the plague, which is potentially dangerous for aerosolized transmission to other cats and human beings (42, 78, 94).

In contrast to cats, dogs and coyotes, which also prey upon infected rodents, typically exhibit clinically inapparent disease. Dogs fed with *Y. pestis* infected guinea pig carcasses showed mild fever, anorexia and lethargy at the initial stage of infection with only 30% of the infected dogs exhibiting clinical sign of enlargement of oro-pharyngeal lymph nodes; however, none of those dogs developed severe disease. All of the infected dogs developed antibodies to F1-antigen as early as 8 days post-infection, which gradually increased to the peak at 3 weeks and then were maintained at the same level for upto 3 months post-exposure. Thereafter, positive serum titers to F1-antigen were present for a year post-infection (77, 94).

D. *Y. pestis* pathogenesis and virulence factors

D1. Early stage of *Y. pestis* pathogenesis and virulence factors

D1a. Intracellular *Y. pestis* pathodynamics

Rodents are considered the natural hosts for *Y. pestis* infection and suffer severe disease with high mortality (100). After the bite of infected fleas, most *Y. pestis* inoculated subcutaneously are phagocytized and killed by neutrophils (81). At the same time, small numbers of *Y. pestis* are also engulfed by macrophages present in the lesion. In contrast to *Y. pestis* in neutrophils, the bacteria phagocytized by the macrophages multiply inside the phagolysosome by presumably evading macrophage antimicrobial activity (45, 81). Subsequently, these *Y. pestis* parasitized macrophages migrate to the local lymph nodes, where the bacteria continuously multiply inside the macrophages until they are released into the extracellular space by cell lysis (112).

Although macrophages have been identified as an important focus of infection during the early stage of the disease, no research has been done specifically focusing on macrophage surface receptors which participate in *Y. pestis* phagocytosis. Based on a recent study by Noel *et al*. (2009), macrophage Fcγ and complement receptors were shown to play a role in *Y. pestis* uptake; however, *Y. pestis* uptake was not completely blocked in the absence of both opsonizing antibody and serum complements in the infection media, indicating that in addition to Fcγ and complement receptors, an as yet unidentified macrophage receptor(s) likely participates in the process of *Y. pestis* phagocytosis (13). Even within Fcγ and complement receptors, sub-types involved in *Y. pestis* phagocytosis have not been identified. During flea bite infection, phagocytosis of

Y. pestis by the local macrophages may not involve either Fcγ or complement receptors because phagocytosis occurs almost instantaneously without *Y. pestis* inducing a significant inflammatory reaction in order to access the serum components for efficient phagocytosis by macrophages. Following the uptake by macrophages, *Y. pestis* containing vacuoles are believed to pass through the regular endocytic pathway and to mature to phagolysosome (45, 92). But a recent study suggests that, by an as yet unclear molecular mechanism, *Y. pestis* may block phagolysosomal acidification, which allows intracellular survival and multiplication (14). In addition to these *Y. pestis* specific events, other macrophage specific innate immune processes are assumed to take place. Particularly, upregulation of genes related to cytokines TNF-α, IFN-γ, macrophage inflammatory protein-1α (MIP-1α), MIP-1β, IL-1α, IL-6 and chemokines IL-8, but down regulation of genes associated with apoptosis was observed in macrophages infected with *Y. pestis* (30, 125).

D1b. *Y. pestis* virulence factors in macrophage infections

During intracellular multiplication in macrophages, *Y. pestis* utilizes various virulence factors to overcome the host antimicrobial activities; the majority of those are chromosomally encoded. A notable insertion sequence present on the *Y. pestis* chromosome that confers a virulence status to pathogenic *Yersinia* species is *IS*100, which is a 102kbp DNA-fragment named as a pigmentation (*pgm*) locus in *Y. pestis*. Functionally, the pigmentation locus is further divided into pigmentation segment and high pathogenic island (HPI), possessing genes for heme storage system (*hmsHFRS* and *hmsT*) and genes for siderophore dependant iron transport system (yersiniabactin) and

pesticin receptor, respectively (92). Depending on *Y. pestis* strains, the pigmentation locus is flanked by approximately 28-nucleotide direct repeats and carries sequence information to transcribe a functional transposase (37, 92). Particularly, genes *ripA* and *ripB* from pigmentation segment encoding, respectively, a putative acetyl-CoA transferase and a monoamine oxidase allow *Y. pestis* to suppress nitric oxide accumulation in the phagolysosome and ensure better survival and multiplication inside macrophages (92). The two-component transcriptional regulator *phoP-phoQ* and its downstream regulated genes, magnesium transporter gene cluster (*mgtC*) and UDP-D-glucose dehydrogenase (*ugd*), are also necessary for *Y. pestis* to maintain viability in a mouse macrophage-like cell line, J774A.1. *Y. pestis* strains with these genes intact are associated with an extension of macrophage phagolysosomes to form spacious vacuoles that may diminish macrophage-mediated antimicrobial activity by diluting the phagolysosomal content. Consistent with this idea, *Y. pestis* mutants for these genes failed to form spacious vacuoles and were defective for intracellular survival in macrophages (45). Similarly, Hfq a chaperon protein stabilizing small, non-coding RNAs (sRNAs) on their target sequences in *Y. pestis* mRNAs is also necessary for *Y. pestis* to survive in a mouse macrophage cell line and to cause infection in mice through subcutaneous or intravenous routes of infection (43). Further, while *Y. pestis* resides inside the phagolysosomes, Braun's lipoprotein in *Y. pestis* outer membrane helps the bacteria to maintain its viability in RAW264.7 cells presumably through facilitating bacterial iron acquisition and transport processes (103). In addition, iron transport systems YfeABC, YfeD, and FeoABC are also thought to facilitate *Y. pestis* iron

acquisition in the phagolysosomal environment. Mutational inactivation of either of these systems significantly decreases bacterial viability inside macrophages (83).

Apart from the virulence genes that ensure *Y. pestis* survival in macrophages, some other *Y. pestis* genes which may not be directly involved in the macrophage infection, but are indispensable for subsequent systemic infection are also activated by intracellular stimuli. The genes encoding the type-III secretion system, F1-capsular antigen and pH6-antigen are notable examples (81). The type-III secretion system is a well studied pathogenic system of *Y. pestis*, which consists of structural components making the needle complex on the surface of the bacteria and of effector proteins delivered through those needles known as *Yersinia* Outer Proteins (YOPs). Expression of this system is tightly regulated by the environmental calcium concentration; low calcium concentration in the phagolysosomal compartments favors the active expression of this system (84, 85). YOPs are preferentially injected into professional phagocytic cells, such as macrophages and dendritic cells, and neutrophils and there interfere with various host cell signaling mechanisms, causing the host cells to undergo a range of physio-morphological changes from decreasing phagocytic activity to apoptosis (65, 72).

The F1-capsular antigens transcribed from the pMT plasmid are extremely thin fimbrial structures which cover the *Y. pestis* surface as a capsule when expressed. Each of these fimbiral structures is a polymer of monomeric proteins called CaF-1 subunits which are 15.6kDa proteins, made up of multiple beta-strands similar to IL-1 and transported across the plasma membrane by a periplasmic chaperon. The F1-antigen is highly expressed at 37^{o}C, especially in the macrophage phagolysosomal environment (1, 26). The presence of F1-antigen on *Y. pestis* surface can mask outward exposure of other *Y.*

pestis surface molecules and hence prevent bacteria-host cell interaction, thereby blocking the phagocytosis of *Y. pestis* by macrophages and neutrophils (70). In contrast to this description, peritoneal macrophages from guinea pig have uptake and subsequent intracellular parasitism of *Y. pestis* expressing F1-antigen (46). This finding in guinea pig suggests that virulence of *Y. pestis* F1-capsular antigen is host specific; the guinea pig macrophages may have subtle changes in the phagocytic receptors, providing for better *Y. pestis* uptake. The other virulence factor, the pH6-antigen, is encoded from *Y. pestis* chromosomal loci *psaA*, which consist of genes *psaEFABC*. This antigen is merely a structural analog of plasmid encoded F1-capsular antigen, and its expression is induced by the acidic environment of macrophage phagolysosomes (66, 87). Protein interaction studies reveal that by mimicking the Fc-receptor for human IgG, pH6-antigen can bind and mask the constant region of IgG molecules attached on *Y. pestis* and thus prevent the antibody mediated phagocytosis of *Y. pestis* by macrophages (127).

The role of *Y. pestis* lipooligosaccharide (LOS) on macrophage infection has also been analyzed in various immunobiology related studies. LOS of *Y. pestis* is anticipated to act through macrophage TLR-4 and CD14 receptor complexes to initiate host chemokine and cytokine responses to infection (120). However, this does not appear to be the case, as mutational inactivation of an essential gene, *ipxM*, involved in lipid A synthesis did not alter the pathogenic process or infection severity in mouse models (5). Similarly, expression of exogenous functional O-antigen in *Y. pestis* incapable of synthesizing its own also did not influence virulence significantly in mouse infections (79). These latter findings question the role of *Y. pestis* LOS in macrophage infection; further research is necessary to understand its role.

D2. *Y. pestis* pathodynamics in local lymph nodes and virulence factors

Y. pestis disseminated via macrophages to local lymph nodes continue to multiply both intra- and extracellularly causing edematous swelling and necrosis of these nodes, which are recognized clinically as buboes (81). During this stage of infection, the extracellular *Y. pestis* expresses a nitric oxide deoxygenase flavohemoglobin which detoxifies nitric oxide which is produced by damaged neutrophils and macrophages. In addition, *Y. pestis* prevents neutrophilic infiltration into the lymph nodes by an unknown mechanism (47, 102). Blockage of the neutrophilic infiltration may benefit *Y. pestis* by controlling the degree of host inflammatory reaction and its negative effects on the progression of the infection.

D3. Systemic dissemination of *Y. pestis* infections and virulence factors

From the local lymph nodes, *Y. pestis* spreads through either lymphatics or blood vessels to various internal organs such as liver, spleen and lung. This spread almost certainly leads to septicemia, disseminated intravascular coagulation (DIC) and death of infected rodents (100). During the systemic dissemination, *Y. pestis* virulence factor plasminogen activator from the pPCP plasmid plays a pivotal role in the disease progression. *Y. pestis* mutant strains for plasminogen activator gene *pla* are severely attenuated for systemic infection in mouse models. However, direct intravenous injection of these mutants cause fatal disease similar to those of wild strains of *Y. pestis* (101). However, *Y. pestis* strains cured of or naturally lacking the pPCP plasmid are fully virulent through aerosolized route in mice and guinea pigs (98), suggesting that the plasminogen activator is predominantly used by *Y. pestis* during the transition of local

infection into the systemic disease and if this stage is bypassed then the virulence factor is unnecessary. Apart from the systemic spread, protease function of the plasminogen activator helps *Y. pestis* degrade residual YOPs in the interstitium during bubonic plague and inactivates various host complement factors and respiratory antimicrobial peptides, respectively, during septicemic and pneumonic infections (40, 107).

D4. Systemic plague and virulence factors

After systemic dissemination, *Y. pestis* bacilli colonize various internal organs, preferentially, liver, spleen and lung. During this stage of infection, *Y. pestis* uses various virulence factors in order to obtain sufficient iron from the infected host and to avoid host immune attacks. *Y. pestis* enzymes phospholipase A and D are used by the bacteria to disrupt the host RBCs in order to acquire iron from the hemoglobin released (36). Further, this process is complemented by upregulation of *Y. pestis* genes associated with iron scavenging, uptake and storage (25). A primary virulence locus involving in this *Y. pestis* iron acquisition process during septicemic plague is the pigmentation (*pgm*) locus. This locus is deleted spontaneously from the chromosome when *Y. pestis* is cultured in an iron rich media (49). Consistent with this *in vitro* observation, pigmentation mutants of *Y. pestis* in animals having abnormally high concentration of iron cause severe disease equivalent to wild type *Y. pestis* infection (21). Similarly, a human patient with hereditary hemochromatosis and resulting high iron load in tissues succumbed to a laboratory-acquired infection of *Y. pestis* mutant strain for the major iron acquisition system (6). However, under normal physiological range of iron concentration, deletion of this locus is detrimental and leads to loss of virulence in many infection models (21). But in

aerosolized exposure, the pigmentation locus is dispensable for *Y. pestis* virulence, as evidenced by the pigmentation locus mutants being equally lethal as wild type *Y. pestis* in normal African green monkeys through respiratory exposure (124). This iron acquisition property of the pigmentation locus is mainly contributed by siderophore dependent iron transport system (yersiniabactin) locating on high pathogenic island of *pgm* locus (92). Yersiniabactin plays an important role in scavenging iron molecules for *Y. pestis* in iron deplete environments (99). Mutation of the whole yersiniabactin operon or part of the coding region (*rip2* gene) leads to loss of virulence in mouse models by subcutaneous route of infection (10). In addition to yersiniabactin, three other ATP-dependent iron transport systems Yiu, Yfe and Yfu have also been reported from this locus (58). Yiu system transcribed from *yiuABCR* operon does not have any detect negative impact on virulence in mouse infections when the system is rendered inactive, but interfering with Yfe system *yfeABCD* and *yfeE* leads to attenuation of virulence (11, 58). Yfu system from *yfuABC* is a "Fur" regulated iron acquisition system, which also acts as a magnesium uptake and utilization system, but the pathogenic role of this system in mammalian host is not yet clear (44). All these iron acquisition systems from HPI are primarily important for *Y. pestis* to acquire sufficient iron for metabolic needs, inactivation of one or more of these systems can decrease the likelihood of *Y. pestis* survival inside the mammalian host.

Hemin storage system is the well studied protein complex transcribed from pigmentation segment of *pgm* locus (92). This system is critical for flea vector life cycle of *Y. pestis*, but is dispensable for mammalian host infection (54). In flea vectors, hemin storage system helps *Y. pestis* form biofilm mass in the flea proventriculus region by the

exopolysaccharide synthetic action of protein HmsT from this system (54, 82). In turn, the protein HmsT is regulated by various co-transcriptors from *hmsHFRS* and *hmsT* operon as well as *phoP-phoQ* transcriptional regulator and quorum sensing molecules such as *luxI*, *luxR*, and *luxS* (15, 16, 114). In addition to this hemin locus, the pigmentation segment has a nutritive iron acquisition system (*hmuRSTUV*), which transports various types of iron sources such as hemin, hemin-albumin and myoglobin into the bacterial cytoplasm. However, mutational inactivation of this locus did not show any significant negative effect on either bacterial growth or infection severity in mouse models (118).

Other major virulence factors involved in the extracellular infection phase of *Y. pestis* are YOPs and a type-III secretion system structural component LcrV from pCD plasmid. The expression of these factors is tightly regulated by environmental Ca++ concentration. Mutational inactivation of regulator genes of YOPs and LcrH leads to attenuation of virulence in mouse infection models (32, 88). YOPs are the primary pathogenic elements of pCD plasmid which disrupt host immune function preferentially targeting antigen presenting cells, such as macrophages and dendritic cells, and neutrophils (72). Among the secretory proteins, YopB and YopD act as a translocon, helping other proteins cross the eukaryotic plasma membrane, especially into the host macrophages (39). Among 14 YOPs reported so far, YopJ is the one studied most widely with respect to its interfering effects on immune cell signaling mechanisms. YopJ blocks toll-like receptor (TLR)-mediated IFN-γ production in human embryonic kidney 293 (HEK293) cells by acting as acetyltransferase to acetylate Ser/Thr residues of MAPK-kinase (MAPKK), which is phosphorylated under normal physiological condition (75,

116). In addition, YopJ also interferes in maturation of dendritic cells by down regulating the vital MAPK/ERK pathway, resulting in inefficient communication between innate and acquired immune systems (50, 69). In rat infections, YopJ was noted to lower the host TNF-α production by depleting the immune cells through induction of caspase-1 mediated apoptosis. Although it plays multiple roles during systemic infection, YopJ mutants were not attenuated with respect to the pathogenic process or infection severity in rats (62, 65).

Other YOPs, YopE, YopK and YopL, likely enhance virulence during the systemic infection, as the triple mutant (YopE, YopK and YopL) failed to colonize the internal organs in mouse infections (110). Similarly, *Y. pseudotuberculosis* YopK, which is highly homologous to *Y. pestis* YopK, also failed to colonize the mouse spleen through either oral or intraperitoneal route of infection when the gene is interrupted (55). The other protein, YopE which is transferred into the eukaryotic cytoplasm through YopB and YopD disrupts Rho-GTPase mediated signaling mechanisms controlling various cellular functions. Sometimes this action is synergistically amplified by protease YopT and Ser/Thr kinase YopO (121). YopM, a leucine rich protein having considerable homology to platelet surface glycoprotein von Willebrand factor shows significant loss of virulence in mouse models when the gene is mutated, likely due to failure of the mutant strains to cause platelet aggregation and its related pathogenic process during the systemic infection (63, 64). YopH plays a role in suppression of adaptive immunity against *Y. pestis* by means of interfering with T-lymphocyte signaling mechanism (3).

E. *Y. pestis* infection of macrophages and disease severity

As explained in the previous sections, host macrophages are the target cells of preference for *Y. pestis* parasitism during the initial stage of flea bite infection. The host macrophages provide a conducive intracellular environment for *Y. pestis* to survive and multiply away from the host innate immune mechanisms (45, 90-92, 112). Based on what is known about *Y. pestis* pathodynamics, infection of rodents depleted of macrophages would suffer diminished severity of *Y. pestis* infection. In this condition, the neutrophils may completely eliminate all the bacilli injected by fleas, and *Y. pestis* may not be able to progress efficiently to the next stage of infection, septicemic plague. Thus, it is reasonable to conjecture that *Y. pestis* infection of host macrophages is a deciding factor for the progression and severity of the infection. In support of this contention, experimental mice depleted of their phagocytic cells by treating with liposomes containing clodronate had fewer number of colony forming units (CFUs) from liver and spleen and resulted in mild or no lesions in these organs for *Y. pestis* infection when compared with that of normal mice (126). Likewise, *Y. pestis* strain CO92 mutants for Braun's lipoprotein gene *lpp*, which failed to survive in *in vitro* macrophage studies, was significantly attenuated for its virulence in mouse infections (103). Further support for the role of host macrophages for *Y. pestis* infection was demonstrated by a study in which infection of mice through peripheral route of inoculation showed that *Y. pestis* predominantly localized in macrophages during the first few days of infection before causing septicemia and death of the infected animals (71).

Although the compelling evidences on involvement of host macrophages in establishment of *Y. pestis* infection are present, no research has been done to examine

whether *Y. pestis* responds differently in macrophages from hosts with varying degrees of severity of infection. One approach to studying this problem would be to compare *Y. pestis* pathodynamics in macrophages from hosts suffering severe disease such as mice and rats with macrophages from hosts only experiencing inapparent or no disease such as dogs or coyotes. To this end, we observed *Y. pestis* infection parameters in primary and tissue culture macrophages originated from mouse and dog. The resulting observations are explained in detail in Chapter 3.

Another aspect of early pathogenesis that needs to be studied further is how *Y. pestis* survives intracellularly in macrophages. It is certain that the host macrophages are used by *Y. pestis* for its benefit as evidenced by various previously published studies (45, 90-92, 112). Further, observation of the intracellular trafficking of *Y. pestis* in macrophages suggests that the vacuoles carrying the bacterium can mature into phagolysosome (45, 92). Macrophages possess a wide spectrum of antimicrobial activities such as phagolysosomal acidic pH; enzymes cathepsins, lipase, nuclease and glycosidase; oxidizing agent; reactive oxygen species; cationic peptides; nitric oxide; and reactive intermediates of nitric oxide (38, 120). In addition, phagolysosomal compartments are low in calcium, iron, magnesium, and manganese concentration, which make the organelle very hostile for the intracellular *Y. pestis* (38, 120). In order to survive in this harsh intracellular environment, *Y. pestis* has to be equipped with various adaptive strategies. Recently, a few of these intracellular adaptive strategies of *Y. pestis* have been explored by various researchers as explained in previous sections (43, 45, 92). However, even within the *Y. pestis* virulence factors reported, some of them such as type-III secretion system, plasminogen activator and pH-6 antigen which have been thought to be

important for macrophage infections may not be required for *Y. pestis* intracellular survival and multiplication (68, 90, 111). Under this circumstance, it is pivotal to know which virulence factors *Y. pestis* relies on to adapt to the macrophage phagolysosomal niche. As an effort to explore this area, we compared intracellular *Y. pestis* protein profiles with those of microbial culture grown *Y. pestis*. This study is presented in Chapter 4. This study was extended to examine expression of *Y. pestis* tellurite resistance genes associated with macrophage infection and presented in Chapter 5.

F. Summary

Y. pestis is a recently evolved pathogen from *Y. pseudotuberculosis* through acquiring of new plasmids and rearranging and reducing the genome. These plasmids are critical for *Y. pestis* pathogenesis and encode various virulence factors necessary for mammalian host infection. The bacterium causes severe infection in the natural rodent host with high mortality; however, in some rodent predators, the disease is mild or inapparent. In natural infection, *Y. pestis* inoculated subcutaneously by the infected flea bite initially multiplies inside the macrophages in the local lymph node and subsequently spreads to various internal organs, resulting in septicemia. Thus, the host macrophages are considered important innate immune cells utilized by *Y. pestis* to establish infection in susceptible hosts. Therefore, to better explain the role of host macrophages for the *Y. pestis* infection severity and to understand the *Y. pestis* virulence factors involved during the macrophage infection, we tested the following hypothesis and made a series of observations and conclusions.

Hypothesis: Differences in *Y. pestis* infection severity between hosts suffering severe disease such as rodents and less severe disease such as dogs may be related to how well *Y. pestis* overcomes the macrophage associated stress during the initial phase of intracellular parasitism.

Conclusion: A study conducted using mouse and dog macrophages supports the hypothesis proposed that, in mouse macrophages, *Y. pestis* can overcome the macrophage associated stress but not in dog macrophages; these findings are presented and discussed in detail in Chapter 3.

Observation: *Y. pestis* intracellular multiplication and survival in macrophages are likely achieved through use of various *Y. pestis* intracellular virulence factors. While many of these virulence factors have been identified, some remain unexplored. As an effort to discover additional intracellularly employed virulence factors, we conducted a comparative proteomics study on *Y. pestis* residing intracellularly in macrophages versus microbial culture grown extracellular *Y. pestis*.

Conclusion: (1) The study revealed that during the macrophage parasitism phase *Y. pestis* employs various bacterial general stress regulator mechanisms to adapt and survive the intracellular niche including newly identified tellurite resistance proteins. Results and discussion pertaining to this area of research are presented in Chapter 4.

(2) As a part of this general stress response, expression of *Y. pestis* tellurite resistance operon was studied and the association of proteins with filamentous cellular morphology related to *Y. pestis* infection of macrophages was examined. These experimental results are presented and discussed in Chapter 5.

References

1. **Abramov, V. M., A. M. Vasiliev, R. N. Vasilenko, N. L. Kulikova, I. V. Kosarev, V. S. Khlebnikov, A. T. Ishchenko, S. MacIntyre, J. R. Gillespie, R. Khurana, T. Korpela, A. L. Fink, and V. N. Uversky.** 2001. Structural and functional similarity between *Yersinia pestis* capsular protein Caf1 and human interleukin-1 beta. Biochemistry **40:**6076-6084.
2. **Achtman, M., K. Zurth, G. Morelli, G. Torrea, A. Guiyoule, and E. Carniel.** 1999. *Yersinia pestis*, the cause of plague, is a recently emerged clone of *Yersinia pseudotuberculosis*. Proc Natl Acad Sci USA **96:**14043-14048.
3. **Alonso, A., N. Bottini, S. Bruckner, S. Rahmouni, S. Williams, S. P. Schoenberger, and T. Mustelin.** 2004. Lck dephosphorylation at Tyr-394 and inhibition of T cell antigen receptor signaling by *Yersinia* phosphatase YopH. J Biol Chem **279:**4922-4928.
4. **Anisimov, A. P., L. E. Lindler, and G. B. Pier.** 2004. Intraspecific diversity of *Yersinia pestis*. Clin Microbiol Rev **17:**434-464.
5. **Anisimov, A. P., R. Z. Shaikhutdinova, L. N. Pan'kina, V. A. Feodorova, E. P. Savostina, O. V. Bystrova, B. Lindner, A. N. Mokrievich, I. V. Bakhteeva, G. M. Titareva, S. V. Dentovskaya, N. A. Kocharova, S. N. Senchenkova, O. Holst, Z. L. Devdariani, Y. A. Popov, G. B. Pier, and Y. A. Knirel.** 2007. Effect of deletion of the *lpxM* gene on virulence and vaccine potential of *Yersinia pestis* in mice. J Med Microbiol **56:**443-453.

6. **Anonymous.** 2011. Fatal laboratory-acquired infection with an attenuated *Yersinia pestis* strain--Chicago, Illinois, 2009. MMWR Morb Mortal Wkly Rep **60:**201-205.

7. **Anonymous.** 1999. Plague manual--epidemiology, distribution, surveillance and control. Wkly Epidemiol Rec **74:**447-481.

8. **Ayyadurai, S., L. Houhamdi, H. Lepidi, C. Nappez, D. Raoult, and M. Drancourt.** 2008. Long-term persistence of virulent *Yersinia pestis* in soil. Microbiology **154:**2865-2871.

9. **Bazanova, L. P., and M. P. Maevskii.** 1996. [The duration of the persistence of the plague microbe in the body of the flea *Citellophilus tesquorum* altaicus]. Med Parazitol (Mosk) **1:**45-48.

10. **Bearden, S. W., J. D. Fetherston, and R. D. Perry.** 1997. Genetic organization of the yersiniabactin biosynthetic region and construction of avirulent mutants in *Yersinia pestis*. Infect Immun **65:**1659-1668.

11. **Bearden, S. W., and R. D. Perry.** 1999. The Yfe system of *Yersinia pestis* transports iron and manganese and is required for full virulence of plague. Mol Microbiol **32:**403-414.

12. **Bizanov, G., and N. D. Dobrokhotova.** 2007. Experimental infection of ground squirrels (*Citellus pygmaeus* Pallas) with *Yersinia pestis* during hibernation. J Infect **54:**198-203.

13. **Bliska, J. B., B. L. Noel, S. Lilo, D. Capurso, and J. Hill.** 2009. *Yersinia pestis* can bypass protective antibodies to LcrV and activation with gamma interferon to

survive and induce apoptosis in murine macrophages. Clin Vaccine Immunol **16:**1457-1466.

14. **Bliska, J. B., C. Pujol, K. A. Klein, G. A. Romanov, L. E. Palmer, C. Cirota, and Z. J. Zhao.** 2009. *Yersinia pestis* can reside in autophagosomes and avoid xenophagy in murine macrophages by preventing vacuole acidification. Infect Immun **77:**2251-2261.

15. **Bobrov, A. G., S. W. Bearden, J. D. Fetherston, A. A. Khweek, K. D. Parrish, and R. D. Perry.** 2007. Functional quorum sensing systems affect biofilm formation and protein expression in *Yersinia pestis*. Adv Exp Med Biol **603:**178-191.

16. **Bobrov, A. G., O. Kirillina, and R. D. Perry.** 2007. Regulation of biofilm formation in *Yersinia pestis*. Genus *Yersinia*: from genomics to function **603:**201-210.

17. **Breneva, N. V., and A. S. Maramovich.** 2008. [Modeling of interaction between *Yersinia pestis* and *Tetrahymena pyriformis* in experimental ecosystems]. Zh Mikrobiol Epidemiol Immunobiol **5:**39-41.

18. **Brubaker, R. R.** 1991. Factors promoting acute and chronic diseases caused by *Yersiniae*. Clin Microbiol Rev **4:**309-324.

19. **Brubaker, R. R.** 1972. The genus *Yersinia*: biochemistry and genetics of virulence. Curr Top Microbiol Immunol **57:**111-158.

20. **Burrows, T. W., and W. A. Gillett.** 1966. Nutritional requirements of some *Pasteurella* species. J General Microbiol **45:**333-348.

21. **Burrows, T. W., and S. Jackson.** 1956. The virulence-enhancing effect of iron on nonpigmented mutants of virulent strains of *Pasteurella pestis*. Br J Exp Pathol **37:**577-583.

22. **Butler, T., Y. S. Fu, L. Furman, C. Almeida, and A. Almeida.** 1982. Experimental *Yersinia pestis* infection in rodents after intragastric inoculation and ingestion of bacteria. Infect Immun **36:**1160-1167.

23. **Chain, P. S., P. Hu, S. A. Malfatti, L. Radnedge, F. Larimer, L. M. Vergez, P. Worsham, M. C. Chu, and G. L. Andersen.** 2006. Complete genome sequence of *Yersinia pestis* strains antiqua and nepal516: evidence of gene reduction in an emerging pathogen. J Bacteriol **188:**4453-4463.

24. **Chain, P. S. G., E. Carniel, F. W. Larimer, J. Lamerdin, P. O. Stoutland, W. M. Regala, A. M. Georgescu, L. M. Vergez, M. L. Land, V. L. Motin, R. R. Brubaker, J. Fowler, J. Hinnebusch, M. Marceau, C. Medigue, M. Simonet, V. Chenal-Francisque, B. Souza, D. Dacheux, J. M. Elliott, A. Derbise, L. J. Hauser, and E. Garcia.** 2004. Insights into the evolution of *Yersinia pestis* through whole-genome comparison with *Yersinia pseudotuberculosis*. Proc Natl Acad Sci USA **101:**13826-13831.

25. **Chauvaux, S., M. L. Rosso, L. Frangeul, C. Lacroix, L. Labarre, A. Schiavo, M. Marceau, M. A. Dillies, J. Foulon, J. Y. Coppee, C. Medigue, M. Simonet, and E. Carniel.** 2007. Transcriptome analysis of *Yersinia pestis* in human plasma: an approach for discovering bacterial genes involved in septicaemic plague. Microbiology **153:**3112-3124.

26. **Chen, T. H., and S. S. Elberg.** 1977. Scanning electron microscopic study of virulent *Yersinia pestis* and *Yersinia pseudotuberculosis* type 1. Infect Immun **15:**972-977.

27. **Ciammaruconi, A., S. Grassi, R. De Santis, G. Faggioni, V. Pittiglio, R. D'Amelio, A. Carattoli, A. Cassone, G. Vergnaud, and F. Lista.** 2008. Fieldable genotyping of *Bacillus anthracis* and *Yersinia pestis* based on 25-loci multi locus VNTR analysis. BMC Microbiol **8:**21-32.

28. **Cui, Y. J., Y. J. Li, O. Gorge, M. E. Platonov, Y. F. Yan, Z. B. Guo, C. Pourcel, S. V. Dentovskaya, S. V. Balakhonov, X. Y. Wang, Y. J. Song, A. P. Anisimov, G. Vergnaud, and R. F. Yang.** 2008. Insight into microevolution of *Yersinia pestis* by clustered regularly interspaced short palindromic repeats. PLoS One **3:**-2652-2662.

29. **Cully, J. F., Jr., T. L. Johnson, S. K. Collinge, and C. Ray.** 2010. Disease limits populations: plague and black-tailed prairie dogs. Vector Borne Zoonotic Dis **10:**7-15.

30. **Das, R., A. Dhokalia, X. Z. Huang, R. Hammamieh, N. Chakraborty, L. E. Lindler, and M. Jett.** 2007. Study of proinflammatory responses induced by *Yersinia pestis* in human monocytes using cDNA arrays. Genes Immun **8:**308-319.

31. **Deng, W., V. Burland, G. Plunkett, 3rd, A. Boutin, G. F. Mayhew, P. Liss, N. T. Perna, D. J. Rose, B. Mau, S. Zhou, D. C. Schwartz, J. D. Fetherston, L. E. Lindler, R. R. Brubaker, G. V. Plano, S. C. Straley, K. A. McDonough, M. L.**

Nilles, J. S. Matson, F. R. Blattner, and R. D. Perry. 2002. Genome sequence of *Yersinia pestis* KIM. J Bacteriol **184:**4601-4611.

32. **Du, Z., Y. Tan, H. Yang, J. Qiu, L. Qin, T. Wang, H. Liu, Y. Bi, Y. Song, Z. Guo, Y. Han, D. Zhou, X. Wang, and R. Yang.** 2009. Gene expression profiling of *Yersinia pestis* with deletion of *lcrG*, a known negative regulator for Yop secretion of type III secretion system. Int J Med Microbiol **299:**355-366.

33. **Dykhuizen, D. E.** 2000. *Yersinia pestis*: an instant species? Trends Microbiol **8:**296-298.

34. **Eppinger, M., P. L. Worsham, M. P. Nikolich, D. R. Riley, Y. Sebastian, S. Mou, M. Achtman, L. E. Lindler, and J. Ravel.** 2010. Genome sequence of the deep-rooted *Yersinia pestis* strain angola reveals new insights into the evolution and pangenome of the plague bacterium. J Bacteriol **192:**1685-1699.

35. **Eskey, C. R., F. M. Prince, and F. B. Fuller.** 1951. Double infection of the rat fleas *X. cheopis* and *N. fasciatus* with *Pasteurella* and *Salmonella*. Public Health Rep **66:**1318-1326.

36. **Feodorova, V. A., and Z. L. Devdariani.** 2002. The interaction of *Yersinia pestis* with erythrocytes. J Med Microbiol **51:**150-158.

37. **Fetherston, J. D., and R. D. Perry.** 1994. The pigmentation locus of *Yersinia pestis* KIM6+ is flanked by an insertion sequence and includes the structural genes for pesticin sensitivity and HMWP2. Mol Microbiol **13:**697-708.

38. **Flannagan, R. S., V. Jaumouille, and S. Grinstein.** 2011. The cell biology of phagocytosis. Annu Rev Pathol **7:**49-86.

39. **Francis, M. S., and H. Wolf-Watz.** 1998. YopD of *Yersinia pseudotuberculosis* is translocated into the cytosol of HeLa epithelial cells: evidence of a structural domain necessary for translocation. Mol Microbiol **29:**799-813.

40. **Galvan, E. M., M. A. Lasaro, and D. M. Schifferli.** 2008. Capsular antigen fraction 1 and Pla modulate the susceptibility of *Yersinia pestis* to pulmonary antimicrobial peptides such as cathelicidin. Infect Immun **76:**1456-1464.

41. **Garcia, E., P. Worsham, S. Bearden, S. Malfatti, D. Lang, F. Larimer, L. Lindler, and P. Chain.** 2007. Pestoides F, an atypical *Yersinia pestis* strain from the former Soviet Union. Adv Exp Med Biol **603:**17-22.

42. **Gasper, P. W., A. M. Barnes, T. J. Quan, J. P. Benziger, L. G. Carter, M. L. Beard, and G. O. Maupin.** 1993. Plague (*Yersinia pestis*) in cats: description of experimentally induced disease. J Med Entomol **30:**20-26.

43. **Geng, J., Y. Song, L. Yang, Y. Feng, Y. Qiu, G. Li, J. Guo, Y. Bi, Y. Qu, W. Wang, X. Wang, Z. Guo, R. Yang, and Y. Han.** 2009. Involvement of the post-transcriptional regulator Hfq in *Yersinia pestis* virulence. PLoS One **4:**6213-6223.

44. **Gong, S., S. W. Bearden, V. A. Geoffroy, J. D. Fetherston, and R. D. Perry.** 2001. Characterization of the *Yersinia pestis* Yfu ABC inorganic iron transport system. Infect Immun **69:**2829-2837.

45. **Grabenstein, J. P., H. S. Fukuto, L. E. Palmer, and J. B. Bliska.** 2006. Characterization of phagosome trafficking and identification of PhoP-regulated genes important for survival of *Yersinia pestis* in macrophages. Infect Immun **74:**3727-3741.

46. **Grebtsova, N. N., A. S. Cherniavskaia, S. A. Lebedeva, and V. S. Ivanova.** 1990. [The phagocytic activity of peritoneal macrophages in relation to *Yersinia pestis* with defective and complete *fra* genes]. Zh Mikrobiol Epidemiol Immunobiol **5:**7-11.

47. **Guinet, F., P. Ave, L. Jones, M. Huerre, and E. Carniel.** 2008. Defective innate cell response and lymph node infiltration specify *Yersinia pestis* infection. PLoS One **3:**1688-1699.

48. **Guiyoule, A., F. Grimont, I. Iteman, P. A. Grimont, M. Lefevre, and E. Carniel.** 1994. Plague pandemics investigated by ribotyping of *Yersinia pestis* strains. J Clin Microbiol **32:**634-641.

49. **Hallett, A. F., M. Isaacson, and K. F. Meyer.** 1973. Pathogenicity and immunogenic efficacy of a live attentuated plaque vaccine in vervet monkeys. Infect Immun **8:**876-881.

50. **Hao, Y. H., Y. Wang, D. Burdette, S. Mukherjee, G. Keitany, E. Goldsmith, and K. Orth.** 2008. Structural requirements for *Yersinia* YopJ inhibition of MAP kinase pathways. PLoS One **3:**1375-1384.

51. **Hillier, S. L., and W. T. Charnetzky.** 1981. Rapid diagnostic test that uses isocitrate lyase activity for identification of *Yersinia pestis*. J Clin Microbiol **13:**661-665.

52. **Hinchliffe, S. J., K. E. Isherwood, R. A. Stabler, M. B. Prentice, A. Rakin, R. A. Nichols, P. C. Oyston, J. Hinds, R. W. Titball, and B. W. Wren.** 2003. Application of DNA microarrays to study the evolutionary genomics of *Yersinia pestis* and *Yersinia pseudotuberculosis*. Genome Res **13:**2018-2029.

53. **Hinnebusch, B. J.** 2005. The evolution of flea-borne transmission in *Yersinia pestis*. Curr Issues Mol Biol **7:**197-212.

54. **Hinnebusch, B. J., R. D. Perry, and T. G. Schwan.** 1996. Role of the *Yersinia pestis* hemin storage (*hms*) locus in the transmission of plague by fleas. Science **273:**367-370.

55. **Holmstrom, A., R. Rosqvist, H. Wolfwatz, and A. Forsberg.** 1995. Virulence plasmid-encoded Yopk is essential for *Yersinia pseudotuberculosis* to cause systemic infection in mice. Infect Immun **63:**2269-2276.

56. **Holt, J. G., N. R. Krieg, P. H. A. Sneath, J. T. Staley, and E. S. Williams.** 1994. Bergey's manual of determinative bacteriology, The Williams & Wilkins Co., Baltimore, Md. **9th edition:**1-8.

57. **Kim, T. J., S. Chauhan, V. L. Motin, E. B. Goh, M. M. Igo, and G. M. Young.** 2007. Direct transcriptional control of the plasminogen activator gene of *Yersinia pestis* by the cyclic AMP receptor protein. J Bacteriol **189:**8890-8900.

58. **Kirillina, O., A. G. Bobrov, J. D. Fetherston, and R. D. Perry.** 2006. Hierarchy of iron uptake systems: Yfu and Yiu are functional in *Yersinia pestis*. Infect Immun **74:**6171-6178.

59. **Koo, J. T., T. M. Alleyne, C. A. Schiano, N. Jafari, and W. W. Lathem.** 2011. Global discovery of small RNAs in *Yersinia pseudotuberculosis* identifies *Yersinia*-specific small, noncoding RNAs required for virulence. Proc Natl Acad Sci USA **108:**709-717.

60. **Larson, C. L., C. B. Philip, W. C. Wicht, and L. E. Hughes.** 1951. Precipitin reactions with soluble antigens from suspensions of *Pasteurella pestis* or from tissues of animals dead of plague. J Immunol **67:**289-298.

61. **Leclercq, A. J., G. Torrea, V. Chenal-Francisque, and E. Carniel.** 2007. 3 IS-RFLP: a powerful tool for geographical clustering of global isolates of *Yersinia pestis*. Adv Exp Med Biol **603:**322-326.

62. **Lemaitre, N., F. Sebbane, D. Long, and B. J. Hinnebusch.** 2006. *Yersinia pestis* YopJ suppresses tumor necrosis factor alpha induction and contributes to apoptosis of immune cells in the lymph node but is not required for virulence in a rat model of bubonic plague. Infect Immun **74:**5126-5131.

63. **Leung, K. Y., B. S. Reisner, and S. C. Straley.** 1990. YopM inhibits platelet-aggregation and is necessary for virulence of *Yersinia pestis* in mice. Infect Immun **58:**3262-3271.

64. **Leung, K. Y., and S. C. Straley.** 1989. The YopM gene of *Yersinia pestis* encodes a released protein having homology with the human platelet-surface protein Gpib-alpha. JBacteriol **171:**4623-4632.

65. **Lilo, S., Y. Zheng, and J. B. Bliska.** 2008. Caspase-1 activation in macrophages infected with *Yersinia pestis* KIM requires the type III secretion system effector YopJ. Infect Immun **76:**3911-3923.

66. **Lindler, L. E., M. S. Klempner, and S. C. Straley.** 1990. *Yersinia pestis* pH 6 antigen: genetic, biochemical, and virulence characterization of a protein involved in the pathogenesis of bubonic plague. Infect Immun **58:**2569-2577.

67. **Lindler, L. E., G. V. Plano, V. Burland, G. F. Mayhew, and F. R. Blattner.** 1998. Complete DNA sequence and detailed analysis of the *Yersinia pestis* KIM5 plasmid encoding murine toxin and capsular antigen. Infect Immun **66:**5731-5742.

68. **Lindler, L. E., and B. D. Tall.** 1993. *Yersinia pestis* pH 6 antigen forms fimbriae and is induced by intracellular association with macrophages. Mol Microbiol **8:**311-324.

69. **Lindner, I., J. Torruellas-Garcia, D. Kolonias, L. M. Carlson, K. A. Tolba, G. V. Plano, and K. P. Lee.** 2007. Modulation of dendritic cell differentiation and function by YopJ of *Yersinia pestis*. Eur J Immunol **37:**2450-2462.

70. **Liu, F., H. Chen, E. M. Galvan, M. A. Lasaro, and D. M. Schifferli.** 2006. Effects of Psa and F1 on the adhesive and invasive interactions of *Yersinia pestis* with human respiratory tract epithelial cells. Infect Immun **74:**5636-5644.

71. **Lukaszewski, R. A., D. J. Kenny, R. Taylor, D. G. Rees, M. G. Hartley, and P. C. Oyston.** 2005. Pathogenesis of *Yersinia pestis* infection in BALB/c mice: effects on host macrophages and neutrophils. Infect Immun **73:**7142-7150.

72. **Marketon, M. M., R. W. DePaolo, K. L. DeBord, B. Jabri, and O. Schneewind.** 2005. Plague bacteria target immune cells during infection. Science **309:**1739-1741.

73. **Matchett, M. R., D. E. Biggins, V. Carlson, B. Powell, and T. Rocke.** 2010. Enzootic plague reduces black-footed ferret (*Mustela nigripes*) survival in Montana. Vector Borne Zoonotic Dis **10:**27-35.

74. **Motin, V. L., A. M. Georgescu, J. M. Elliott, P. Hu, P. L. Worsham, L. L. Ott, T. R. Slezak, B. A. Sokhansanj, W. M. Regala, R. R. Brubaker, and E. Garcia.** 2002. Genetic variability of *Yersinia pestis* isolates as predicted by PCR-based *IS*100 genotyping and analysis of structural genes encoding glycerol-3-phosphate dehydrogenase (*glpD*). J Bacteriol **184:**1019-1027.

75. **Mukherjee, S., G. Keitany, Y. Li, Y. Wang, H. L. Ball, E. J. Goldsmith, and K. Orth.** 2006. *Yersinia* YopJ acetylates and inhibits kinase activation by blocking phosphorylation. Science **312:**1211-1214.

76. **Nikul'shin, S. V., T. G. Onatskaia, L. M. Lukanina, and A. I. Bondarenko.** 1992. [Associations of the soil amoeba *Hartmannella rhysodes* with the bacterial causative agents of plague and pseudotuberculosis in an experiment]. Zh Mikrobiol Epidemiol Immunobiol **10:**2-5.

77. **Orloski, K. A., and M. Eidson.** 1995. *Yersinia pestis* infection in three dogs. J Am Vet Med Assoc **207:**316-318.

78. **Orloski, K. A., and S. L. Lathrop.** 2003. Plague: a veterinary perspective. J Am Vet Med Assoc **222:**444-448.

79. **Oyston, P. C., J. L. Prior, S. Kiljunen, M. Skurnik, J. Hill, and R. W. Titball.** 2003. Expression of heterologous O-antigen in *Yersinia pestis* KIM does not affect virulence by the intravenous route. J Med Microbiol **52:**289-294.

80. **Parkhill, J., B. W. Wren, N. R. Thomson, R. W. Titball, M. T. Holden, M. B. Prentice, M. Sebaihia, K. D. James, C. Churcher, K. L. Mungall, S. Baker, D. Basham, S. D. Bentley, K. Brooks, A. M. Cerdeno-Tarraga, T. Chillingworth, A. Cronin, R. M. Davies, P. Davis, G. Dougan, T. Feltwell, N. Hamlin, S.**

Holroyd, K. Jagels, A. V. Karlyshev, S. Leather, S. Moule, P. C. Oyston, M. Quail, K. Rutherford, M. Simmonds, J. Skelton, K. Stevens, S. Whitehead, and B. G. Barrell. 2001. Genome sequence of *Yersinia pestis*, the causative agent of plague. Nature **413:**523-527.

81. **Perry, R. D., and J. D. Fetherston.** 1997. *Yersinia pestis*--etiologic agent of plague. Clin Microbiol Rev **10:**35-66.

82. **Perry, R. D., T. S. Lucier, D. J. Sikkema, and R. R. Brubaker.** 1993. Storage reservoirs of hemin and inorganic iron in *Yersinia pestis*. Infect Immun **61:**32-39.

83. **Perry, R. D., I. Mier, Jr., and J. D. Fetherston.** 2007. Roles of the Yfe and Feo transporters of *Yersinia pestis* in iron uptake and intracellular growth. Biometals **20:**699-703.

84. **Perry, R. D., S. C. Straley, J. D. Fetherston, D. J. Rose, J. Gregor, and F. R. Blattner.** 1998. DNA sequencing and analysis of the low-Ca^{2+}-response plasmid pCD1 of *Yersinia pestis* KIM5. Infect Immun **66:**4611-4623.

85. **Pollack, C., S. C. Straley, and M. S. Klempner.** 1986. Probing the phagolysosomal environment of human macrophages with a Ca^{2+}-responsive operon fusion in *Yersinia pestis*. Nature **322:**834-836.

86. **Prentice, M. B., and L. Rahalison.** 2007. Plague. Lancet **369:**1196-1207.

87. **Price, S. B., M. D. Freeman, and K. S. Yeh.** 1995. Transcriptional analysis of the *Yersinia pestis* pH6 antigen gene. J Bacteriol **177:**5997-6000.

88. **Price, S. B., and S. C. Straley.** 1989. *lcrH*, a gene necessary for virulence of *Yersinia pestis* and for the normal response of *Y. pestis* to ATP and calcium. Infect Immun **57:**1491-1498.

89. **Protsenko, O. A., A. A. Filippov, and V. V. Kutyrev.** 1991. Integration of the plasmid encoding the synthesis of capsular antigen and murine toxin into *Yersinia pestis* chromosome. Microb Pathog **11:**123-128.

90. **Pujol, C., and J. B. Bliska.** 2003. The ability to replicate in macrophages is conserved between *Yersinia pestis* and *Yersinia pseudotuberculosis*. Infect Immun **71:**5892-5899.

91. **Pujol, C., and J. B. Bliska.** 2005. Turning *Yersinia* pathogenesis outside in: subversion of macrophage function by intracellular *Yersiniae*. Clin Immunol **114:**216-226.

92. **Pujol, C., J. P. Grabenstein, R. D. Perry, and J. B. Bliska.** 2005. Replication of *Yersinia pestis* in interferon gamma-activated macrophages requires *ripA*, a gene encoded in the pigmentation locus. Proc Natl Acad Sci USA **102:**12909-12914.

93. **Robert D. Perry, and J. D. Fetherston.** 2007. The genus *Yersinia*--from genomics to function. Advances in experimental medicine and biology (Springer Science+Business Media) **603:**2-16.

94. **Rust, J. H., Jr., D. C. Cavanaugh, R. O'Shita, and J. D. Marshall, Jr.** 1971. The role of domestic animals in the epidemiology of plague. I. Experimental infection of dogs and cats. J Infect Dis **124:**522-526.

95. **Rust, J. H., Jr., D. N. Harrison, J. D. Marshall, Jr., and D. C. Cavanaugh.** 1972. Susceptibility of rodents to oral plague infection: a mechanism for the persistence of plague in inter-epidemic periods. J Wildl Dis **8:**127-133.

96. **Rust, J. H., Jr., B. E. Miller, M. Bahmanyar, J. D. Marshall, Jr., S. Purnaveja, D. C. Cavanaugh, and U. S. Hla.** 1971. The role of domestic

animals in the epidemiology of plague. II. Antibody to *Yersinia pestis* in sera of dogs and cats. J Infect Dis **124:**527-531.

97. **Salkeld, D. J., M. Salathe, P. Stapp, and J. H. Jones.** 2010. Plague outbreaks in prairie dog populations explained by percolation thresholds of alternate host abundance. Proc Natl Acad Sci USA **107:**14247-14250.

98. **Samoilova, S. V., L. V. Samoilova, I. N. Yezhov, I. G. Drozdov, and A. P. Anisimov.** 1996. Virulence of pPst+ and pPst- strains of *Yersinia pestis* for guinea-pigs. J Med Microbiol **45:**440-444.

99. **Schubert, S., S. Cuenca, D. Fischer, and J. Heesemann.** 2000. High-pathogenicity island of *Yersinia pestis* in *Enterobacteriaceae* isolated from blood cultures and urine samples: prevalence and functional expression. J Infect Dis **182:**1268-1271.

100. **Sebbane, F., D. Gardner, D. Long, B. B. Gowen, and B. J. Hinnebusch.** 2005. Kinetics of disease progression and host response in a rat model of bubonic plague. Am J Pathol **166:**1427-1439.

101. **Sebbane, F., C. O. Jarrett, D. Gardner, D. Long, and B. J. Hinnebusch.** 2006. Role of the *Yersinia pestis* plasminogen activator in the incidence of distinct septicemic and bubonic forms of flea-borne plague. Proc Natl Acad Sci USA **103:**5526-5530.

102. **Sebbane, F., N. Lemaitre, D. E. Sturdevant, R. Rebeil, K. Virtaneva, S. F. Porcella, and B. J. Hinnebusch.** 2006. Adaptive response of *Yersinia pestis* to extracellular effectors of innate immunity during bubonic plague. Proc Natl Acad Sci USA **103:**11766-11771.

103. **Sha, J., S. L. Agar, W. B. Baze, J. P. Olano, A. A. Fadl, T. E. Erova, S. Wang, S. M. Foltz, G. Suarez, V. L. Motin, S. Chauhan, G. R. Klimpel, J. W. Peterson, and A. K. Chopra.** 2008. Braun lipoprotein (Lpp) contributes to virulence of *Yersiniae*: potential role of Lpp in inducing bubonic and pneumonic plague. Infect Immun **76:**1390-1409.

104. **Shen, X., Q. Wang, L. Xia, X. Zhu, Z. Zhang, Y. Liang, H. Cai, E. Zhang, J. Wei, C. Chen, Z. Song, H. Zhang, D. Yu, and R. Hai.** 2010. Complete genome sequences of *Y. pestis* from natural foci in China. J Bacteriol **192:**3551-3552.

105. **Simond, M., M. L. Godley, and P. D. Mouriquand.** 1998. Paul-Louis Simond and his discovery of plague transmission by rat fleas: a centenary. J R Soc Med **91:**101-104.

106. **Skurnik, M., A. Peippo, and E. Ervela.** 2000. Characterization of the O-antigen gene clusters of *Yersinia pseudotuberculosis* and the cryptic O-antigen gene cluster of *Yersinia pestis* shows that the plague bacillus is most closely related to and has evolved from *Y. pseudotuberculosis* serotype O:1b. Mol Microbiol **37:**316-330.

107. **Sodeinde, O. A., A. K. Sample, R. R. Brubaker, and J. D. Goguen.** 1988. Plasminogen activator/coagulase gene of *Yersinia pestis* is responsible for degradation of plasmid-encoded outer membrane proteins. Infect Immun **56:**2749-2752.

108. **Song, Y., Z. Tong, J. Wang, L. Wang, Z. Guo, Y. Han, J. Zhang, D. Pei, D. Zhou, H. Qin, X. Pang, J. Zhai, M. Li, B. Cui, Z. Qi, L. Jin, R. Dai, F. Chen, S. Li, C. Ye, Z. Du, W. Lin, J. Yu, H. Yang, P. Huang, and R. Yang.** 2004.

Complete genome sequence of *Yersinia pestis* strain 91001, an isolate avirulent to humans. DNA Res **11:**179-197.

109. **Sprague, L. D., H. C. Scholz, S. Amann, H. J. Busse, and H. Neubauer.** 2008. *Yersinia similis* species nov. Int J Syst Evol Micr **58:**952-958.

110. **Straley, S. C., and M. L. Cibull.** 1989. Differential clearance and host-pathogen interactions of YopE$^-$ and YopK$^-$ YopL$^-$ *Yersinia pestis* in BALB/c mice. Infect Immun **57:**1200-1210.

111. **Straley, S. C., and P. A. Harmon.** 1984. Growth in mouse peritoneal macrophages of *Yersinia pestis* lacking established virulence determinants. Infect Immun **45:**649-654.

112. **Straley, S. C., and P. A. Harmon.** 1984. *Yersinia pestis* grows within phagolysosomes in mouse peritoneal macrophages. Infect Immun **45:**655-659.

113. **Sulakvelidze, A.** 2000. *Yersiniae* other than *Y. enterocolitica, Y. pseudotuberculosis*, and *Y. pestis*: the ignored species. Microbes and Infection **2:**497-513.

114. **Sun, Y. C., A. Koumoutsi, and C. Darby.** 2009. The response regulator PhoP negatively regulates *Yersinia pseudotuberculosis* and *Yersinia pestis* biofilms. FEMS Microbiol Lett **290:**85-90.

115. **Surgalla, M. J., and E. D. Beesley.** 1969. Congo red-agar plating medium for detecting pigmentation in *Pasteurella pestis*. Appl Microbiol **18:**834-837.

116. **Sweet, C. R., J. Conlon, D. T. Golenbock, J. Goguen, and N. Silverman.** 2007. YopJ targets TRAF proteins to inhibit TLR-mediated NF-kappaB, MAPK and IRF3 signal transduction. Cell Microbiol **9:**2700-2715.

117. **Thomas, C. U., and P. E. Hughes.** 1992. Plague surveillance by serological testing of coyotes (*Canis latrans*) in Los Angeles County, California. J Wildl Dis **28:**610-613.

118. **Thompson, J. M., H. A. Jones, and R. D. Perry.** 1999. Molecular characterization of the hemin uptake locus (*hmu*) from *Yersinia pestis* and analysis of *hmu* mutants for hemin and hemoprotein utilization. Infect Immun **67:**3879-3892.

119. **Toma, S.** 1986. Human and nonhuman infections caused by *Yersinia pseudotuberculosis* in Canada from 1962 to 1985. J Clin Microbiol **24:**465-466.

120. **Underhill, D. M., and A. Ozinsky.** 2002. Phagocytosis of microbes: complexity in action. Annu Rev Immunol **20:**825-852.

121. **Viboud, G. I., and J. B. Bliska.** 2005. *Yersinia* outer proteins: role in modulation of host cell signaling responses and pathogenesis. Annu Rev Microbiol **59:**69-89.

122. **Wang, X. Y., Y. P. Han, Y. J. Li, Z. B. Guo, Y. J. Song, Y. F. Tan, Z. M. Du, A. Rakin, D. S. Zhou, and R. F. Yang.** 2007. *Yersinia* genome diversity disclosed by *Yersinia pestis* genome-wide DNA microarray. Canadian J Microbiol **53:**1211-1221.

123. **Waters, L. S., and G. Storz.** 2009. Regulatory RNAs in bacteria. Cell **136:**615-628.

124. **Welkos, S., M. L. Pitt, M. Martinez, A. Friedlander, P. Vogel, and R. Tammariello.** 2002. Determination of the virulence of the pigmentation-deficient and pigmentation$^-$/plasminogen activator$^-$ deficient strains of *Yersinia pestis* in

non-human primate and mouse models of pneumonic plague. Vaccine **20:**2206-2214.

125. **Yang, R. F., and B. Li.** 2008. Interaction between *Yersinia pestis* and the host immune system. Infect Immun **76:**1804-1811.

126. **Ye, Z., E. J. Kerschen, D. A. Cohen, A. M. Kaplan, N. van Rooijen, and S. C. Straley.** 2009. $Gr1^+$ cells control growth of YopM-negative *Yersinia pestis* during systemic plague. Infect Immun **77:**3791-3806.

127. **Zav'yalov, V. P., V. M. Abramov, P. G. Cherepanov, G. V. Spirina, T. V. Chernovskaya, A. M. Vasiliev, and G. A. Zav'yalova.** 1996. pH6 antigen (PsaA protein) of *Yersinia pestis*, a novel bacterial Fc-receptor. FEMS Immunol Med Microbiol **14:**53-57.

128. **Zharinova, N. V., G. D. Briukhanova, O. V. Maletskaia, N. S. Tsareva, and T. M. Luneva.** 2008. [Relations of the causative agents of plague and listeriosis during their simultaneous stay in the flea *Citellophilus tesquorum at* different environmental temperatures]. Med Parazitol (Mosk) **1:**41-43.

129. **Zhou, D., Y. Han, Y. Song, P. Huang, and R. Yang.** 2004. Comparative and evolutionary genomics of *Yersinia pestis*. Microbes Infect **6:**1226-1234.

130. **Zhou, D. S., Z. Z. Tong, Y. J. Song, Y. P. Han, D. C. Pei, X. Pang, J. H. Zhai, M. Li, B. Z. Cui, Z. Z. Qi, L. X. Jin, R. X. Dai, Z. M. Du, J. Wang, Z. B. Guo, J. Wang, P. T. Huang, and R. F. Yang.** 2004. Genetics of metabolic variations between *Yersinia pestis* biovars and the proposal of a new biovar, microtus. J Bacteriol **186:**5147-5152.

Table 1. *Y. pestis* biovars and strains, and their genomic properties

Biovars	Historical perspective	Strains	*pgm* locus[†]	Plasmids				Reference
				pCD	pPCP	pMT	pCRY[*]	
Antiqua	Justinian plague	Angola	+	+	+	+[¥]	-	(34)
		Antiqua	+	+	+	+	-	(23)
		Nepal516	+	+	+	+	-	(23)
		Z176003	+	+	+	+	-	(104)
		Pestoides F[§]	+	+	-	+[Ψ]	-	(41)
Mediaevalis	Black Death	KIM5	-	+	+	+	-	(126)
		KIM5+	+	+	+	+	-	(81)
		KIM6	-	-	+	+	-	(14)
		KIM6+	+	-	+	+	-	(45)
		KIM10	-	-	-	+	-	(14)
		KIM10+	+	-	-	+	-	(45)
Orientalis	Modern plague	CO92	+	+	+	+	-	(80)
Microtus	-	91001[#]	+	+	+	+	+	(108)

[†], pigmentation locus; *, cryptic plasmid; [¥], integrated pMT-pPCP plasmid; [Ψ], larger pMT plasmid (137kbp); [§], pathogenic to humans through aerosolized route of infection; [#], non pathogenic to humans.

CHAPTER III

YERSINIA PESTIS FILAMENTOUS MORPHOLOGY DURING INTRACELLULAR PARASITISM OF MACROPHAGES FROM HOSTS WITH HIGH AND LOW SUSCEPTIBILITY

Abstract

Yersinia pestis, the etiological agent of plague, causes severe disease in natural rodent hosts but mild to inapparent disease in certain rodent predators such as dogs. *Y. pestis* initiates infection in susceptible hosts by accessing subcutaneous tissue in which it parasitizes and multiplies intracellularly in macrophages during the early stage of infection. Therefore, it was hypothesized that *Y. pestis* infection severity may be related to the extent to which the bacterium overcomes the initial host macrophage associated stress. To test this hypothesis, *Y. pestis* infection progress was observed in mouse splenic and dog peripheral blood derived macrophages, and various parameters associated with this infection were measured in mouse and dog macrophage-like tissue culture cells RAW264.7 and DH82, respectively. In all macrophages, at 2.5 h post infection (p.i.), a fraction of intracellular *Y. pestis* assumed filamentous morphology with filaments containing multiple genomes per colony forming unit (CFU). On progress of the infection, filamentous *Y. pestis* transitioned back to coccobacilli in mouse splenic and RAW264.7 macrophages. This change in *Y. pestis* morphology was associated with spacious extension of the *Yersinia* containing vacuole (YCV) in mouse splenic and RAW264.7 macrophages, and a more rapid increase of CFUs than the respective genomic equivalences (GEs) and of lysis of RAW264.7 cells. In dog peripheral blood macrophages, filamentous *Y. pestis* became coccobacilli at 7.5 h p.i., similar to what was observed in mouse macrophage infections. However, in dog macrophages these coccobacilli were in tight YCV and were killed by 27.5 h p.i. In DH82 cells, filamentous *Y. pestis* were present throughout the infection without noticeable structural change in YCV or significant host cell death. This observation was supported by a static GE to CFU

ratio of ≈ 4 in DH82 cell from 2.5 to 27.5 h p.i. Overall, these results support the hypothesis that *Y. pestis* in mouse or other similar highly susceptible host macrophages survive and replicate, which may aid in the development of severe systemic infection. However, in dog or other low susceptible hosts, macrophages appear to restrict the growth of *Y. pestis* at the intracellular parasitism phase, resulting in mild to inapparent disease.

Introduction

The Gram-negative bacterium *Yersinia pestis,* the etiological agent of plague, causes severe disease in natural rodents hosts such as mice, ground squirrels and prairie dogs, but mild to inapparent disease in some rodent predators such as domestic dogs and coyotes (1, 10, 25, 34). *Y. pestis* is maintained in rodent populations in the endemic areas as a flea transmitted disease (1, 34). Rodent predators acquire the infection by either ingestion of infected rodents or via bite of *Y. pestis* infected rodent fleas (5, 18, 33, 48). The mechanism underlying the difference in susceptibility of rodents and canines to infection by *Y. pestis* is not understood.

The high lethality of *Y. pestis* infection in rodents is demonstrated by the periodic extinction of local rodent populations during seasonal epizootics as well as by high mortality rates in experimental infection studies in rodents. In brown Norway rats, intradermal inoculation of 5×10^2 CFU per animal, to mimic the natural flea bite transmission, caused 100% mortality within 3 to 15 days depending on the site of inoculation (50). Shortly after the intradermal injection, reddish papular eruptions occur

at the site, followed by enlargement of the local lymph nodes, septicemia and death of infected animals (50). Similar disease progression and mortality was observed for infection by parenteral inoculation or infected flea bites in mouse models, with infected animals succumbing to the disease within 2 to 8 days post-infection depending on the inoculation dose (51, 52). Following the bite of an infected flea or experimental injection, subcutaneous *Y. pestis* are phagocytized by tissue neutrophils and macrophages (26, 29, 34). *Y. pestis* are readily killed by neutrophils, but this initial neutrophilic restriction of *Y. pestis* is only effective for the first few hours post-infection; thereafter, expression of anti-phagocytic factor F1-antigen reduces this process (11, 34, 53). In contrast to killing by neutrophils, *Y. pestis* survives inside rodent macrophages during the early stage of infection (34). Phagosomes containing *Y. pestis* mature from early endosomes to phagolysosomes, but the bacteria are able to survive and multiply, thereby allowing dissemination while evading host innate immunity (6, 19, 39-41, 55, 56). While residing in phagolysosomes, *Y. pestis* expresses various stress response and virulence genes such as type-III secretion system, and F1- and pH6-antigens; and modifies the phagolysosomes into spacious vacuoles to adapt for progression of the infection by systemic dissemination (15, 27, 28, 36). Depletion of macrophages in mice by treatment with clodronate-liposomes diminished the severity of infection by *Y. pestis* as indicated by a marked reduction in lesions in spleens and livers of inoculated animals (62). Overall, infection studies support the role of *Y. pestis* infection of host macrophages in establishing local infection and systemic dissemination of infection following introduction of *Y. pestis* into the host through flea bites (53).

In contrast to flea transmission in natural rodent hosts, rodent predators acquire *Y. pestis* primarily by ingestion of infected rodents (33, 48). Some rodent predators such as ferrets and cats are highly susceptible to infection by *Y. pestis*, developing lymphadenopathy of the lymph nodes of the head or neck and subsequent systemic dissemination similar to the disease progression observed in rodents (16). In experimental infection studies in which cats ingested infected rodents, 80 to 100% of exposed cats developed clinical illness with 38 to 42% mortality (12, 16). Although domestic cats and dogs in endemic regions likely have similar rates of exposure to *Y. pestis* infected rodents, there are many more case reports in the literature of clinical disease in cats than in dogs, suggesting that the latter are less susceptible (12, 16, 42, 60). In one of the few case reports of plague in dogs, the clinical signs of mild fever, malaise, stomatitis, and transient submandibular lymph node swelling were observed (33). Unlike experimentally infected cats, dogs infected experimentally with *Y. pestis* through either oral or subcutaneous route exhibited only mild clinical signs of short duration with no mortality (46). The mechanism by which some species are less susceptible to infection by *Y. pestis* than others may be related to how well *Y. pestis* overcomes stress associated with intracellular parasitism of host macrophages. Although natural rodent hosts and canid rodent predators are infected via different routes, it appears likely that *Y. pestis* utilizes the same mechanism of evasion of the host innate immunity by intracellular parasitism of host macrophages and subsequent systemic dissemination in hosts with both high and low susceptibility.

During *Y. pestis* infection, macrophages can employ a wide spectrum of antimicrobial defenses including phagolysosomal acidification; enzymatic actions from

cathepsins, lipase, nuclease and glycosidase; reactions of oxidizing agents and reactive oxygen species; and effects of cationic peptides, nitric oxide and reactive intermediates of nitric oxide. Further, by the action of natural resistance-associated macrophage protein (NRAMP), many phagolysosomal metal ions such as iron, calcium, magnesium and manganese are sequestered, making the organelle very hostile for the intracellular *Y. pestis* (13, 58). In order to adapt to this harsh intracellular environment, *Y. pestis* relies on various general stress regulators, mechanisms helping *Y. pestis* to reduce the phagolysosomal nitric oxide level, and various ion utilization systems (19, 35, 38, 41).

Based on these observations, we hypothesized that differences in host susceptibility to *Y. pestis* infection between highly susceptible rodents and less susceptible dogs may be related to whether *Y. pestis* is able to overcome macrophage imposed stress during the intracellular parasitism phase of infection. In agreement with our hypothesis, *Y. pestis* in mouse macrophages showed intracellular survival for the experimental period of 27.5h, and the intracellular *Y. pestis* mediated morphological changes and cell lysis of the infected macrophages. However, in dog macrophages, intracellular *Y. pestis* was either killed by or at least restricted from inflicting damages to the macrophages.

Materials and methods

Bacterial strains and culture conditions

Y. pestis strain KIM62053.1+ *hms*$^{+}$ *psn*$^{+}$ *psa*$^{-}$ (Δ*psa*2053.1) *Ybt*$^{+}$ *Lcr*$^{-}$ derived from KIM62053.1 (2) provided by Dr. Robert Perry, University of Kentucky was used in all experiments except where noted. For fluorescent imaging experiments, KIM62053.1+ was transformed with a modified green fluorescent protein expression plasmid (pGFPuv, Clontech, Mountain View, CA, USA) by electroporation as described elsewhere (9, 61). Isolated colonies on Brain Heart Infusion (BHI) (Difco, Becton Dickinson Company, Franklin Lakes, NJ, USA) agar plates grown for 36 h at 26^{o}C were inoculated into BHI broth (Difco) and cultured overnight at 26^{o}C with 160 rpm shaking.

Isolation of mouse splenic macrophages

Splenic macrophages were used as an appropriate alternate to blood macrophages due to the difficulty of collecting a sufficient volume of blood to isolate a sufficient minimum number of macrophages. Splenic macrophages were isolated from 7 to 11 week old, female C57BL/6J mice (The Jackson Laboratory, Maine, USA). Briefly, spleens from mice euthanized with 70% CO_2 were collected sterilely in 10-15 mL of Dulbecco's Modified Eagle's Medium (DMEM) (Invitrogen, USA) supplemented with 20% fetal bovine serum (FBS) (Hyclone laboratories) and 50 µg/mL of gentamicin sulfate (Sigma-Aldrich), and therein the same media, spleens were thoroughly minced using a sterile scalpel blade. The resulting cell suspension was passed successively through sterile nylon mesh of 160, 75, 15 µm sizes to get a cell debris free homogenous cell suspension, and

thereafter, the cell concentration was adjusted to 2 x 10^6 viable cells/mL in the same media. Finally, each 6 mL of this cell suspension was cultured overnight in a 25 cm^2, poly-D-lysine coated tissue culture flask (Becton Dickinson labware, MA, USA) at 37^oC with 5% CO_2, followed by single removal of non-adherent cells by washing with sterile PBS. The attached cells were further cultured for 3 days in a fresh batch of the same DMEM media. Subsequently, the cell layers were changed into RPMI-1640 media (Sigma-Aldrich, USA) supplemented with 20% FBS, 2 g/L sodium bicarbonate and no antibiotic for 2 days prior to use.

Isolation of mouse bone marrow derived macrophages

Adherent macrophages of bone marrow origin were isolated from femurs and tibias of 7 to 11 week old, female C57BL/6J mice (The Jackson Laboratory, Maine 04609, USA). Briefly, femurs and tibias from mice euthanized with 70% CO_2 were collected sterilely by blunt dissection, both ends of each bone removed, and the bone marrow cavity flushed into DMEM (Invitrogen) supplemented with 20% fetal bovine serum (FBS) (Hyclone laboratories) and 50 µg/mL of gentamicin sulfate (Sigma-Aldrich) with 3-5 mL of the same media per bone using 10 cc syringe and 23 gauge (0.6 x 19.0 mm) needles. The resulting cells were washed thrice with 30-50 mL of sterile PBS containing 50 µg/mL of gentamicin and collected by centrifugation at 250xg for 10 min at room temperature, and the cell concentration was adjusted to 2x10^6 viable cells/mL in DMEM with 20% FBS and 50 µg/mL gentamicin. Finally, each 6 mL of this cell suspension was cultured in a 25 cm^2, poly-D-lysine coated tissue culture flask (Becton Dickinson labware, MA, USA) at 37^oC with 5% CO_2 for 3 days. Afterwards, the cell

layers were changed into RPMI-1640 media (Sigma-Aldrich) supplemented with 20% FBS, 2 g/L sodium bicarbonate and no antibiotic for 2 days.

Isolation of dog peripheral blood derived macrophages

Blood was collected from healthy adult dogs via venipuncture and anticoagulated with 10% sodium citrate (Sigma-Aldrich). Anticoagulant peripheral blood was diluted 2-fold with PBS containing 50 µg/mL gentamicin, and the diluted blood was gently overlaid on sterile Histopaque®-1083 (Sigma-Aldrich) at the ratio of 2:1 and centrifuged at 800xg for 15 min at room temperature. From the multilayer separation, buffycoat was collected by aspiration and washed thrice with sterile PBS containing 50 µg/mL gentamicin and collected each time by centrifugation at 250xg for 10 min at room temperature. The resulting cell pellet was resuspended in DMEM with 20% FBS and 50 µg/mL gentamicin at the rate of 2 X 10^6 viable cells/mL, and then 6 mL/25 cm^2 poly-D-lysine coated flask was cultured overnight at 37^{o}C with 5% CO_2 tension, followed by washing out the non-adherent cells once with sterile PBS. The cell layers were further cultured for 3 days in fresh batch of the same Dulbecco's media. Subsequently, gentamicin was removed and the cells were kept in RPMI-1640 media with 20% FBS with no antibiotic for another 2 days prior to use.

Tissue culture cells and growth conditions

Mouse macrophage cell line RAW264.7 was provided by Dr. Guolong Zhang, Department of Animal Science, Oklahoma State University, and dog macrophage cell line DH82 was provided by Dr. Susan E. Little, Department of Veterinary Pathobiology,

Oklahoma State University. Both cell lines were cultured at 37^{o}C with 5% CO_2 tension in RPMI-1640 media with 10% FBS.

Infection of primary macrophage isolates

For infection of primary macrophage isolates, *Y. pestis* strain KIM6-2053.1+ was grown in BHI broth at 26°C as described above, and the inocula quantified by OD_{600nm} as compared with a standard curve for CFU/OD_{600nm}. At the time of infection, 6 mL of an inocula of 4.0-8.3 X 10^6 *Y. pestis* in RPMI-1640 with 10% FBS media was added to each 25 cm^2 flask containing 0.81-1.7 X 10^6 macrophages, yielding a multiplicity of infection of 5:1. To initiate the infection, the flasks were centrifuged at 800×g for 3 min to enhance macrophage-bacteria contact and then incubated at 37^{o}C under 5% CO_2 concentration for 30 min. Subsequently, adherent macrophages were washed gently thrice with 6 to 7 mL of sterile PBS and treated with 6 mL of RPMI-1640 with 10% FBS media containing 50 µg/mL gentamicin for 2 h under the same incubation conditions to kill extracellular bacteria. At the end of gentamicin exposure, macrophages were once again washed gently thrice with 6 to 7 mL of PBS and then 6 mL of antibiotic-free RPMI-1640 with 10% FBS media were added. From the resulting infection, samples were collected for light and transmission electron microscopic studies at various post-infection intervals. At 2.5 h post infection (p.i.), samples were collected following removal of the gentamicin media and PBS washes by treating with 0.05% trypsin-EDTA (Mediatech Inc., Manassas, VA 20109, USA) at 37^{o}C for 1 to 3 min; however, at 7.5 and 27.5 h p.i., 2 h prior to sampling, the infected adherent macrophages were treated with RPMI-1640 with 10% FBS media and 50 µg/mL of gentamicin for 2 h to kill any extracellular *Y. pestis*.

Infection of tissue culture cells

To prepare tissue culture cells for infection, RAW264.7 and DH82 cell monolayers grown in 75 cm^2 tissue culture flasks were released into the fresh RPMI-1640 with 10% FBS media using cell scraper (BD Falcon, Biosciences discovery labware, Bedfor, MA01730, USA) and number of cells per unit volume were counted by using hemocytometer. Prior to use in assays, tissue culture cell viability was assessed by trypan blue exclusion assay with >95% viability required for subsequent use. Infection of RAW264.7 and DH82 macrophage cell lines with *Y. pestis* KIM6+ were carried out in 96-well flat-bottom plates (FALCON flat bottom polystyrene plate, Becton Dickinson Company, NJ, USA). Prior to infection, 100 µL of cell suspensions containing $1x10^6$ RAW264.7 viable cells/mL of RPMI-1640 with 10% FBS were sub-cultured in wells A1 to A3 of the top row of 96-well flat-bottom tissue culture plates and in the same way DH82 cells were sub-cultured in wells A7 to A9. These plates were incubated at 37^oC with 5% CO_2 concentration for 12 to 16 h. For infection, 100 µL of RPMI-1640 with 10% FBS media containing $5×10^6$ *Y. pestis* KIM6+ cultured overnight at 26^oC was added to each well of A1-3 and A7-9 of all plates yielding a MOI of 5:1. The resulting infection was carried out at 37^oC with 5% CO_2 for 30 min and then treated with 50 µg/mL gentamicin for 2 h as above mentioned for primary macrophage infections. At 0 h p.i., replica of inocula and tissue culture cells with which the infection had started were taken as such for analysis. For 0.5 and 2.5 h p.i., samples were obtained immediately before adding gentamicin and antibiotic-free media, respectively. At 1.25 and 2.0 h p.i., samples were obtained after removal of the gentamicin media and washing thrice with PBS. Prior to 5.0, 7.5, 12.5, 18.5 and 27.5 h p.i. sampling, the tissue layers were treated for a second

time with RPMI-1640 with 10% FBS media contained 50 µg/mL of gentamicin for 2 h as mentioned above.

Determination of colony forming units

CFUs were determined using a novel high-throughput assay developed by Nizet and colleagues in which infected tissue culture cells in 96-well plates are lyzed, serial dilution, and microcolonies of intracellular bacteria are grown in soft agar in the 96-well plates and counted to determine the CFUs (31, 61). At the time of sampling, media from wells was aspirated, adherent tissue culture cells washed gently thrice with 100 µL of PBS, and the final wash transferred laterally to wells in the A row of the plate. Following washing and transfer of the final wash, 100 µL of 0.1% Triton X-100 in sterile PBS was added to wells A1-3 and A7-9, and the plates were incubated for 10 min at 37^{o}C with 160 rpm on an oscillating shaker to allow lysis and release of intracellular *Y. pestis* into the media. Eighty µL of PBS were added to wells B1 to H12, and the cell lysates and wash solutions in row A were serially diluted 5-fold in PBS by transferring 20 µL from each row to the next from row A to row H. Subsequently, 80 µL of bacterial suspension left in each well of 96-well plate was overlaid gently with 120 µL of 0.83% Bacto-agar (Becton Dickinson and company, MD, USA) maintained at 45 to 48^{o}C. Finally, the plates were incubated at 26^{o}C for 16 to 24 h, and the resulting micro-colonies were counted using an inverted light microscope. Before adopting this micro-plate based colony counting, accuracy of the method was compared with conventional CFU determinations using a 10 cm agar plate method, which is described in detail by Wendte *et. al*., 2011 (61).

Determination of genomic equivalences

To determine the total number of *Y. pestis* comprised of culturable, viable but non-culturable, and dead bacteria in samples at various post-infection time points, GEs were determined using PCR. A 90 bp fragment from the single copy *Y. pestis* specific '*fur*' gene was amplified using forward primer 5'-TCT GGA AGT GTT GCA AAA TCC TG-3' and reverse primer, 5'- AAG CCA ATC TCT TCA CCA ATA TCG-3'. PCR reactions were carried out with 300 nM of each primer at 20 µL volume using the Fast SYBR green master mix (Applied Biosystems) according to the manufacture's instruction (initial enzyme activation at 95^{o}C for 20 sec, followed by 40 cycles of denaturation at 95^{o}C for 3 sec and annealing/extension at 60^{o}C for 30 sec). Standard curves of threshold cycle (ct) values versus bacterial number were prepared by spiking known CFUs of *Y. pestis* strain KIM6+ into samples containing 1x10^{6} RAW264.7 or DH82 cells/mL. The assay was initiated immediately after adding the bacteria into the cell suspension by first heat bursting at 95^{o}C for 10 min, and after centrifugation at 1,000×g for 1 min, 2 µL of supernatant was used to determine the ct-value using a 7500 Fast Real-Time PCR system (Applied Biosystems). For samples containing infected macrophages, the assay was initiated by heat burst, and the resulting samples were assayed as described above.

Determination of infected macrophage counts

To determine the number of macrophages at a particular infection interval, counts of macrophages were conducted. At each sampling period, infected RAW264.7 and DH82 cells in wells of replica plates were released by gentle pipetting and dilution in

0.4% trypan blue-PBS dye. Using a hemocytometer and microscope, the number of viable and non-viable macrophages was determined.

Determination of the percent infectivity

At each infection interval, samples of *Y. pestis* infected RAW264.7 and DH82 cells were cytospun (Statspin Cytofuge, Norwood, MA02062, USA) onto glass microscope slides at low speed for 5 min and stained with Wright Giemsa stain. Using a light microscope at 1,000x magnification, approximately 400 macrophages per sample were examined to count the number of macrophages which had at least one detectable intracellular bacterium, and from these values, the percent infectivity was calculated.

Calculation of CFUs and GEs per macrophage

At each infection interval, number of CFUs and GEs per macrophage was calculated from the CFUs, GEs and macrophage number per mL and percent infectivity of the corresponding interval using the formulas:

$$\text{CFUs per macrophage} = \left[\frac{\text{CFUs/mL}}{\text{Total macrophages/mL}}\right] \times \text{percent infectivity as a fraction}$$

$$\text{GEs per macrophage} = \left[\frac{\text{GEs/mL}}{\text{Total macrophages/mL}}\right] \times \text{percent infectivity as a fraction}$$

Here, total macrophages/mL represents the sum of trypan blue positive and negative cells per mL at each infection interval.

Macrophage cytotoxicity assay

Replica samples of RAW264.7 and DH82 cells infected with *Y. pestis* were used for the cytotoxicity assay. At each infection interval, the activity of the eukaryotic cytoplasmic enzyme lactate dehydrogenase (LDH) in the extracellular media was measured as an indicator of macrophage cell lysis. The LDH activity was measured using the CytoTox-ONE^{TM} Homogenous Membrane Integrity Assay kit (Promega) in a POLAR star OPTIMA (BMG labtechnologies Inc.) at excitation and emission of 560 and 590 nm, respectively. From these values, percent cytotoxicity was calculated using the formula:

$$\% \text{ Cytotoxicity} = \left[\frac{\text{(LDH release from infected cells - release from uninfected cells)}}{\text{(LDH release from positive control - release from uninfected cells)}}\right] \times 100$$

Positive control release is the maximum LDH release from uninfected macrophages induced by cell lysis with 0.1% Triton X-100.

Infection of tissue culture macrophages in antibiotic free condition

In our standard infection protocol, co-occurrence of filamentous *Y. pestis* intracellularly and the presence of gentamicin in the extracellular media as part of the infection procedure raised concern that gentamicin may play a role in this filamentation process. To assess this concern, RAW264.7 and DH82 cells were infected in the same manner as the standard protocol for 30 min at 37^{o}C, however, in place of gentamicin containing RPMI with 10% FBS media, Hank's balanced salt solution (HBSS) with 10% FBS was used for the remaining period of the experiment. From the infection, samples for light microscopic studies were conducted at 2.5 and 5 h p.i.

Microscopic studies

Morphological features of intracellular *Y. pestis* and of infected macrophages were examined using microscopy.

(i) Fluorescent microscopy

RAW264.7 and DH82 cells infected with *Y. pestis* strain KIM6+ GFPuv as described above were sampled between 3 to 4 h p.i. At the time of sampling, infected macrophages from 96-well tissue culture plates were directly released by using pipetting force into PBS supplemented with 10% FBS. From the suspension, a thin layer of wet films were prepared between microscopic glass slide and cover slip, and the wet mount preparations were observed directly under fluorescent microscope (Eclipse 80i, Nikon Instruments Inc., Melville, NY, U.S.A.) using a UV-filter.

(ii) Light microscopy

Y. pestis infected macrophage cell lines, RAW264.7 and DH82, and primary macrophage isolates from mouse spleen and bone marrow and dog peripheral blood were spun onto microscopic slides at slow speed for 5 min using a cytocentrifuge (Statspin Cytofuge, Norwood, MA, USA), and the slides stained with Wright Giemsa stain. The stained slides were examined at 1,000x magnification using light microscopy.

(iii) Transmission electron microscopy (TEM)

Primary macrophage isolates from mouse spleen and dog peripheral blood and tissue culture cell lines RAW264.7 and DH82 were infected as described above and sampled at 2.5, 7.5 and 27.5 h p.i. During sampling, infected primary macrophage isolates were released into RPMI-1640 with 10% FBS media at the intended sampling intervals by using trypsin as explained elsewhere, then collected at 250xg for 10 min, and

finally fixed with 2.5% (Vol/Vol) glutaraldehyde in PBS for 1 h at room temperature. After fixing, the cells were changed into PBS as noted above and kept at 4^{o}C until processing. In case of tissue culture macrophages, infected cells in 25 cm^{2} flasks were fixed therein for 15 min on ice with 2.5% (Vol/Vol) glutaraldehyde in PBS. Subsequently, the fixed cells were transferred using a CytoOne® cell scraper (USA Scientific Inc., Ocala, FL34478, USA) into the above noted glutaraldehyde solution to fix further for 45 min at room temperature. Thereafter, the fixed cells were collected by centrifuging at 250xg for 10 min at room temperature, suspended in PBS and maintained at 4^{o}C for further processing. For this processing, cells were postfixed with 1% osmium tetroxide (Polysciences Inc., Warrington, PA) in PBS for 1 h. Subsequently, cells washed thrice with PBS were en bloc stained with 1% aqueous uranyl acetate (Ted Pella Inc., Redding, CA) for 1 h, dehydrated in ascending grades of ethanol and then embedded in Eponate resin (Ted Pella Inc., Redding, CA). Ultra-thin sections of 90 nm were prepared using a Leica Ultracut UCT ultramicrotome (Leica Microsystems Inc., Bannock-burn, IL, USA) and stained with uranyl acetate and lead citrate (Sigma, St Louis, MO). Finally these sections were examined in a JEOL 1,200 EX transmission electron microscopy (JEOL USA Inc., Peabody, MA, USA).

Morphometric analysis of TEM images

Electron microscopic images were assessed using gimp® photo-editing software version 2.6. Based on 1 µm measure bar provided on the image, bacterial length was measured. The bacteria longer than 5 µm, double the size of maximum length of normal *Y. pestis* (0.5-08 x 1-2.5 µm), were considered to be filamentous *Y. pestis*. In addition,

intracellular *Y. pestis* with irregular morphology such as vacuoles or unevenly distributed electron dense aggregates on cross section were scored as dead bacteria. For infected macrophages, the percentage of cells which had spacious extension of YCV and normal nuclear and mitochondrial morphological features were quantified.

Statistical analysis

Wherever applicable, data were compared for statistical significance through student's t-test. The resulting analysis was reported as significant difference at p-value 0.01 or 0.05 for a given parameter. For the analysis, mean value of a particular parameter at a given p.i. from mouse splenic macrophage infection was statistically compared with the corresponding value from dog peripheral blood derived macrophage infection. Similarly, the analysis was carried out between RAW264.7 and DH2 cell infections.

Results

Intracellular parasitism of mouse and dog macrophages by *Y. pestis*

We hypothesized that differences in host susceptibility to *Y. pestis* infection between highly susceptible rodents and less susceptible dogs may be related to whether *Y. pestis* is able to overcome macrophage imposed stress during the intracellular parasitism phase of infection. To this end, morphological changes of *Y. pestis* in primary macrophages derived from mouse spleen and bone marrow and dog peripheral blood were monitored. These cells were infected with *Y. pestis* strain KIM6+, and macrophage

and bacterial morphology observed over a 27.5 h infection period by light and electron microscopy. *Y. pestis* infections of mouse macrophages have been previously reported, but infections of dog macrophages have not. As has been previously reported for mouse macrophages (4), intracellular *Y. pestis* in splenic macrophages appeared primarily as coccobacilli in tight YCV at 2.5 h p.i. (Fig. 1). In addition, some of the intracellular *Y. pestis* were filamentous in structure, having partial or no visible septation along the bacterial length under light microscope. Morphology at 7.5 h p.i. was similar, but many macrophages exhibited spacious YCVs. At 27.5 h p.i., many of the splenic macrophages appeared larger with foamy cytoplasm, and *Y. pestis* had bipolar rod appearance. In agreement with the light microscopic observations, morphometric analysis on TEM images showed the similar sequence of morphological changes in both intracellular *Y. pestis* and splenic macrophages (Fig. 2) (Table 1A). At 2.5 h p.i., on an average 11% of the intracellular *Y. pestis* per macrophage was filamentous in shape with a mean length of 6.8 µm. The number of filamentous *Y. pestis* quantified by transmission electron microscopy may under estimate the actual number because only those filamentous bacteria in a longitudinal axis can be observed in the planar sections. These intracellular bacteria were morphologically intact and contained within tight YCV. At 7.5 h p.i., no filamentous *Y. pestis* were observed, but the number of intact coccobacilli per macrophage increased noticeably. This increase was also accompanied with spacious extension of YCV in 82% of the infected macrophages. At 27.5 h p.i., few splenic macrophages were observed, suggesting that macrophages lost viability between 7.5 and 27.5 h p.i. Those remaining macrophages had only low number of intact coccobacilli in tight YCVs. Overall, microscopic examinations of mouse splenic macrophages infected

with *Y. pestis* indicates that the bacteria in the macrophages assume filamentous morphology at the initial stage of infection as an adaptation to the stressful intracellular environment. Subsequently by extending YCVs into spacious compartments at 7.5 h p.i., intracellular *Y. pestis* return to normal coccobacillary shape, continue intracellular multiplication and may have been released from non-viable macrophages at 27.5 h p.i..

In contrast to *Y. pestis* infection of splenic macrophages, *Y. pestis* in mouse bone marrow macrophages did not exhibit stress morphology. Throughout 27.5 h of infection, morphological features of intracellular *Y. pestis* did not change appreciably, maintaining bipolar coccobacillary morphology (Fig. 3). In addition, bone marrow macrophages exhibited no obvious extension of YCV. These observations are compatible with the naïve bone marrow macrophages being less efficient in exerting antibacterial defense against *Y. pestis*, resulting in no stress related structural changes in the intracellular bacteria (30, 57).

Intracellular *Y. pestis* in dog macrophages underwent a distinctive sequence of morphological alteration during 27.5 h of infection. Similar to mouse splenic macrophage infections, a fraction of the intracellular *Y. pestis* exhibited filamentous morphology, and *Y. pestis* were contained within tight YCVs (Fig. 1). At 7.5 h p.i., most intracellular *Y. pestis* exhibited coccobacillary morphology with only a few filamentous forms present. By 27.5 h p.i., intracellular *Y. pestis* appeared poorly stained by Wright Giemsa stain and granular with inconspicuous coccobacillary morphology, suggesting that these bacteria had been killed. In contrast to the marked changes in morphology of intracellular *Y. pestis*, changes in the morphological features of the dog macrophages were restricted to increased foamy cytoplasm at 7.5 and 27.5 h p.i. The TEM images from samples at 2.5

and 7.5 h p.i. mirrored the corresponding pictures of light microscopy (Fig. 2) (Table 1A). At 2.5 h p.i., a majority of the intracellular *Y. pestis* were intact, having evenly distributed electron dense materials on cross sections typical of normal bacterial morphology. At 7.5 h p.i., coccobacilli appeared to be enclosed in individual tight YCVs, but the number of intact coccobacilli per macrophage increased significantly from 2.5 h p.i., compatible with transition of filamentous *Y. pestis* to coccobacilli. At 27.5 h p.i., intracellular *Y. pestis* appeared to be housed in YCV with double membranes in 80% of the infected macrophages; however, most of these intracellular coccobacilli exhibited irregular morphology consisting of vacuolation and uneven distribution of electron dense aggregates on cross sections, compatible with killing of the bacteria by the dog macrophages. Particularly, these disfigured bacteria were either partially or completely digested by the macrophages to condensed electron dense remnants inside the expanded periplasmic space. These findings suggest that in dog peripheral blood macrophages, although intracellular *Y. pestis* exhibit similar stress morphology as in mouse splenic macrophages, *Y. pestis* in dog macrophages failed to extend YCV at 7.5 h p.i., possibly facilitating killing of *Y. pestis* by the macrophages.

Intracellular *Y. pestis* parasitism of mouse and dog macrophage-like cell lines

In order to better quantify and compare intracellular parasitism of *Y. pestis* in macrophages from hosts having different susceptibility to infection, CFUs and GEs per macrophage were measured and light and electron microscopic images obtained for *Y. pestis* infection of mouse and dog macrophage-like RAW264.7 and DH82 cell lines. Further, under light microscope a number of macrophages which had observable

intracellular *Y. pestis* were counted as percentage of infectivity. Throughout the infection, approximately 90 to 100% of RAW264.7 and 90 to 95% of DH82 cells had at least one detectable *Y. pestis* per macrophage (Fig. 4). During the initiation of infection from 0 to 2.5 h, *Y. pestis* CFUs per macrophage decreased, but GEs increased for both RAW264.7 and DH82 cells (Fig. 5). Both Wright Giemsa stained light and transmission electron microscopic images at 2.5 h p.i., showed numerous filamentous *Y. pestis* present (Figs. 6 and 7) (Table 1B), suggesting that the decrease in CFUs and accompanying increase in GEs reflected filamentous growth of *Y. pestis* in both macrophage-like cell lines. This filamentous change was also evidenced under UV-fluorescent microscope in *Y. pestis* strain KIM6+ GFPuv infection of RAW264.7 and DH82 cells at 3 to 4 h p.i. (Fig. 8). From 2.5 to 7.5 h p.i., in RAW264.7 cells, some filamentous intracellular *Y. pestis* reverted to coccobacilli, but still an average of 6.4% of intracellular *Y. pestis* per macrophage were filamentous (Table 1B). YCV in infected RAW264.7 cells had gradually increased into spacious compartments and at 7.5 h p.i., 64% of the total infected cells had moderate extension of YCV in electron micrographs (Table 1B, Fig. 7). Between 7.5 to 12.5 h p.i., the spacious extension of YCV induced by intracellular *Y. pestis* was very prominent; furthermore, this extension was accompanied with conversion of filamentous *Y. pestis* into coccobacilli. In agreement with these microscopic observations, CFUs per RAW264.7 cell increased at a rapid rate and finally equalled the corresponding GEs by 18.5 h p.i. (Fig. 5A).

In DH82 cells, light and transmission electron microscopic images showed presence of filamentous *Y. pestis* throughout the experiment (Figs. 6B and 7) (Table 1B). Supporting this observation, CFUs per DH82 cell also lagged significantly behind the

respective GEs for 27.5 h of infection (Fig. 5B). Furthermore, at 27.5 h p.i. in DH82 cells, 29% of intracellular *Y. pestis* showed loss of viable bacterial morphology in TEM images (Fig. 7). These results suggest that *Y. pestis* in RAW264.7 cells experienced and then likely overcame the macrophage stress. But in DH82 cells, *Y. pestis* likely failed to overcome the intracellular stress resulting in loss of viability as evidenced in TEM images at 27.5 h p.i. Further, the filamentous morphology of *Y. pestis* in RAW264.7 and DH82 cells is most likely an adaptive strategy for retaining viability in the intracellular environment. This change was not caused by gentamicin that was used to kill the extracellular bacteria as part of the experimental procedure explained in materials and methods. At 2.5 and 5.0 h p.i., RAW264.7 and DH82 cells infected and maintained in antibiotic free condition also had the filamentous *Y. pestis* similar to other experiments as noted above (Fig. 9).

Morphology and cytotoxicity of *Y. pestis* infected RAW264.7 and DH82 cells

At 2.5 h p.i., *Y. pestis* inside the macrophages appeared to be contained in tight YCVs (Figs. 6 and 7) for both RAW264.7 and DH82 cells, but by 7.5 h p.i., YCV were spacious containing multiple bacteria for RAW264.7 cells, but YCV in DH82 cells appeared unchanged morphologically from the 2.5 h p.i. time interval. In RAW264.7 cells, this spacious extension of YCV was very prominent at 12.5 h p.i. and persisted throughout the remaining period of the experiment. At later p.i. times, the number of RAW264.7 cells decreased suggesting infection associated macrophage death; whereas, DH82 cell numbers declined only slightly (Fig. 10).

As previously reported in mouse J774A.1 macrophage-like cell lines (54), *Y. pestis* infection is associated with loss of macrophage viability. Using the trypan blue dye exclusion method with RAW264.7 cells revealed approximately 50% loss of cell viability, but only approximately 20% loss of cell viability in *Y. pestis* infected DH82 cells (Fig. 10A). To further characterize this cell death, lactate dehydrogenase leakage was determined. As shown in Figure 11, RAW264.7 cells infected with *Y. pestis* experience rapid cell lysis as indicated by specific LDH leakage during the initial 2.5 h p.i. period, and then slower, steady lysis through 27.5 h p.i. resulting in 45% lysis of infected cells as compared with uninfected control RAW264.7 cells exhibiting 0% cell lysis. In contrast, *Y. pestis* infection of DH82 cells exhibited cell lysis of approximately 10% for the entire infection period, which was not statistically significantly higher than was that of uninfected control groups. These results show that *Y. pestis* infection of RAW264.7 cells causes cell lysis, which may release *Y. pestis* to the extracellular space in infected animals potentially initiating septicemic plague.

Discussion

Although *Y. pestis* infects various animal species, infection severity differs from species to species. Rodents are the natural hosts and suffer severe disease with high mortality, but some rodent predators such as dogs and coyotes experience only mild or inapparent disease (1, 10, 25, 34, 46, 47, 59). This variation in infection severity among susceptible hosts may be related to the extent to which *Y. pestis* overcomes the initial host macrophage mediated stress. The host macrophages are the primary cells used by *Y.*

pestis entering through peripheral route of infection to evade the host immune mechanism and to multiply intracellularly during the early stage of infection (6, 19, 29, 34, 39-41, 53, 56, 62). The goal of our experimental study was to better understand *Y. pestis* responses to macrophages from mice and dogs, as high and low susceptible hosts, respectively. We hypothesized that *Y. pestis* in macrophages of highly susceptible hosts likely overcomes the intracellular antimicrobial stresses and multiplies intracellularly. Whereas, in macrophages of low susceptible hosts, *Y. pestis* fails to overcome the intracellular defense mechanisms and are eventually killed by the macrophages.

In this experimental study, we found that a fraction of intracellular *Y. pestis* in host macrophages assumes filamentous morphology with multiple copies of genome per bacterium likely induced as a result of macrophage associated stress. This filamentation of *Y. pestis* was frequently noticed during the early stage of infection in both primary and tissue culture macrophages (Figs. 1, 2, 6 and 7). Similar filamentous stress response have been observed for uropathogenic *E. coli* in mouse urinary bladder epithelial cells, *Legionella* spp. in Vero cell line, *Mycobacterium tuberculosis* in human macrophage cell line THP-1, and *Salmonella enterica* serovar Typhimurium in mouse bone marrow and RAW264.7 macrophages (7, 21, 24, 32, 44, 45). The antibiotic gentamicin used in our infection protocol is also known to induce filamentous changes in exposed bacteria (17). However, in our study, when gentamicin was omitted from the infection protocol, filamentous *Y. pestis* were still observed supporting intracellular stress as the cause rather than gentamicin (Fig. 9).

Y. pestis filamentation response in macrophages may be an adaptive strategy to cope with intracellular antibacterial defense mechanisms in addition to stress relievers

such as general stress regulation and inhibition of acidification of YCV (4, 19, 38). Evidently, for *Salmonella typhimurium* filamentous changes in primary mouse bone marrow macrophages or in RAW264.7 cell line are associated with exposure to NADPH oxidase, reactive oxygen species, nitric oxide or proteases associated with phagosome, and further, this structural change is positively influenced by IFN-gamma priming of macrophages or presence of cationic antimicrobial peptides during the infection (44, 45, 49). In support of filamentation as a specific adaptive change induced by intracellular stress, *Y. pestis* in naïve bone marrow macrophages, which are considered to be less efficient in their antimicrobial defense mechanisms (30, 57), did not change into filamentous shape during 27.5 h of infection (Fig. 3). In addition, *Y. pestis* SOS response to DNA damage occurring intracellularly is also known to cause the bacterium to undergo filamentous shape by interfering with cell division process as observed in other bacteria (3, 7, 43). Presumably, filamentation by *Y. pestis* is an adaptive strategy to survive the hostile intracellular environment; this structural alteration prevents the passing of damaged genomic copies to the daughter cells, by extending the time frame for DNA repair (22, 23).

In addition to antimicrobial intracellular stressors, insufficiency of essential nutrients in the macrophage phagolysosomal environment may also trigger the filamentation process in *Y. pestis*; particularly, low calcium in YCV may favor the filamentation of *Y. pestis* in macrophages (20, 37, 63). Further research will need to be done on this area to better understand the molecular-bridging machinery connects the external stimuli to the bacterial cell division process. Although filamentous stress response has been reported for other bacteria, filamentation of *Y. pestis* in macrophages is

new to this field of study; furthermore, we conclude that *Y. pestis* filamentous response to intracellular parasitism employs same type of molecular mechanism in mouse and dog macrophages.

The filamentous morphology of *Y. pestis* reverted to coccobacillary form both in mouse splenic and tissue culture macrophages at later stages of infection (Figs.1, 2, 6A and 7). However, the progression of *Y. pestis* morphologic change occurred more rapidly in splenic macrophages than in tissue culture cells (Figs. 1 and 2). For splenic macrophages, by 7.5 h p.i., the majority of intracellular *Y. pestis* converted back to coccobacilli, which were loosely confined within the spacious YCV. Based on the scarcity of splenic macrophages in samples at 27.5 h p.i., it is believed that most of these infected macrophages may have been lysed, thereby releasing intracellular *Y. pestis*. Most splenic macrophages in these samples had *Y. pestis* with morphology similar to early infection suggesting that these macrophages may have been previously uninfected cells which were re-infected by the released *Y. pestis*. Whereas in case of RAW264.7 cells, increasing number of coccobacilli were noticed after 7.5 h p.i., as indicated between 7.5 to 18.5 h p.i. by increased CFUs with the same GEs (Figs. 5A, 6A and 7). This difference between mouse primary and tissue culture macrophage may be due to subtle difference in the gene repertoire for the bacterial defense mechanisms (30). In accordance with the microscopic observation, after 7.5 h p.i., CFUs per RAW264.7 cell increased at a rapid rate and equalled the corresponding GEs likely as the result of cell division of filaments having multiple copies of genome into many single GE copy coccobacilli (Fig. 5A). Reversion of *Y. pestis* from filaments to coccobacilli in mouse macrophages reflects release of bacteria from the intracellular stresses. The molecular machinery which

mediates the transition from filamentous *Y. pestis* to the normal coccobacillary morphology is largely unknown; nevertheless, products of *Y. pestis* genes y2313, y2315 and y2316 are believed to play a role in this process. These genes are expressed in mouse macrophage cell line J774A.1 at 4 h p.i, and mutational inactivation was associated with retention of filamentous intracellular *Y. pestis* for at least 24 h of infection (14).

In addition to conversion from filamentous to coccobacillary morphology as an indication of overcoming macrophage imposed stress, *Y. pestis* in mouse splenic and tissue culture macrophages also cause spacious vacuolar extension of YCV (Figs. 1, 2, 6A and 7). This vacuolar extension is consistent with previous report in J774A.1 macrophages infected with *Y. pestis* KIM6. After 8 h p.i., YCVs were actively extended by the intracellular *Y. pestis*, and this extension process was dependent on presence of intact copies of PhoP-PhoQ transcriptional regulator (19). However, the precise molecular mechanism governing this process is unknown. *Y. pestis* mediated extension of YCV would likely benefit the bacterium by dilution of phagolysosomal content thereby reducing their antimicrobial activity.

In contrast to these changes in mouse macrophages, *Y. pestis* in dog tissue culture macrophages retained filamentous shape throughout 27.5 h of infection, which also observed by CFUs and GEs per macrophage with 4-fold less CFUs per DH82 cell than the respective GEs for the entire period of infection (Figs. 5B, 6B and 7). This suggests that *Y. pestis* in DH82 cells may not efficiently overcome the intracellular stress, and consequently, the bacterium is susceptible to macrophage killing as evidenced by presence of disintegrating coccobacilli in YCV at 27.5 h p.i. (Fig. 7). In dog peripheral blood mononuclear cells, *Y. pestis* converted from filamentous forms to coccobacilli at

7.5 h p.i. but failed to modify YCV and remained in tight YCV, suggesting that intracellular *Y. pestis* are still controlled by macrophage defense mechanisms (Figs. 1 and 2). These coccobacilli eventually died within YCVs due to macrophage killing. This initial failure of intracellular parasitism phase by *Y. pestis* likely leads to less severe disease in dogs and certain other carnivores such as coyotes (34, 46, 47, 59).

Apart from the vacuolar extension of YCV, mouse and dog tissue culture macrophages markedly differed in the loss of viability from *Y. pestis* infection for the period of 27.5 h p.i. (Figs. 10 and 11). For the infection, RAW264.7 cells exhibited upto 45% cell lysis in contrast to approximately 10% for DH82 cells (Fig. 11). High percentage of LDH leakage in RAW264.7 cells may be associated with spacious extension of YCV leading to lysis of infected macrophages. Furthermore, this finding in RAW264.7 cells agrees with the prevailing speculation that cell lysis is the primary mean of *Y. pestis* release from the infected macrophages (40). In contrast, restriction of intracellular *Y. pestis* to retention of filamentous shape in tight, unmodified YCV for the entire infection may account for the failure of *Y. pestis* to induce lysis of DH82 cells. Similar observations have been made for filamentous *Burkholderia pseudomallei* in THP-1 cells (8).

In conclusion, our results clearly demonstrate that *Y. pestis* in host macrophages assume filamentous morphology during initial stage of exposure to intracellular stress likely as a structural adaptation used by the bacterium to prolong the survivability under harsh conditions. These filamentous *Y. pestis* in mouse macrophages eventually returned into regular coccobacillary form, which was associated with actively extending YCV into spacious compartment and also causing extensive macrophage cell lysis. However, in dog

macrophages, *Y. pestis* was either restricted to remain in filamentous structure for an extended period of time and then were killed by the macrophages or changed into coccobacilli but eventually killed by the macrophages due to failure to form spacious extension of YCV. Therefore, severity of infections and fatal outcomes thereof in rodents and other highly susceptible hosts may be the consequence of failure to restricting *Y. pestis* growth at the macrophage parasitism phase. In contrast, superior control of the progress of *Y. pestis* intracellular parasitism in dog macrophages is associated with mild disease.

References

1. **Anonymous.** 1999. Plague manual--epidemiology, distribution, surveillance and control. Wkly Epidemiol Rec **74:**447-481.
2. **Bearden, S. W., J. D. Fetherston, and R. D. Perry.** 1997. Genetic organization of the yersiniabactin biosynthetic region and construction of avirulence mutants in *Yersinia pestis*. Infect Immun **65:**1659-1668.
3. **Bi, E., and J. Lutkenhaus.** 1993. Cell division inhibitors SulA and MinCD prevent formation of the FtsZ ring. J Bacteriol **175:**1118-1125.
4. **Bliska, J. B., C. Pujol, K. A. Klein, G. A. Romanov, L. E. Palmer, C. Cirota, and Z. J. Zhao.** 2009. *Yersinia pestis* can reside in autophagosomes and avoid xenophagy in murine macrophages by preventing vacuole acidification. Infect Immun **77:**2251-2261.
5. **Boone, A., J. P. Kraft, and P. Stapp.** 2009. Scavenging by mammalian carnivores on prairie dog colonies: implications for the spread of plague. Vector Borne Zoonotic Dis **9:**185-190.
6. **Cavanaugh, D. C., and R. Randall.** 1959. The role of multiplication of *Pasteurella pestis* in mononuclear phagocytes in the pathogenesis of flea-borne plague. J Immunol **83:**348-363.
7. **Chauhan, A., M. V. Madiraju, M. Fol, H. Lofton, E. Maloney, R. Reynolds, and M. Rajagopalan.** 2006. *Mycobacterium tuberculosis* cells growing in macrophages are filamentous and deficient in FtsZ rings. J Bacteriol **188:**1856-1865.

8. **Chen, K., G. W. Sun, K. L. Chua, and Y. H. Gan.** 2005. Modified virulence of antibiotic-induced *Burkholderia pseudomallei* filaments. Antimicrob Agents Chemother **49:**1002-1009.

9. **Conchas, R. F., and E. Carniel.** 1990. A highly efficient electroporation system for transformation of *Yersinia*. Gene **87:**133-137.

10. **Cully, J. F., Jr., T. L. Johnson, S. K. Collinge, and C. Ray.** 2010. Disease limits populations: plague and black-tailed prairie dogs. Vector Borne Zoonotic Dis **10:**7-15.

11. **Du, Y., R. Rosqvist, and A. Forsberg.** 2002. Role of fraction 1 antigen of *Yersinia pestis* in inhibition of phagocytosis. Infect Immun **70:**1453-1460.

12. **Eidson, M., J. P. Thilsted, and O. J. Rollag.** 1991. Clinical, clinicopathologic, and pathologic features of plague in cats: 119 cases (1977-1988). J Am Vet Med Assoc **199:**1191-1197.

13. **Flannagan, R. S., V. Jaumouille, and S. Grinstein.** 2011. The cell biology of phagocytosis. Annu Rev Pathol **7:**49-86.

14. **Fukuto, H. S., A. Svetlanov, L. E. Palmer, A. W. Karzai, and J. B. Bliska.** 2010. Global gene expression profiling of *Yersinia pestis* replicating inside macrophages reveals the roles of a putative stress-induced operon in regulating type III secretion and intracellular cell division. Infect Immun **78:**3700-3715.

15. **Galyov, E. E., O. Smirnov, A. V. Karlishev, K. I. Volkovoy, A. I. Denesyuk, I. V. Nazimov, K. S. Rubtsov, V. M. Abramov, S. M. Dalvadyanz, and V. P. Zav'yalov.** 1990. Nucleotide sequence of the *Yersinia pestis* gene encoding F1

antigen and the primary structure of the protein. Putative T and B cell epitopes. FEBS Lett **277:**230-232.

16. **Gasper, P. W., A. M. Barnes, T. J. Quan, J. P. Benziger, L. G. Carter, M. L. Beard, and G. O. Maupin.** 1993. Plague (*Yersinia pestis*) in cats: description of experimentally induced disease. J Med Entomol **30:**20-26.

17. **Gilleland, L. B., H. E. Gilleland, J. A. Gibson, and F. R. Champlin.** 1989. Adaptive resistance to aminoglycoside antibiotics in *Pseudomonas aeruginosa*. J Med Microbiol **29:**41-50.

18. **Gould, L. H., J. Pape, P. Ettestad, K. S. Griffith, and P. S. Mead.** 2008. Dog-associated risk factors for human plague. Zoonoses Public Health **55:**448-454.

19. **Grabenstein, J. P., H. S. Fukuto, L. E. Palmer, and J. B. Bliska.** 2006. Characterization of phagosome trafficking and identification of PhoP-regulated genes important for survival of *Yersinia pestis* in macrophages. Infect Immun **74:**3727-3741.

20. **Hall, P. J., G. C. Yang, R. V. Little, and R. R. Brubaker.** 1974. Effect of Ca^{2+} on morphology and division of *Yersinia pestis*. Infect Immun **9:**1105-1113.

21. **Henry, T., F. Garcia-del Portillo, and J. P. Gorvel.** 2005. Identification of *Salmonella* functions critical for bacterial cell division within eukaryotic cells. Mol Microbiol **56:**252-267.

22. **Imlay, J. A., and S. Linn.** 1987. Mutagenesis and stress responses induced in *Escherichia coli* by hydrogen peroxide. J Bacteriol **169:**2967-2976.

23. **Justice, S. S., D. A. Hunstad, L. Cegelski, and S. J. Hultgren.** 2008. Morphological plasticity as a bacterial survival strategy. Nat Rev Microbiol **6:**162-168.

24. **Justice, S. S., D. A. Hunstad, P. C. Seed, and S. J. Hultgren.** 2006. Filamentation by *Escherichia coli* subverts innate defenses during urinary tract infection. Proc Natl Acad Sci USA **103:**19884-19889.

25. **Kartman, L., F. M. Prince, S. F. Quan, and H. E. Stark.** 1958. New knowledge on the ecology of sylvatic plague. Ann NY Acad Sci **70:**668-711.

26. **Laws, T. R., M. S. Davey, R. W. Titball, and R. Lukaszewski.** 2010. Neutrophils are important in early control of lung infection by *Yersinia pestis*. Microbes Infect **12:**331-335.

27. **Lindler, L. E., and B. D. Tall.** 1993. *Yersinia pestis* pH 6 antigen forms fimbriae and is induced by intracellular association with macrophages. Mol Microbiol **8:**311-324.

28. **Liu, F., H. Chen, E. M. Galvan, M. A. Lasaro, and D. M. Schifferli.** 2006. Effects of Psa and F1 on the adhesive and invasive interactions of *Yersinia pestis* with human respiratory tract epithelial cells. Infect Immun **74:**5636-5644.

29. **Lukaszewski, R. A., D. J. Kenny, R. Taylor, D. G. Rees, M. G. Hartley, and P. C. Oyston.** 2005. Pathogenesis of *Yersinia pestis* infection in BALB/c mice: effects on host macrophages and neutrophils. Infect Immun **73:**7142-7150.

30. **Marim, F. M., T. N. Silveira, D. S. Lima, Jr., and D. S. Zamboni.** 2010. A method for generation of bone marrow-derived macrophages from cryopreserved mouse bone marrow cells. PLoS One **5:** 15263-15271.

31. **Nizet, V., A. L. Smith, a. P. M. Sullam, and C. E. Rubens.** 1998. A simple microtiter plate screening assay for bacterial invasion or adherence. Methods Cell Sci. **20:**107-111.

32. **Ogawa, M., A. Takade, H. Miyamoto, H. Taniguchi, and S. Yoshida.** 2001. Morphological variety of intracellular microcolonies of *Legionella* species in Vero cells. Microbiol Immunol **45:**557-562.

33. **Orloski, K. A., and M. Eidson.** 1995. *Yersinia pestis* infection in three dogs. J Am Vet Med Assoc **207:**316-318.

34. **Perry, R. D., and J. D. Fetherston.** 1997. *Yersinia pestis*--etiologic agent of plague. Clin Microbiol Rev **10:**35-66.

35. **Perry, R. D., I. Mier, Jr., and J. D. Fetherston.** 2007. Roles of the Yfe and Feo transporters of *Yersinia pestis* in iron uptake and intracellular growth. Biometals **20:**699-703.

36. **Perry, R. D., S. C. Straley, J. D. Fetherston, D. J. Rose, J. Gregor, and F. R. Blattner.** 1998. DNA sequencing and analysis of the low-Ca^{2+}-response plasmid pCD1 of *Yersinia pestis* KIM5. Infect Immun **66:**4611-4623.

37. **Pollack, C., S. C. Straley, and M. S. Klempner.** 1986. Probing the phagolysosomal environment of human macrophages with a Ca^{2+}-responsive operon fusion in *Yersinia pestis*. Nature **322:**834-836.

38. **Ponnusamy, D., S. D. Hartson, and K. D. Clinkenbeard.** 2011. Intracellular *Yersinia pestis* expresses general stress response and tellurite resistance proteins in mouse macrophages. Vet Microbiol **150:**146-151.

39. **Pujol, C., and J. B. Bliska.** 2003. The ability to replicate in macrophages is conserved between *Yersinia pestis* and *Yersinia pseudotuberculosis*. Infect Immun **71:**5892-5899.

40. **Pujol, C., and J. B. Bliska.** 2005. Turning *Yersinia* pathogenesis outside in: subversion of macrophage function by intracellular *Yersiniae*. Clin Immunol **114:**216-226.

41. **Pujol, C., J. P. Grabenstein, R. D. Perry, and J. B. Bliska.** 2005. Replication of *Yersinia pestis* in interferon gamma-activated macrophages requires *ripA*, a gene encoded in the pigmentation locus. Proc Natl Acad Sci USA **102:**12909-12914.

42. **Rollag, O. J., M. R. Skeels, L. J. Nims, J. P. Thilsted, and J. M. Mann.** 1981. Feline plague in New Mexico: report of five cases. J Am Vet Med Assoc **179:**1381-1383.

43. **Romberg, L., and P. A. Levin.** 2003. Assembly dynamics of the bacterial cell division protein FTSZ: poised at the edge of stability. Annu Rev Microbiol **57:**125-154.

44. **Rosenberger, C. M., and B. B. Finlay.** 2002. Macrophages inhibit *Salmonella typhimurium* replication through MEK/ERK kinase and phagocyte NADPH oxidase activities. J Biol Chem **277:**18753-18762.

45. **Rosenberger, C. M., R. L. Gallo, and B. B. Finlay.** 2004. Interplay between antibacterial effectors: A macrophage antimicrobial peptide impairs intracellular *Salmonella* replication. Proc Natl Acad Sci USA **101:**2422-2427.

46. **Rust, J. H., Jr., D. C. Cavanaugh, R. O'Shita, and J. D. Marshall, Jr.** 1971. The role of domestic animals in the epidemiology of plague. I. Experimental infection of dogs and cats. J Infect Dis **124:**522-526.

47. **Rust, J. H., Jr., B. E. Miller, M. Bahmanyar, J. D. Marshall, Jr., S. Purnaveja, D. C. Cavanaugh, and U. S. Hla.** 1971. The role of domestic animals in the epidemiology of plague. II. Antibody to *Yersinia pestis* in sera of dogs and cats. J Infect Dis **124:**527-531.

48. **Salkeld, D. J., and P. Stapp.** 2006. Seroprevalence rates and transmission of plague (*Yersinia pestis*) in mammalian carnivores. Vector Borne Zoonotic Dis **6:**231-239.

49. **Schapiro, J. M., S. J. Libby, and F. C. Fang.** 2003. Inhibition of bacterial DNA replication by zinc mobilization during nitrosative stress. Proc Natl Acad Sci USA **100:**8496-8501.

50. **Sebbane, F., D. Gardner, D. Long, B. B. Gowen, and B. J. Hinnebusch.** 2005. Kinetics of disease progression and host response in a rat model of bubonic plague. Am J Pathol **166:**1427-1439.

51. **Sebbane, F., C. O. Jarrett, D. Gardner, D. Long, and B. J. Hinnebusch.** 2006. Role of the *Yersinia pestis* plasminogen activator in the incidence of distinct septicemic and bubonic forms of flea-borne plague. Proc Natl Acad Sci USA **103:**5526-5530.

52. **Sha, J., J. J. Endsley, M. L. Kirtley, S. M. Foltz, M. B. Huante, T. E. Erova, E. V. Kozlova, V. L. Popov, L. A. Yeager, I. V. Zudina, V. L. Motin, J. W. Peterson, K. L. DeBord, and A. K. Chopra.** 2011. Characterization of an F1

deletion mutant of *Yersinia pestis* CO92, pathogenic role of F1 antigen in bubonic and pneumonic plague, and evaluation of sensitivity and specificity of F1 antigen capture-based dipsticks. J Clin Microbiol **49:**1708-1715.

53. **Smiley, S. T.** 2008. Immune defense against pneumonic plague. Immunol Rev **225:**256-271.

54. **Spinner, J. L., K. S. Seo, J. L. O'Loughlin, J. A. Cundiff, S. A. Minnich, G. A. Bohach, and S. D. Kobayashi.** 2010. Neutrophils are resistant to *Yersinia* YopJ/P-induced apoptosis and are protected from ROS-mediated cell death by the type III secretion system. PLoS One **5:**9279-9288.

55. **Straley, S. C., and P. A. Harmon.** 1984. Growth in mouse peritoneal macrophages of *Yersinia pestis* lacking established virulence determinants. Infect Immun **45:**649-654.

56. **Straley, S. C., and P. A. Harmon.** 1984. *Yersinia pestis* grows within phagolysosomes in mouse peritoneal macrophages. Infect Immun **45:**655-659.

57. **Tsang, A. W., K. Oestergaard, J. T. Myers, and J. A. Swanson.** 2000. Altered membrane trafficking in activated bone marrow-derived macrophages. J Leukoc Biol **68:**487-494.

58. **Underhill, D. M., and A. Ozinsky.** 2002. Phagocytosis of microbes: complexity in action. Annu Rev Immunol **20:**825-852.

59. **Vernati, G., W. H. Edwards, T. E. Rocke, S. F. Little, and G. P. Andrews.** 2011. Antigenic profiling of *Yersinia pestis* infection in the Wyoming coyote (*Canis latrans*). J Wildl Dis **47:**21-29.

60. **Watson, R. P., T. W. Blanchard, M. G. Mense, and P. W. Gasper.** 2001. Histopathology of experimental plague in cats. Vet Pathol **38:**165-172.

61. **Wendte, J. M., D. Ponnusamy, D. Reiber, J. L. Blair, and K. D. Clinkenbeard.** 2011. *In vitro* efficacy of antibiotics commonly used to treat human plague against intracellular *Yersinia pestis*. Antimicrob Agents Chemother **55:**3752-3757.

62. **Ye, Z., E. J. Kerschen, D. A. Cohen, A. M. Kaplan, N. van Rooijen, and S. C. Straley.** 2009. Gr1+ cells control growth of YopM-negative *Yersinia pestis* during systemic plague. Infect Immun **77:**3791-3806.

63. **Young, K. D.** 2006. The selective value of bacterial shape. Microbiol Mol Biol Rev **70:**660-703.

Table 1A. Morphometric analysis of intracellular *Y. pestis* and primary macrophages from TEM images

Parameter		Mouse splenic macrophages			Dog peripheral blood derived macrophages		
Hours post infection		**2.5**	**7.5**	**27.5**	**2.5**	**7.5**	**27.5**
Filamentous *Y.*	% filamentous *Y.*	10.8 ± 11.1	0	0	8.5 ± 8.8	0	0.4 ± 1.7
pestis	*pestis* / macrophage*						
	Length (in µM)	6.8 ± 1.6	-	-	8.4 ± 2.5	-	5.8
	Range (in µM)	5.1 - 10.5	-	-	5.1 - 12.5	-	5.8
Intact *Y. pestis* / macrophage		18 ± 13.2	38.7 ± 13.9	7.6 ± 3.6##	23.9 ± 13.9	33 ± 12.5	2.3 ± 2.1##
Disfigured *Y. pestis* / macrophage		2 ± 2.2¥	2.8 ± 2.1	0.6 ± 0.7$$	0.9 ± 1¥	3 ± 2.2	16.7 ± 6.4$$
YCV	Spacious extension (in	33	82	0	20	5	80
	% of macrophages)						
Morphology of macrophage nucleus		Normal#	Normal	Normal	Normal	Normal	Normal
Morphology of macrophage mitochondria		Normal@	Normal	Normal	Normal	Normal	Normal

Note: Mean value of a particular parameter at 2.5, 7.5 or 27.5 h p.i. from mouse splenic macrophage infection was statistically compared with the corresponding value from dog peripheral blood derived macrophage infection
*, *Y. pestis* longer than 5µM
#, Heterochromatin at the periphery and euchromatin at the center
@, Sharp and visible cristae
¥, $p<0.05$; ##, $$, $p<0.01$

Table 1B. Morphometric analysis of intracellular *Y. pestis* and tissue culture macrophage cell lines from TEM images

Parameter		RAW264.7 cells			DH82 cells		
Hours post infection		**2.5**	**7.5**	**27.5**	**2.5**	**7.5**	**27.5**
Filamentous *Y. pestis*	% filamentous *Y. pestis* / macrophage	22.6 ± 33.1	6.4 ± 9.7$^{\psi}$	2.5 ± 4.2	17.5 ± 28.8	27.6 ± 26.6 $^{\psi}$	26.3 ± 33.2
	Length (in µM)	6.9 ± 1.9	5.6 ± 0.6$^{\$}$	5.8 ± 0.7	7.2 ± 3.1	6.5 ± 1.4$^{\$}$	6.9 ± 1.5
	Range (in µM)	5.2 - 11.1	5 - 6.8	5.1 - 6.6	5 - 14.9	5 - 9.3	5 - 9.3
Intact *Y. pestis* / macrophage		13.8 ± 9.1	16.5 ± 9.7§§	14.3 ± 7.8†	10.1 ± 5.8	7.7 ± 6.7§§	7.2 ± 6.1†
Disfigured *Y. pestis* / macrophage		0.8 ± 1.1	0.6 ± 0.9	2.1 ± 1.4	0.7 ± 0.8	0.8 ± 1.1	2.1 ± 1.9
YCV	Spacious extension (in % of macrophages)	13	64	73	18	23	18
Morphology of macrophage nucleus		Normal	Normal	Normal	Normal	Normal	Normal
Morphology of macrophage mitochondria		Normal	Normal	Normal	Normal	Normal	Normal

Note: Mean value of a particular parameter at 2.5, 7.5 or 27.5 h p.i. from RAW264.7 cell infection was statistically compared with the corresponding value from DH82 cell infection
ψ, $, †, $p<0.05$; §§, $p<0.01$

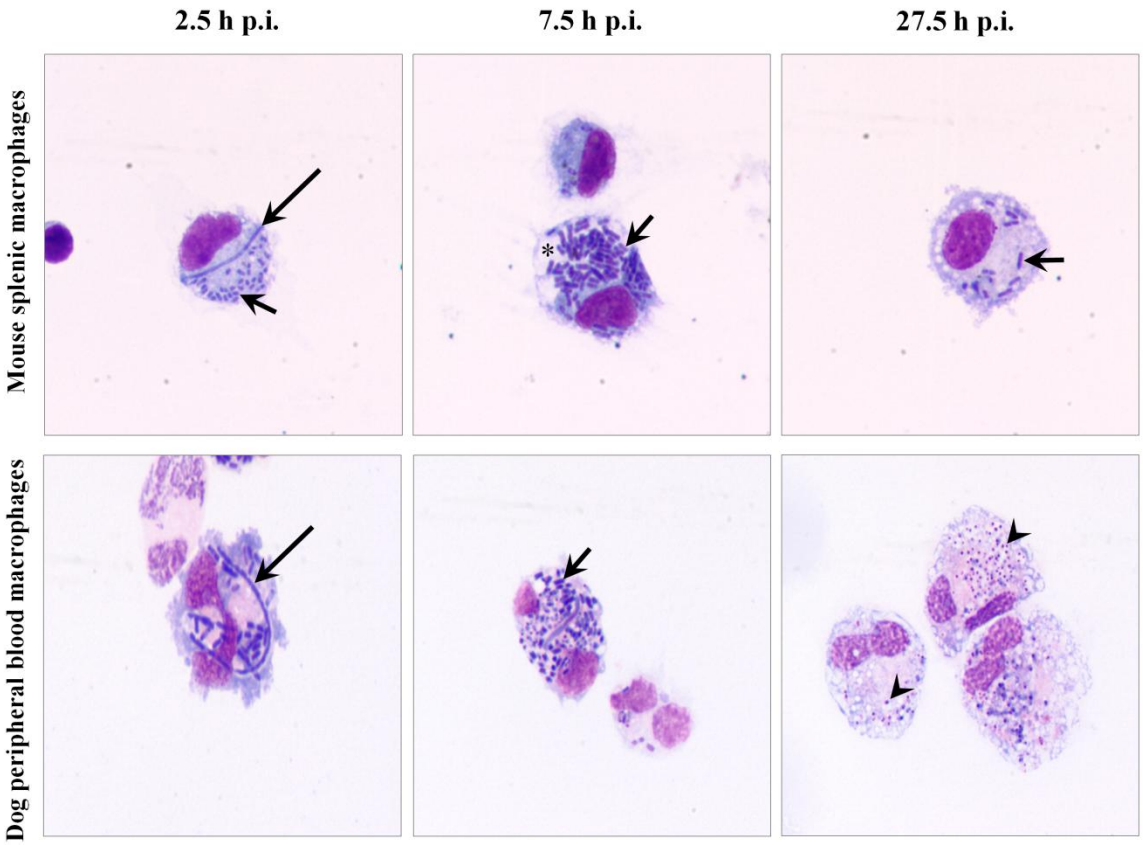

Fig. 1. Intracellular *Y. pestis* in primary macrophages. *Y. pestis* strain KIM6+ infected primary macrophages from mouse spleen (top row) and dog peripheral blood (bottom row) were sampled at 2.5, 7.5 and 27.5 h p.i. and observed under light microscope by staining with Wright Giemsa. Long arrows, short arrows and arrow heads represent filamentous, coccobacillary and degraded coccobacillary *Y. pestis*, respectively. Asterisk indicates spacious vacuolar extension of phagolysosomes. Images are at 1,000x magnification.

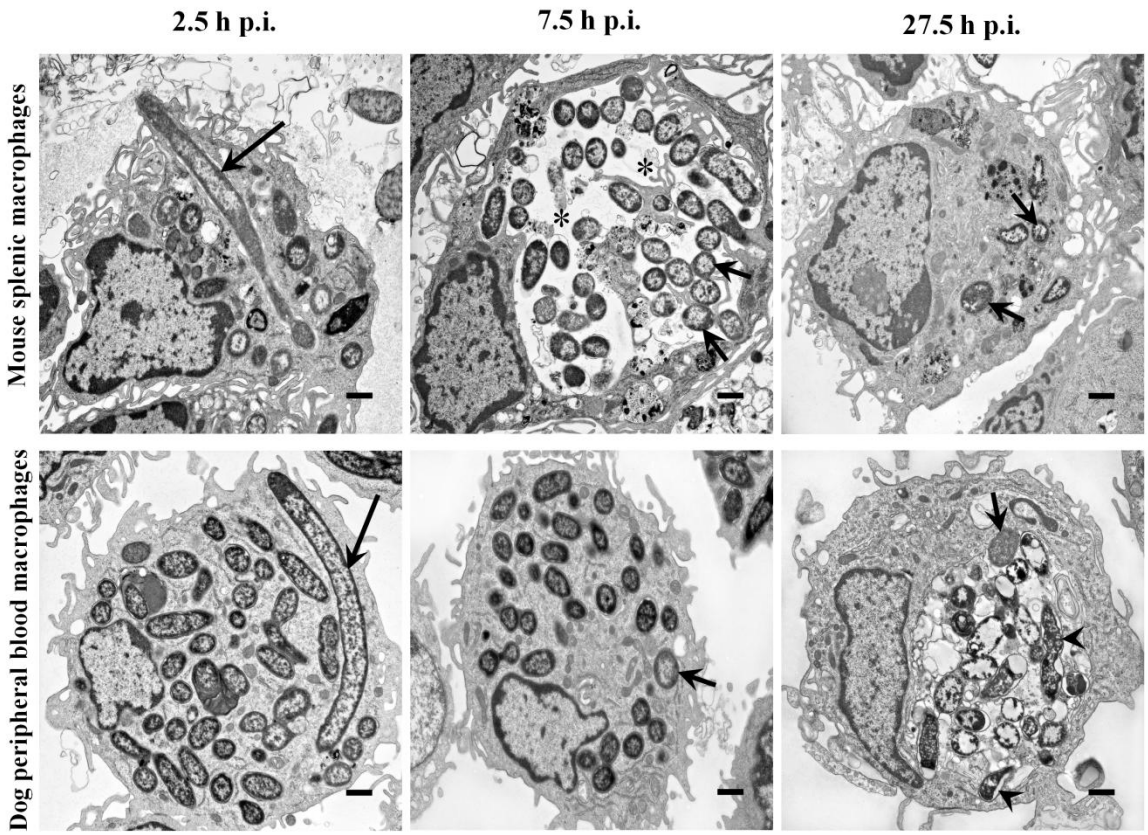

Fig. 2. Ultrastructural features of intracellular *Y. pestis* and infected primary macrophages. Primary macrophages from mouse spleen (top row) and dog peripheral blood (bottom row) infected with *Y. pestis* strain KIM6+ were glutaraldehyde fixed at 2.5, 7.5 and 27.5 h p.i. and examined in transmission electron microscopy. Long arrows, short arrows and arrow heads represent filamentous, coccobacillary and degraded coccobacillary *Y. pestis*, respectively. Asterisks indicate spacious vacuolar extension of phagolysosomes. The images are at 6,000x magnification and cross bars represent 1µm.

Fig. 3. Intracellular *Y. pestis* in mouse bone marrow macrophages. Macrophages cultured for 5 days were infected with *Y. pestis* strain KIM6+ and sampled at 2.5, 7.5 and 27.5 h p.i. The samples were prepared for the light microscopic examination by staining with Wright Giemsa stain. Arrows indicate the actively dividing normal sized coccobacillus of intracellular *Y. pestis*. Images are at 1,000x magnification.

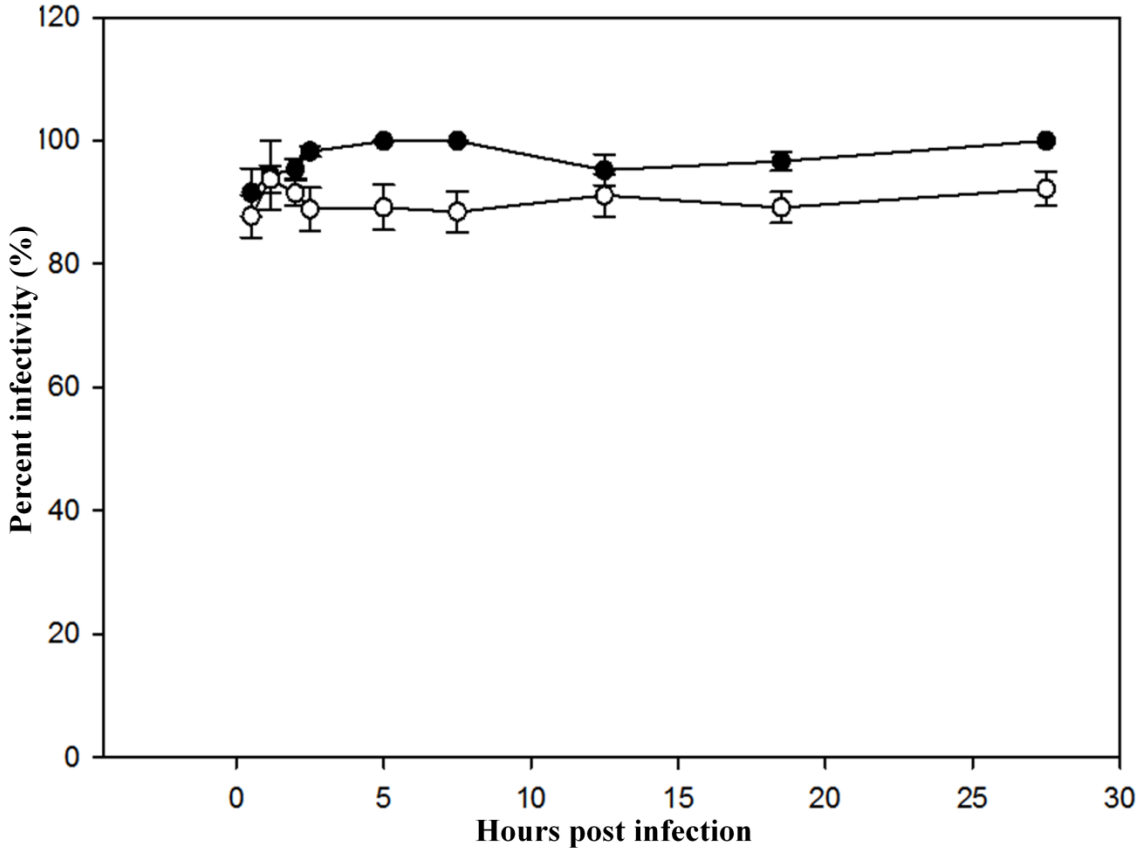

Fig. 4. Percent of infectivity for tissue culture macrophages to *Y. pestis* infection. *Y. pestis* strain KIM6+ infected RAW264.7 (—●—) and DH82 (—○—)cells were sampled at various p.i. intervals to examine under light microscope for the presence of intracellular bacteria. Approximately 400 cells per replicate were randomly counted to calculate the percentage of infectivity (n=3). The values are reported as mean ± SEM.

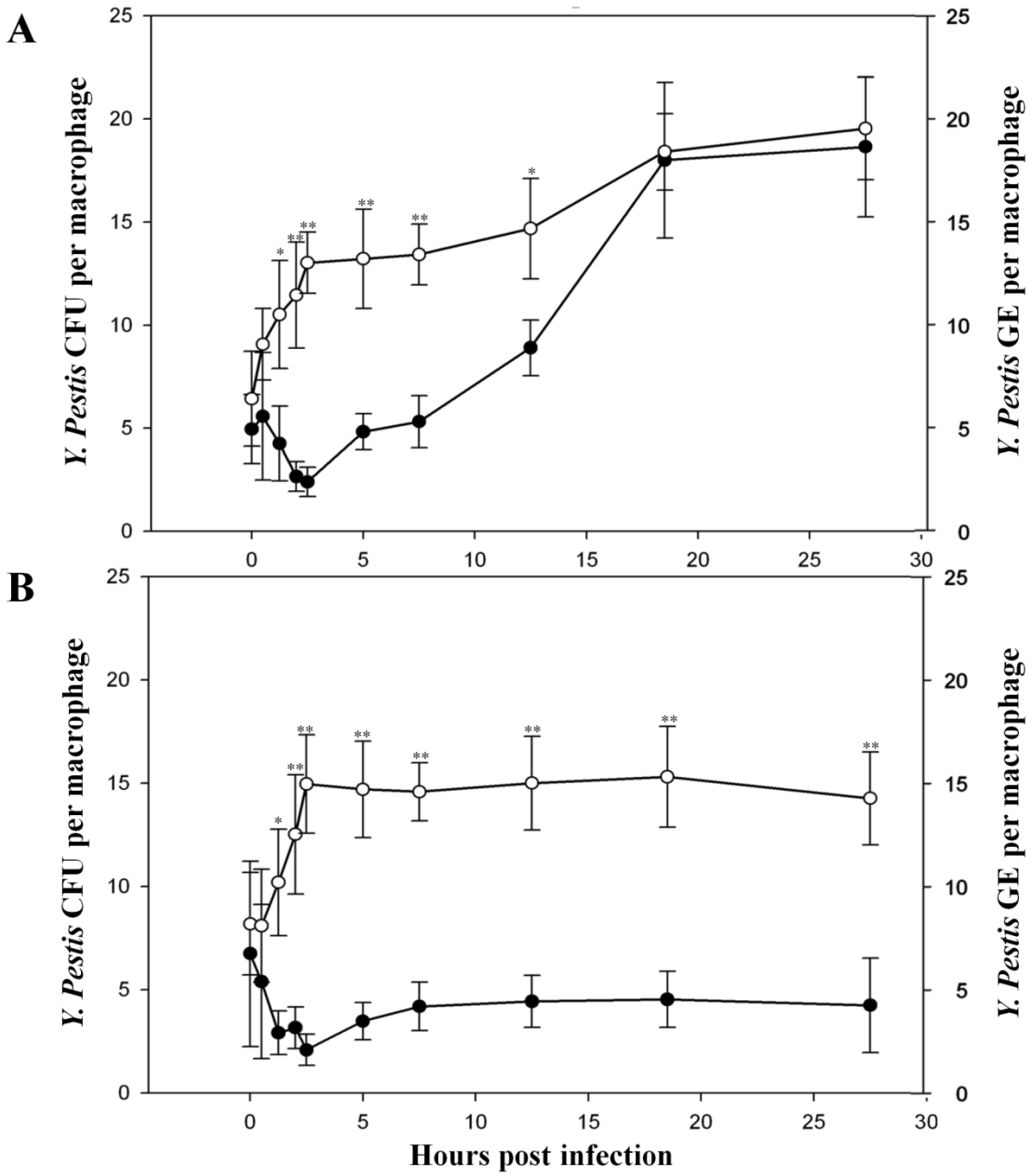

Fig. 5. Intracellular CFUs and GEs per tissue culture macrophage. CFUs (—●—) and GEs (—○—) as, respectively, culturable and total *Y. pestis* per RAW264.7 (A) and DH82 (B) were calculated for various intervals from 0 to 27.5 h p.i. using microplate based colony counting and qPCR described in materials and methods section (n=3). The results are

expressed as mean ± SEM. Asterisks on error bars represent, at the respective interval, statistical difference (∗, $p < 0.05$; ∗∗, $p < 0.01$) between the mean values of GEs and CFUs.

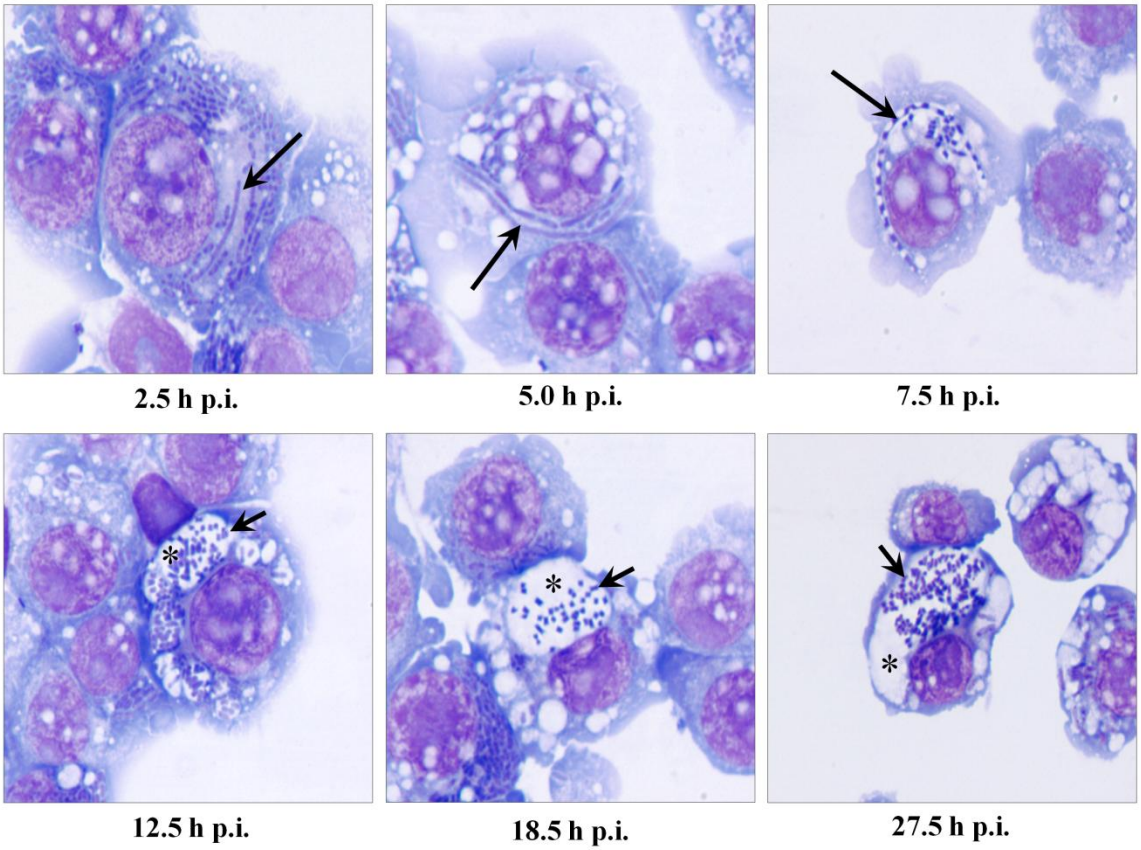

Fig. 6A. Morphological features of intracellular *Y. pestis* and infected RAW264.7 cells. *Y. pestis* strain KIM6+ infected RAW264.7 cells were sampled from 2.5 to 27.5 h p.i. and observed under light microscope by staining with Wright Giemsa. Filamentous and coccobacillary forms of intracellular *Y. pestis* and spacious phagolysosomal extensions were determined at 1,000x magnification. Long and short arrows indicate filamentous and coccobacillary form of intracellular *Y. pestis*, respectively. Asterisk indicates spacious vacuolar extension of phagolysosome.

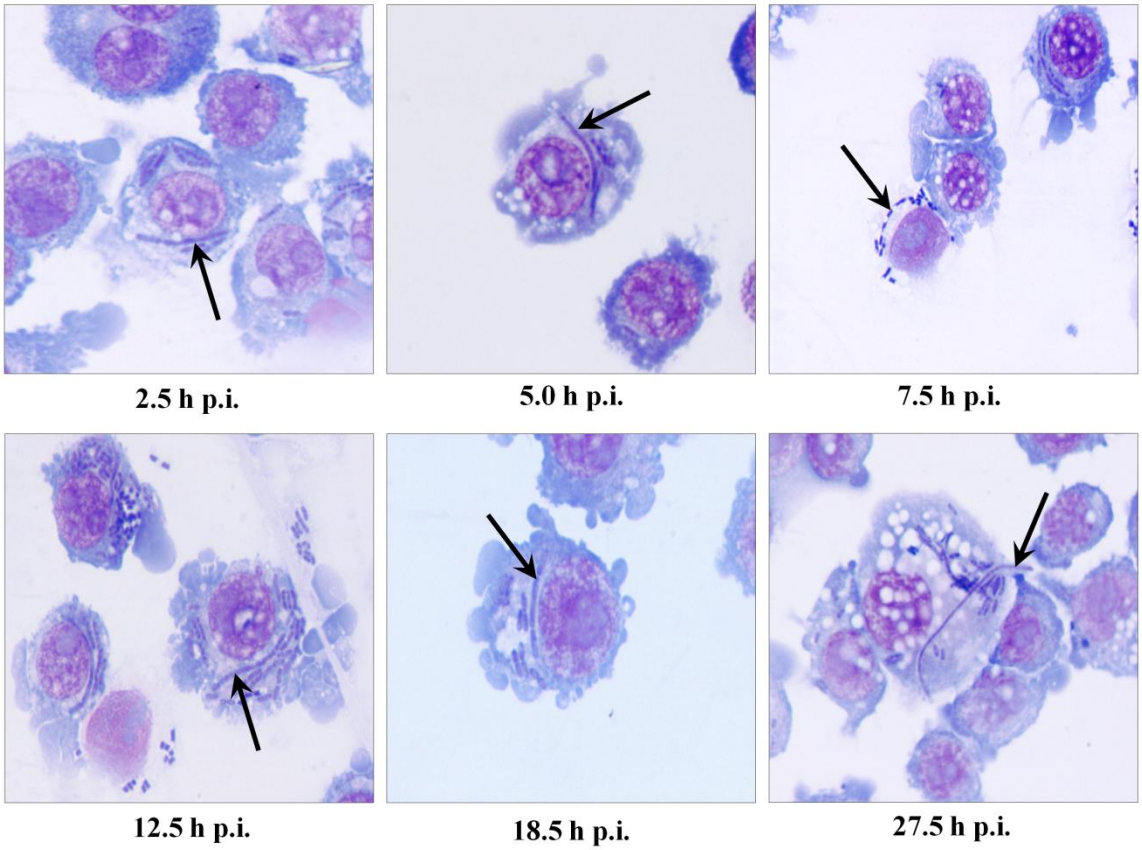

Fig. 6B. Morphological features of intracellular *Y. pestis* and infected DH82 cells. *Y. pestis* strain KIM6+ infected DH82 cells were sampled from 2.5 to 27.5 h p.i. and observed under light microscope by staining with Wright Giemsa. Filamentous intracellular (long arrows) *Y. pestis* were determined at 1,000x magnification.

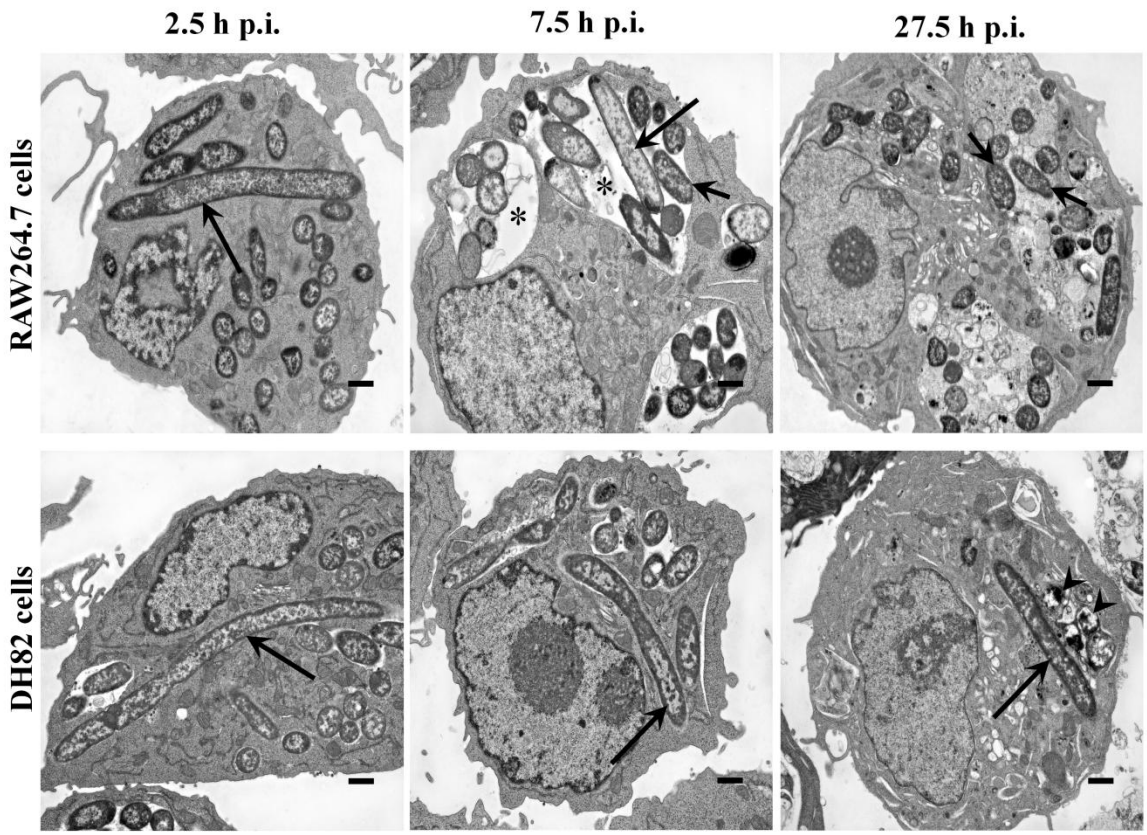

Fig. 7. Ultrastructural features of intracellular *Y. pestis* and infected tissue culture cells. *Y. pestis* strain KIM6+ infected RAW264.7 (top row) and DH82 (bottom row) cells were sampled at 2.5, 7.5 and 27.5 h p.i. and examined in transmission electron microscope. Long and short arrows indicate filamentous and coccobacillary form of intracellular *Y. pestis*, respectively. Arrow heads point out the degraded intracellular *Y. pestis*. Asterisks indicate spacious vacuolar extension of phagolysosomes. The images are at 6,000x magnification and cross bars represent 1µm.

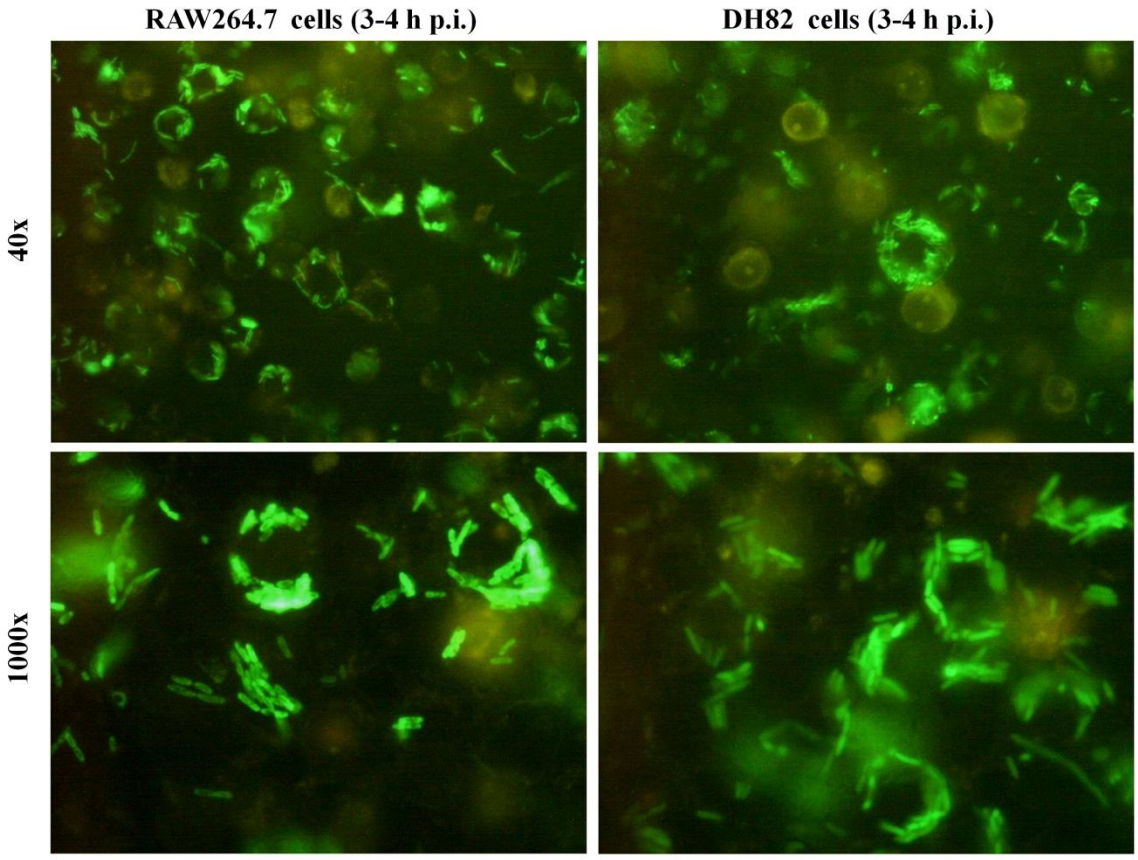

Fig. 8. Morphological features of *Y. pestis* strain KIM6+ GFPuv in tissue culture cells. *Y. pestis* strain KIM6+ GFPuv infected RAW264.7 (1st column) and DH82 (2nd column) cells collected at 3 to 4 h p.i. were observed under fluorescent microscope as wet mount preparations.

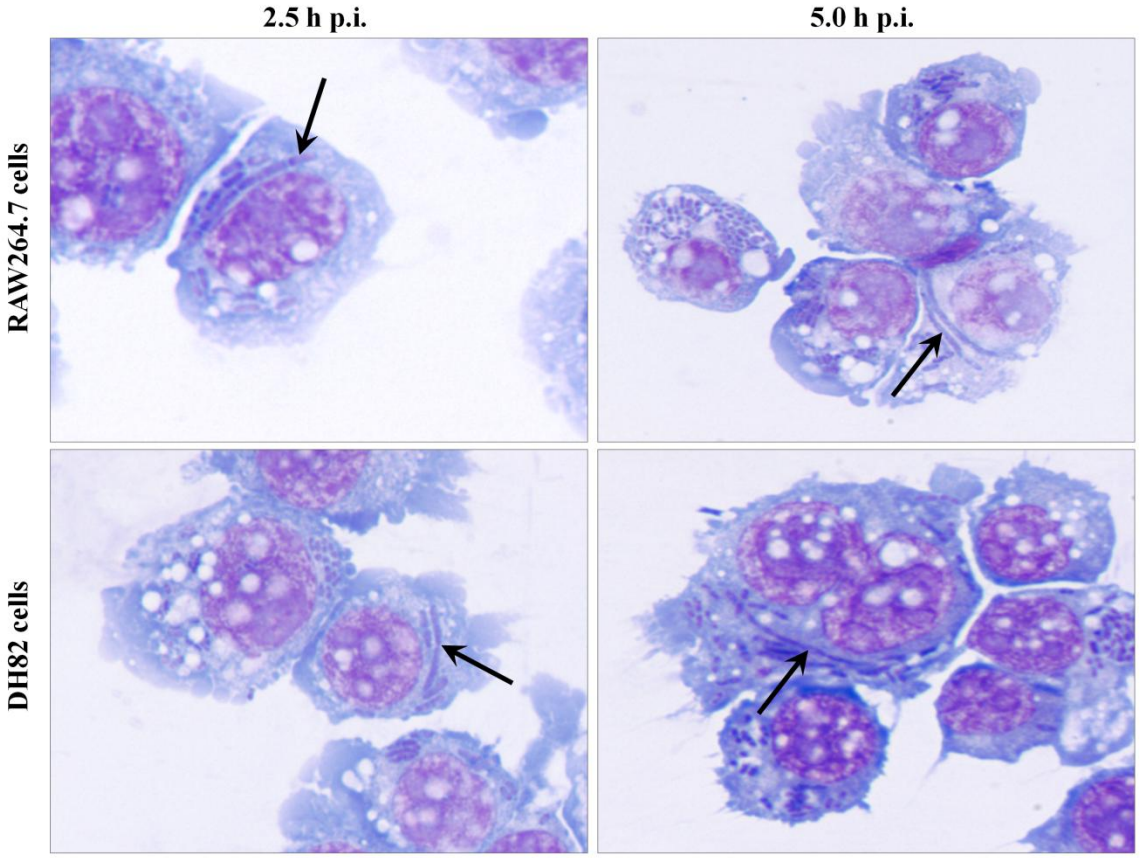

Fig. 9. Morphological features of intracellular *Y. pestis* in antibiotic-free media. RAW264.7 and DH82 cells were infected with *Y. pestis* strain KIM6+ for 30 min in RPMI-1640 with 10% FBS media and then changed to HBSS with 10% FBS. Infected macrophages were sampled at 2.5 and 5 h p.i. to light microscopic examination. Arrows indicate filamentous *Y. pestis*. Images are presented at 1,000x magnification.

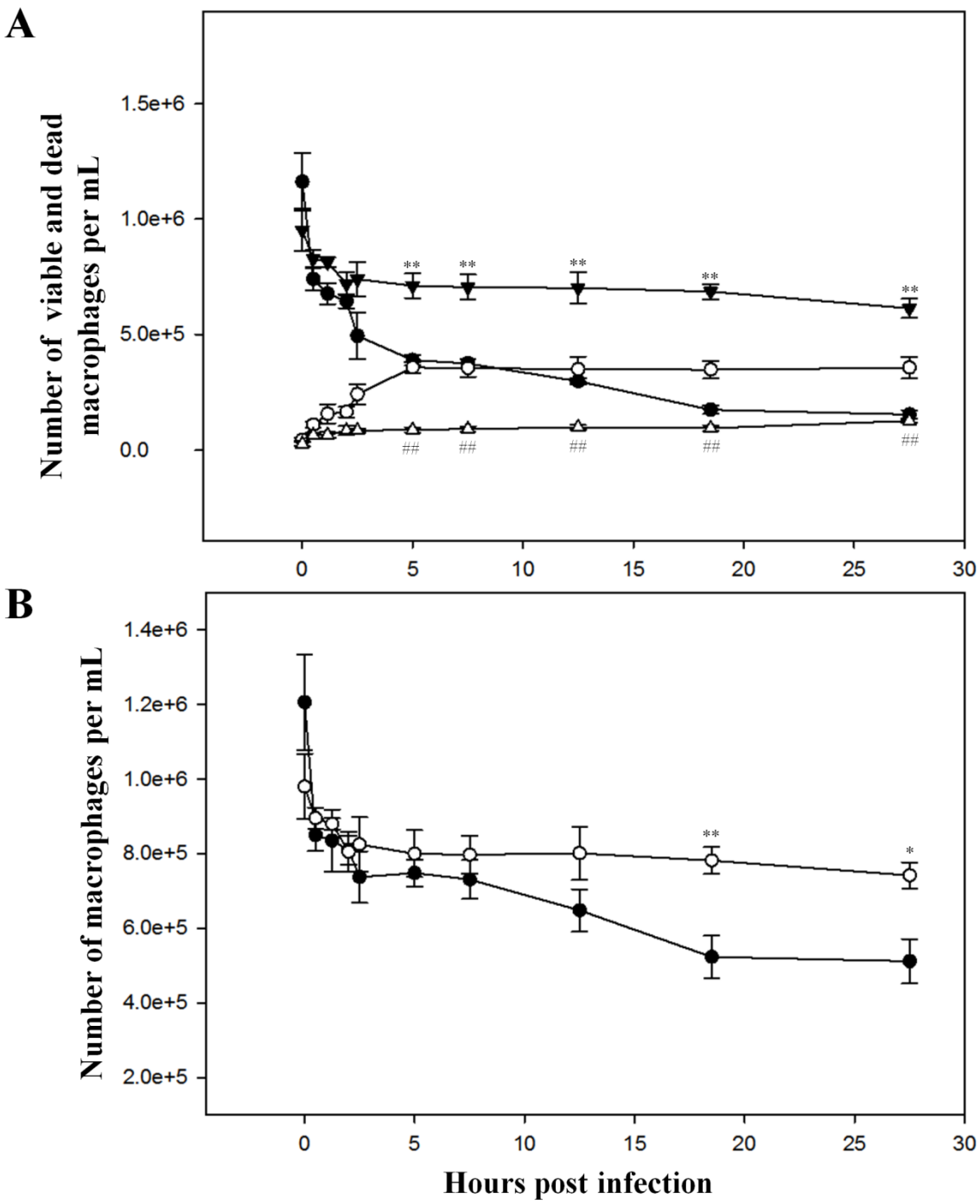

Fig. 10. Tissue culture macrophage counts for *Y. pestis* infection in trypan blue assay. (A): *Y. pestis* strain KIM6+ infected tissue culture macrophages were sampled at different p.i. to enumerate a number of trypan blue positive (dead) and negative (viable) cells. The

resulting viable RAW264.7 (●) and DH82 (▼), and dead RAW264.7 (○) and DH82 (△) cells are reported here (n=3). The values are represented as mean ± SEM. Statistically significant difference ($p < 0.01$) was indicated for viable counts of RAW264.7 vs. DH82 cells (**), and dead counts of RAW264.7 vs. DH82 cells (##) at each infection interval. (B): A number of macrophages per mL of infective material at different p.i. were also calculated for RAW264.7 (●) and DH82 (○)cells by adding a number of viable and dead counts at each infection interval (n=3). The data are shown as mean ± SEM. Asterisks on error bars represent, at the respective interval, statistical difference (*, $p < 0.05$; **, $p < 0.01$) between the total macrophage counts of RAW264.7 and DH82 cells per mL.

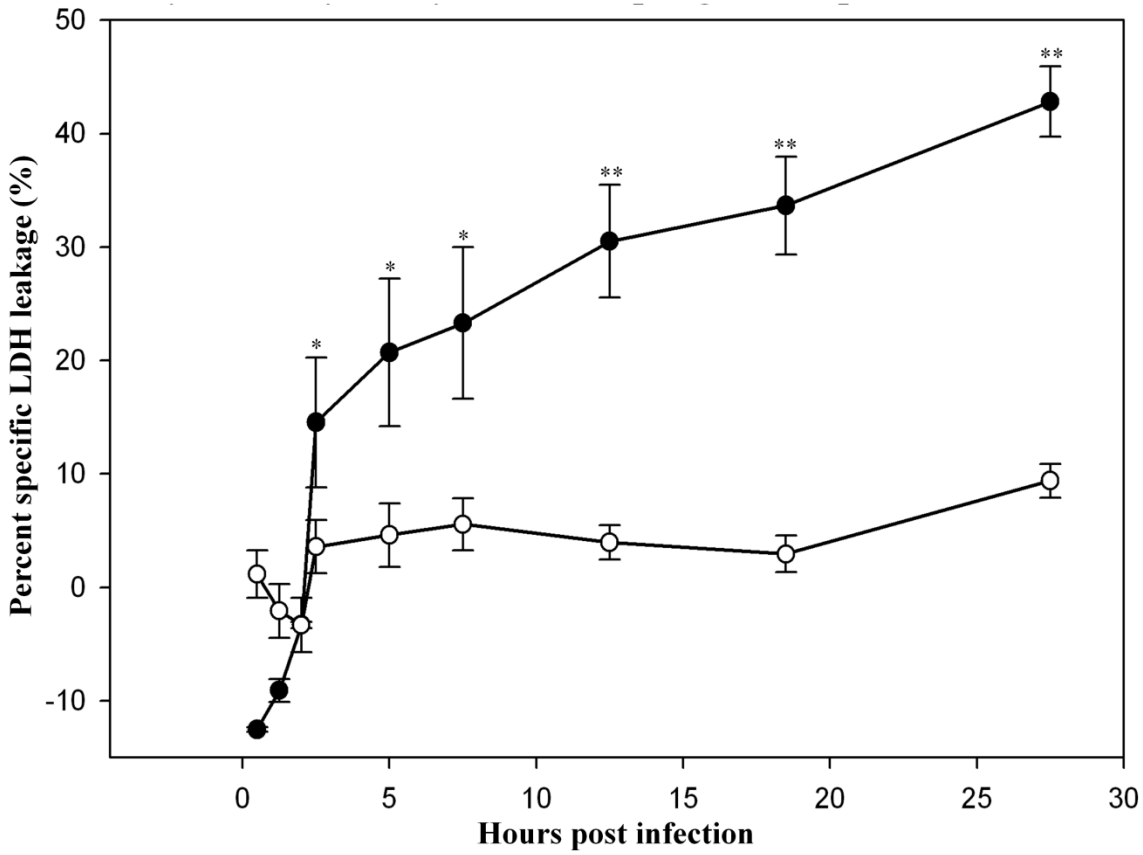

Fig. 11. Cytotoxicity assay of tissue culture cells to *Y. pestis* infection. Concentration of macrophage cytoplasmic enzyme LDH in the extracellular media as the consequence of cell lysis to *Y. pestis* infection was measured for RAW264.7 (—●—) and DH82 (—○—) cells (n=3). The data are shown as mean ± SEM. Asterisks on error bars represent, at the respective interval, statistical difference (∗, $p < 0.05$; ∗∗, $p < 0.01$) between the means percentage specific LDH leakage of RAW264.7 and DH82 cells.

CHAPTER IV

INTRACELLULAR *YERSINIA PESTIS* EXPRESSES GENERAL STRESS RESPONSE AND TELLURITE RESISTANCE PROTEINS IN MOUSE MACROPHAGES

(This chapter was published in a peer reviewed journal as: **Ponnusamy, D., S. D. Hartson, and K. D. Clinkenbeard.** 2011. Intracellular *Yersinia pestis* expresses general stress response and tellurite resistance proteins in mouse macrophages. Vet Microbiol **150:**146-151. The related copyright agreement is attached in the appendix)

Abstract

Yersinia pestis inoculated subcutaneously via fleabite or experimental injection in natural rodent hosts multiply initially in macrophage phagolysosomes. Survival and multiplication of *Y. pestis* in this acidic low [Ca^{2+}] and [Mg^{2+}] environment likely necessitates compensatory mechanisms involving expression of specific proteins compared to those expressed during extracellular growth. A proteomics approach was used to identify these proteins using mouse macrophage RAW264.7 cells infected with *Y. pestis* strain KIM6-2053.1+ for 8 h. Intracellular *Y. pestis* protein samples were prepared by detergent lysis of infected RAW264.7 cells, isolation of intracellular *Y. pestis* by differential centrifugation, and sonication of isolated *Y. pestis*. Protein samples were similarly prepared from *Y. pestis* grown extracellularly in tissue culture media. Two intracellular and extracellular *Y. pestis* protein samples were analyzed by two-dimensional polyacrylamide gel electrophoresis and compared *in silico* identifying 12 protein spots present in both intracellular samples but absent in extracellularly grown *Y. pestis.* Mass spectrometry analysis of these identified nine proteins at a high level of confidence in the *Y. pestis* genome: superoxide dismutase-A (SodA), inorganic pyrophosphatase, autonomous glycyl radical cofactor GrcA, molecular chaperone DnaK, serine endoprotease GsrA, global DNA-binding transcriptional dual regulator H-NS, urease subunit gamma UreA, and tellurite resistance proteins TerD and TerE. These results support the involvement of various general stress response regulators of *Y. pestis* during the intracellular parasitism of host macrophages as well as identification of UreA, TerD and TerE with as yet unknown roles in the process of intracellular survival of *Y. pestis.*

Introduction

Yersinia pestis causes flea-transmitted natural epizootics in rodents (10). *Y. pestis* inoculated via flea bite into the host subcutis persists locally or is phagocytized by neutrophils and tissue macrophages. Neutrophils effectively kill phagocytized *Y. pestis*, but *Y. pestis* is able to survive and multiply in macrophage phagolysosomes in which it evades host innate immunity and disseminate systemically (5, 7, 10, 16).

In order to survive and multiply intracellularly in host macrophage phagolysosomes, *Y. pestis* must withstand the harsh antimicrobial environment. *In vitro* simulation of phagolysosomal environment by lowering culture media [Mg^{2+}] revealed up-regulation of various genes from the pCD1 plasmid, F1- and pH6-antigens loci and Mg^{2+} and iron transporting systems (24). Similarly, *Y. pestis* recovered from buboes exhibited differential expression of genes related with oxidative and nitrosative stresses and iron transport and storage systems (17). However, although transcripts for these virulence genes were detected in phagolysosomes, *Y. pestis* mutants for plasmids pCD1 and pPCP1 and chromosomal loci for various genes including pH6-antigen and chromosomal type-III secretion system did not markedly influence survival of these mutants inside macrophages (8, 11, 19). Studies to identify virulence factors critical for the intracellular lifestyle of *Y. pestis* have identified transcriptional regulator PhoP, possible nitric oxide repressors *ripA* and *ripB* genes from pigmentation locus, and RNA-binding protein Hfq as potentially important (6, 7, 13). Apart from these virulence factors, it is likely that many of the factors involved in the intracellular lifestyle of *Y. pestis* have yet to be identified. A proteomics approach to identification such proteins specifically expressed in host macrophages compared to bacteria grown in microbial

culture is reported. Nine proteins expressed in intracellular *Y. pestis* were identified and consisted primarily of general stress response proteins anticipated to be involved in intracellular survival, but additional proteins for tellurite resistance TerD and TerE were identified with as yet unknown roles in the process of intracellular survival and proliferation of *Y. pestis*.

Materials and methods

Bacterial strain and growth conditions

Y. pestis strain KIM62053.1+ *hms*$^{+}$ *psn*$^{+}$ *psa*$^{-}$ (Δ*psa2053.1*) *ybt*$^{+}$ *lcr*$^{-}$**,** generous gift from Dr. Robert Perry, University of Kentucky (2), was grown on 10 cm Brain Heart Infusion (BHI) (Difco, Becton Dickinson company, USA) agar plates, and following 36 h culture at 26^{o}C, single colonies were used to inoculate 25 mL BHI broth for overnight culture at 26^{o}C with 160 rpm.

Tissue culture cell and growth conditions

Mouse macrophage cell line RAW264.7 (American Type Culture Collection) (23) was cultured at 37°C with 5% CO_2 in RMPI 1640 media (Sigma-Aldrich) supplemented with 2 g/L sodium bicarbonate and 10% fetal bovine serum (Hyclone laboratories).

Infection of tissue culture cells

To prepare RAW264.7 cells for infection with *Y. pestis*, $300x10^6$ RAW264.7 cells were infected with $1,500x\ 10^6$ CFU *Y. pestis*, yielding a multiplicity of infection (MOI) of 5. The RAW264.7 cells were dispensed equally into six 225 cm^2 tissue culture flasks ($50x10^6$ cells per flask) and incubated at 37°C with 5% CO_2 overnight to form monolayers. Following aspiration of tissue culture media from flasks, monolayers were infected by addition of 50 mL per flask of $5x10^6$ CFU/mL *Y. pestis* KIM62053.1+ ($250x10^6$ CFU per flask) grown as described above and incubated 30 min at 37°C with 5% CO_2. Infection was terminated by removal of the bacteria containing media from the flasks followed by washing the RAW264.7 cells thrice with sterile phosphate buffer saline (PBS) and then adding 50 mL/flask of RPMI 1640 media containing 50 µg/mL gentamicin and incubated for an additional 2 h under the same incubation conditions. An 8 h intracellular growth period was initiated by removal of gentamicin containing media, washing flasks three times with sterile PBS, replacement of media with RPMI 1640 media without gentamicin and incubation at 37°C with 5% CO_2.

Isolation of intracellular *Y. pestis*

Following 8 h incubation, RPMI 1640 media were removed from flasks, and the infected RAW264.7 cells were washed three times with sterile PBS to remove any extracellular bacteria. RAW264.7 cells were then lysed by addition of 20 ml of PBS containing 0.1% Triton X-100 to each flask and gentle agitation for 10 min at 37^oC. Lysates were pooled in ice-cooled centrifuge tubes and centrifuged at 600xg for 10 min in 4^oC; the resulting supernatant was carefully decanted; the pellet discarded; and

centrifugation of supernatant repeated twice at the same centrifugal force to completely as possible remove all eukaryotic cellular debris. Finally, the intracellular *Y. pestis* were collected by centrifugation at 8,000xg for 15 min in 4^{o}C.

Preparation of extracellular *Y. pestis*

Y. pestis KIM62053.1+ grown overnight at 26^{o}C in BHI broth was diluted 100-fold in 50 mL of RPMI 1640 media and grown for 8 h at 37^{o}C. Bacteria were collected by centrifugation at 8,000xg for 15 min in 4^{o}C.

Preparation of protein samples

Bacterial pellets for intracellular and extracellular *Y. pestis* KIM62053.1+ were individually washed three times in ice cold 40 mL of 10 mM Tris, 250 mM sucrose, pH 7.0 and were resuspended in 2 mL of 20 mM Tris, pH 8.0. Phenylmethanesulfonylfluoride (PMSF, Calbiochem) was added to the resuspended bacteria to a final concentration of 2 mM, and the suspensions sonicated on ice for 60 bursts with the setting of 1 sec on and off at moderate power (10pts/20pts) in Misonix Microson XL2000 Ultrasonic Cell Disruptor^{TM} (Misonix, Inc; USA). The sonicated bacterial lysates were treated with 125 U/mL of benzonase (Sigma-Aldrich) for 1 h at 37^{o}C with gentile agitation. To prepare the samples for two-dimensional separation, sample buffer was added to all the samples to a final concentration of 0.5% Triton X-100, 20 mM Tris, 7 M urea, 2 M thiourea, 4% CHAPS (w/v), 30 mM DTT, 2 mM TBP and 2% Bio-lyte 3/10 (Ampholyte, Bio-Rad Laboratories) and shaken at every 10 min intervals for 30 min at 4^{o}C. To remove any insoluble materials, the samples were

subjected to centrifugation at 16,000xg for 20 min at 20^{o}C, and the resulting debris-free protein samples cleaned with ReadyPrep™ 2-D Cleanup Kit (Bio-Rad Laboratories) according to the manufacturer's instructions. Subsequently, the protein pellets were redissolved in rehydration buffer consisting of 7 M urea, 2 M thiourea, 4% CHAPS, 30 mM DTT, 2 mM TBP, 0.5% Bio-lyte and 0.002% bromophenol blue (w/v), and the protein concentration of each sample was measured by a Bradford assay (Bradford assay kit, Thermo-scientific, Pierce Biotechnology).

Two- dimensional electrophoresis and gel image analysis

Proteins from intracellular and extracellular *Y. pesitis* (200 µg bacterial protein per fraction) were focused individually in pH 3-10, 11 cm ReadyStrips™ IPG strips (Bio-Rad Laboratories), followed by a second-dimension SDS-PAGE electrophoresis on Criterion™ precast 8-16% gradient gels (Bio-Rad Laboratories) using a standard protocol. The resulting gels were stained with Coomassie brilliant blue G-250 and imaged with a VersaDoc™ Imaging System (Bio-Rad Laboratories). Using PDQuest™ 2-D Analysis Software (Bio-Rad Laboratories), a master gel image of extracellular protein spots was created by merging the images of the two extracellular-derived *Y. pestis* samples, and then, this master gel image was compared individually with the images of two intracellular-derived *Y. pestis* samples. The protein spots present on both gels of intracellular-derived *Y. pestis*, but absent from the master image of extracellular-derived *Y. pestis*, were selected for further analysis.

Tryptic digestion and MALDI-TOF analysis

Those protein spots identified to be reproducibly present in samples from intracellular *Y. pestis*, but absent in extracellular-derived *Y. pestis*, were excised. Gel plugs were washed three times in 50% v/v acetonitrile (ACN)/50 mM ammonium bicarbonate, then dehydrated in 100% ACN and dried at room temperature. The dried gel plugs were rehydrated with ice-cold trypsin (8 µg/mL) in 50 mM ammonium bicarbonate, and digested overnight at 37^{o}C. The resulting peptide fragments were extracted in 50% ACN /0.1% trifluoroacetic acid (TFA). Peptide extracts were dried to reduce their volume to ≈ 10 µL and were then mixed with one volume of 10 mg/mL α-cyano-4-hydroxycinnamic acid (CHCN) freshly dissolved in 50% ACN/0.1% TFA. Peptide ions were analyzed using a Voyager DE-PRO mass spectrometer (Applied Biosystems) operated in positive-ion, reflectron mode, and calibrated using a known mixture of synthetic peptides (external calibation). For each spectrum, Data Explorer v4.0 was used to extract the five most intense mono-isotopic m/z's within each 100-m/z interval. Alternatively, weaker spectra enjoyed manually optimized peak detection windows that were set slightly above the baseline noise threshold. Monoisotopic peptide masses were searched using MASCOT v2.2 (MatrixScience) in a local protein sequences database, consisting of 64,322 mouse sequences (taxonomy ID 10090) downloaded from UniProtKP database on June 30, 2010, and 8,265 *Yersinia pestis* CO92 sequence (txid214092) downloaded from NCBInr on June 30, 2010. Search were conducted stating cleavage with trypsin (allowing one missed cleavage), a stated mass accuracy of 100 ppm, and included the following variable peptide modifications: acetylation of protein N-termini, formylation of protein N-termini, cyclization of N-terminal Gln to

pyroglutamate, oxidation of Met, and acrylamide modifications of Cys (propionamide-Cys). Protein identifications were accepted if their MASCOT probability based MOWSE scores (PBM) were statistically significant, if the PBM of the top-ranked candidate was markedly superior to that of the next-ranked candidate, and if experimental peptide masses showed systematic discrepancies vs. hypothetical calculated peptide masses.

Results

Preparation of protein samples from *Y. pestis* grown in mouse macrophage RAW264.7 cells and in tissue culture media

In order to generate protein samples for intracellular *Y. pestis* with sufficient material to allow detection and identification of proteins present at low concentrations, $3.0x10^8$ RAW264.7 cells were infected with *Y. pestis* strain KIM6-2053.1+ for 8 h which yielded approximately $2x10^9$ CFUs for analysis. Infected RAW264.7 cells were lysed with 0.1% Triton X-100, intracellular *Y. pestis* isolated by differential centrifugation and subjected to sonication to prepare the intracellular protein samples. Two samples prepared for intracellularly grown *Y. pestis* yielded 291 and 332 µg protein and two samples of extracellularly grown *Y. pestis* yielded 1780 and 2070 µg protein. To identify proteins differentially expressed by intracellular *Y. pestis*, the four protein samples were subjected to two-dimensional gel electrophoresis. A master gel image of extracellular protein spots was created *in silico* by merging the images of the two extracellular protein images. *In silico* comparison of the two images for intracellular protein samples

identified 21 and 37 protein spots present in the intracellular but not in the extracellular protein samples. Out of these, 12 protein spots were common to both of the intracellular protein samples (Fig 1).

Protein profiles of *Y. pestis* grown in mouse macrophage cell line

Proteins unique to the intracellular *Y. pestis* protein samples were identified by searching their experimental peptide mass fingerprints against a database of known proteins. This approach is an accepted technique for protein identifications, particularly when analyzing proteins separated on two-dimensional gels (3). This resulted in the confident identification of nine *Y. pestis* proteins specific to intracellular growth, and three contaminating RAW264.7 proteins (Table 1).

After searching experimental peptide fingerprints with Mascot, superoxide dismutase SodA, inorganic pyrophosphatase, autonomous glycyl radical cofactor GrcA, molecular chaperone DnaK, serine endoprotease GsrA, global DNA-binding transcriptional dual regulator H-NS, urease subunit gamma UreA, and tellurite resistance proteins TerD and TerE were identified as yielding significant Mascot scores ($p<0.05$), indicating a non-random identification of these candidates. Moreover, Mascot scores for all these candidates were notably higher than those of the next-ranked candidates, indicating that there were no reasonable alternative identifications for these proteins. In addition, these experimental peptides represented a high percentage of each candidates' sequence (from 29 to 81%), further supporting arguments for valid identifications. Deviations between calculated vs. experimental peptide m/z's (mass error) were systematic with respect to peptide mass, consistent with minor imperfections in

instrument's calibration. These systematic mass error further argued for the validity of these identifications, because random matches between experimental vs. calculated peptides typically generate random mass errors.

In addition, RAW264.7 host cell contaminants, mitochondrial aldehyde dehydrogenase, ribonuclease inhibitor and ADP/ATP translocase were also identified as a strong candidate with favorable parameters (Table 1).

Discussion

In the rodent hosts, *Y. pestis* initially multiplies inside the macrophage phagolysosomes to escape host innate immunity prior to initiation of systemic infection (7, 16). The physiological mechanisms by which *Y. pestis* manages to survive and multiply inside phagolysosomes are not completely understood. Hence, studying intracellular grown *Y. pestis* protein profiles with reference to the protein profiles of *Y. pestis* cultured extracellularly may help to identify the proteins involving in the intracellular lifestyle of *Y. pestis*. Using two-dimensional electrophoresis and peptide mass fingerprinting, we identified nine *Y. pestis* proteins specific to intracellular growth (Table 1). While multiplying inside the macrophages, *Y. pestis* expressed a battery of proteins related with various aspects of stress ameliorators such as enzymes SodA, inorganic pyrophosphatase, and GrcA; proteins mediating responses to abnormally folded proteins such as chaperon DnaK and GsrA; transcriptional regulator such as DNA binding protein H-NS; as well as proteins not previously implicated in intracellular

survival such as urease subunit gamma UreA and tellurite resistance proteins TerD and TerE.

As a facultative intracellular pathogen at the initial stage of infection (12), it is reasonable to suppose that *Y. pestis* might induce expression of stress regulators to mediate survival and multiplication inside phagolysosomes. Concordant with this supposition, transcriptome analysis of *Y. pestis* residing in the buboes of experimentally infected rat revealed the expression of various genes related with oxidative and nitric oxide stresses and iron metabolisms including SodA and GrcA genes (17). Similarly, mRNAs corresponding to the proteins identified reported herein TerD, TerE, DnaK, inorganic pyrophosphatase and UreA were up regulated between 2- to 5.5-fold during chloramphenicol treatment of *Y. pestis* culturing at 37^{o}C, and in the same manner, polymyxin treatment at 26^{o}C induced 3.3-fold increased expression of DnaK (14, 24).

UreA is a product of polycistronic operon *UreABCEFGD* which forms a functional tri-heterotrimeric complex UreABC with the help of accessory proteins UreE, UreF, UreG, and UreD (15, 18). However, in *Y. pestis* insertion of an extra guanine residue in poly-G stretch of the open reading frame for UreD produces a truncated version of the protein resulting in failure to form an active urease in this species. Spontaneous deletion of this inserted G and subsequent reactivation of urease can occur at high frequency, especially in the presence of urea in the media (4, 15). Irrespective of its functional status, urease does not appear to have significant influence on *Y. pestis* experimental infection dynamics in a mouse model (15); however, under certain as yet undefined conditions of intracellular *Y. pestis* growth, UreA expression reported herein may be important for the intracellular lifestyle of *Y. pestis*.

Perhaps the most novel of the intracellular *Y. pestis* proteins identified herein were tellurite resistance proteins TerD and TerE. Tellurite sensitivity is common in Gram-negative bacteria, and tellurite resistance (Te^R) loci which also confer phage incompatibility are commonly carried on large R-plasmids (R478), but the Te^R loci in *Y. pestis* is chromosomal (9, 20). The R478 type Te^R loci consist of a *terZABCDE* operon, although the *ter* operon of some other Gram-negative bacteria lack *terD* and *terE*. Transposon insertion in *terZ, terC* and *terD* in *Escherichia coli* render mutants phage-compatible and sensitive to tellurite (22). The TerD and TerE proteins have extensive amino acid homology with the carboxy terminus of a cyclic AMP binding protein (CABP1) of the eukaryotic slime mold *Dictyostelium discoideum* (20). CABP1 is a cytoplasmic protein consisting of two subunits differing only by a 37 amino acid truncation in N-terminus of subunit-2 (1). Although the functional activities of TerD and TerE in Te^R are unknown, some have speculated that these proteins may have a primary function other than tellurite resistance, possibly by detoxifying antimicrobial compounds produced by host macrophages (20). Some evidence exists to support this contention in *Proteus mirabilis* in which expression of the *ter* operon is associated with oxidative stress as well as tellurite exposure (21).

It is unlikely that the proteomic screen presented here identified all of the factors involved in the intracellular lifestyle of *Y. pestis*. There are almost certainly some proteins that were either lost during processing or present at concentrations too low to detect. Nevertheless, the proteomics screen did identify several proteins previously implicated in intracellular residence of *Y. pestis* as detected by DNA microarrays or mutant screens in animal models. These proteins likely allow the bacteria to survive and

proliferate in the harsh phagolysosomal environment by down-regulating the expressions of unnecessary genes, controlling various metabolic process, renaturing or facilitating degradation of denatured proteins, and detoxifying host antimicrobial compounds. Furthermore, identification of tellurite resistance proteins TerD and TerE expression in *Y. pestis* infected macrophages suggests that these proteins may be previously underappreciated as potential virulence factors.

References

1. **Bain, G., and A. Tsang.** 1991. Disruption of the gene encoding the p34/31 polypeptides affects growth and development of Dictyostelium discoideum. Mol Gen Genet **226:**59-64.
2. **Bearden, S. W., J. D. Fetherston, and R. D. Perry.** 1997. Genetic organization of the yersiniabactin biosynthetic region and construction of avirulence mutants in *Yersinia pestis*. Infect Immun **65:**1659-1668.
3. **Bradshaw, R. A., A. L. Burlingame, S. Carr, and R. Aebersold.** 2006. Reporting protein identification data: the next generation of guidelines. Mol Cell Proteomics **5:**787-788.
4. **Brubaker, R. R., and A. Sulen.** 1971. Mutations influencing the assimilation of nitrogen by *Yersinia pestis*. Infect Immun **3:**580-588.
5. **Cavanaugh, D. C., and R. Randall.** 1959. The role of multiplication of *Pasteurella pestis* in mononuclear phagocytes in the pathogenesis of flea-borne plague. J Immunol **83:**348-363.
6. **Geng, J., Y. Song, L. Yang, Y. Feng, Y. Qiu, G. Li, J. Guo, Y. Bi, Y. Qu, W. Wang, X. Wang, Z. Guo, R. Yang, and Y. Han.** 2009. Involvement of the post-transcriptional regulator Hfq in *Yersinia pestis* virulence. PLoS One **4:**6213-6223.
7. **Grabenstein, J. P., H. S. Fukuto, L. E. Palmer, and J. B. Bliska.** 2006. Characterization of phagosome trafficking and identification of PhoP-regulated genes important for survival of *Yersinia pestis* in macrophages. Infect Immun **74:**3727-3741.

8. **Lindler, L. E., and B. D. Tall.** 1993. *Yersinia pestis* pH6 antigen forms fimbriae and is induced by intracellular association with macrophages. Mol Microbiol **8:**311-324.

9. **Parkhill, J., B. W. Wren, N. R. Thomson, R. W. Titball, M. T. Holden, M. B. Prentice, M. Sebaihia, K. D. James, C. Churcher, K. L. Mungall, S. Baker, D. Basham, S. D. Bentley, K. Brooks, A. M. Cerdeno-Tarraga, T. Chillingworth, A. Cronin, R. M. Davies, P. Davis, G. Dougan, T. Feltwell, N. Hamlin, S. Holroyd, K. Jagels, A. V. Karlyshev, S. Leather, S. Moule, P. C. Oyston, M. Quail, K. Rutherford, M. Simmonds, J. Skelton, K. Stevens, S. Whitehead, and B. G. Barrell.** 2001. Genome sequence of *Yersinia pestis,* the causative agent of plague. Nature **413:**523-527.

10. **Perry, R. D., and J. D. Fetherston.** 1997. *Yersinia pestis*--etiologic agent of plague. Clin Microbiol Rev **10:**35-66.

11. **Pujol, C., and J. B. Bliska.** 2003. The ability to replicate in macrophages is conserved between *Yersinia pestis* and *Yersinia pseudotuberculosis*. Infect Immun **71:**5892-5899.

12. **Pujol, C., and J. B. Bliska.** 2005. Turning *Yersinia* pathogenesis outside in: subversion of macrophage function by intracellular *Yersiniae*. Clin Immunol **114:**216-226.

13. **Pujol, C., J. P. Grabenstein, R. D. Perry, and J. B. Bliska.** 2005. Replication of *Yersinia pestis* in interferon gamma-activated macrophages requires *ripA*, a gene encoded in the pigmentation locus. Proc Natl Acad Sci USA **102:**12909-12914.

14. **Qiu, J., D. Zhou, L. Qin, Y. Han, X. Wang, Z. Du, Y. Song, and R. Yang.** 2006. Microarray expression profiling of *Yersinia pestis* in response to chloramphenicol. FEMS Microbiol Lett **263:**26-31.

15. **Sebbane, F., A. Devalckenaere, J. Foulon, E. Carniel, and M. Simonet.** 2001. Silencing and reactivation of urease in *Yersinia pestis* is determined by one G residue at a specific position in the *ureD* gene. Infect Immun **69:**170-176.

16. **Sebbane, F., D. Gardner, D. Long, B. B. Gowen, and B. J. Hinnebusch.** 2005. Kinetics of disease progression and host response in a rat model of bubonic plague. Am J Pathol **166:**1427-1439.

17. **Sebbane, F., N. Lemaitre, D. E. Sturdevant, R. Rebeil, K. Virtaneva, S. F. Porcella, and B. J. Hinnebusch.** 2006. Adaptive response of *Yersinia pestis* to extracellular effectors of innate immunity during bubonic plague. Proc Natl Acad Sci USA **103:**11766-11771.

18. **Sebbane, F., M. A. Mandrand-Berthelot, and M. Simonet.** 2002. Genes encoding specific nickel transport systems flank the chromosomal urease locus of pathogenic *Yersiniae*. J Bacteriol **184:**5706-5713.

19. **Straley, S. C., and P. A. Harmon.** 1984. Growth in mouse peritoneal macrophages of *Yersinia pestis* lacking established virulence determinants. Infect Immun **45:**649-654.

20. **Taylor, D. E.** 1999. Bacterial tellurite resistance. Trends Microbiol **7:**111-115.

21. **Toptchieva, A., G. Sisson, L. J. Bryden, D. E. Taylor, and P. S. Hoffman.** 2003. An inducible tellurite-resistance operon in *Proteus mirabilis*. Microbiology **149:**1285-1295.

22. **Whelan, K. F., R. K. Sherburne, and D. E. Taylor.** 1997. Characterization of a region of the *IncHI*2 plasmid R478 which protects *Escherichia coli* from toxic effects specified by components of the tellurite, phage, and colicin resistance cluster. J Bacteriol **179:**63-71.

23. **Zauberman, A., S. Cohen, E. Mamroud, Y. Flashner, A. Tidhar, R. Ber, E. Elhanany, A. Shafferman, and B. Velan.** 2006. Interaction of *Yersinia pestis* with macrophages: limitations in YopJ-dependent apoptosis. Infect Immun **74:**3239-3250.

24. **Zhou, D., Y. Han, J. Qiu, L. Qin, Z. Guo, X. Wang, Y. Song, Y. Tan, Z. Du, and R. Yang.** 2006. Genome-wide transcriptional response of *Yersinia pestis* to stressful conditions simulating phagolysosomal environments. Microbes Infect **8:**2669-2678.

Table 1. Mascot search summary of *Y. pestis* proteins expressed inside a mouse macrophage cell line

Spot No	ID	Gene locus tag in *Y. pestis* CO92 genome	Mascot^R PBM score/ Mascot^R threshold ($p > 0.05$)	PBM score of next ranked candidate	No of peptides matched / Searched	% of sequence coverage	Calculated MW / Apparent MW (kDa)	Calculated pI / Apparent pI	e-value
1	Superoxide dismutase-A (SOD-A)	YPO4061	99/61	58	9/31	37	23.223/25	5.89/5.7	8.3e-006
2	Inorganic diphosphatase	YPO3521	81/61	62	6/15	29	19.602/25	4.91/5.2	0.00056
3	Autonomous glycyl radical cofactor GrcA	YPO2705	95/61	58	9/54	81	14.344/15	4.72/4.0	0.000025
4	Molecular chaperone DnaK	YPO0468	306/61	64	30/43	55	68.982/75	4.86/4.8	1.8e-026
5	Serine endoprotease (GsrA)	YPO3382	85/61	42	21/110	45	49.836/53	8.81/8.2	0.00022
6	Global DNA-binding transcriptional dual regulator H-NS	YPO2175	126/61	44	12/42	65	15.009/15	5.26/4.1	1.8e-008
7	Urease gamma subunit (UreA)	YPO2339	76/61	54	7/16	71	11.042/10	5.35/4.2	0.002
8	Tellurite resistance protein-D (TerD)	YPO0298	78/61	50	8/28	48	20.563/22	4.77/4.5	0.0012
9	Tellurite resistance protein-E (TerE)	YPO0299	92/61	45	13/74	64	20.663/24	4.65/4.3	0.000048
10	Mitochondrial-Aldehyde dehydrogenase	Mouse	90/61	50	13/39	25	56.502/80	7.53/6.1	0.000066
11	Ribonuclease inhibitor	Mouse	76/61	58	12/54	38	49.784/34	4.69/4.1	0.002
12	ADP/ATP translocase	Mouse	63/61	54	9/44	22	35.235/32	9.62/8.7	0.033

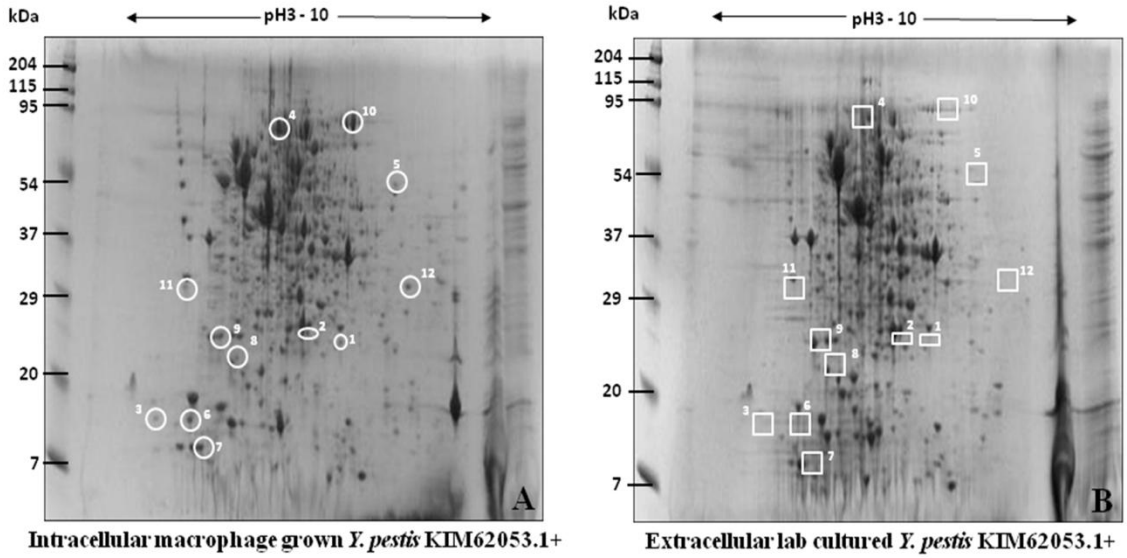

Fig.1. Coomassie brilliant blue G-250 stained two-dimensional gels of intracellular macrophage grown (A) and extracellular lab cultured (B) Y. pestis KIM62053.1+ protein samples. Protein spots marked (O) in KIM62053.1+ intracellular bacteria (A) are absent in corresponding location (□) in KIM62053.1+ extracellularly cultured (B) protein samples. The identity of protein spots marked (O) in KIM62053.1+ intracellular bacteria (A) is in Table 1.

CHAPTER V

EXPRESSION OF *YERSINIA PESTIS* TELLURITE RESISTANCE OPERON DURING MOUSE MACROPHAGE INFECTION

Abstract

The etiologic agent of plague *Yersinia pestis* causes severe disease in natural rodent hosts as a flea borne infection. In rodents, *Y. pestis* inoculated subcutaneously is phagocytized by local tissue macrophages in which the bacterium subsequently multiplies during the initial stage of infection before causing septicemic plague. In our previous experiments, intracellular *Y. pestis* in macrophages exhibited stress induced filamentous cellular morphology with 4-fold higher genomic equivalences (GEs) per colony forming unit (CFU) ratio. Further, during macrophage infections, *Y. pestis* proteins TerD and TerE were observed in protein samples from intracellular but not from extracellular *Y. pestis*. In laboratory adapted *E. coli*, expression of *ter* operon genes *terZ*, *-A*, *-B*, and *-C* from pathogenic *E. coli* caused the bacterium to assume filamentous cellular morphology similar to *Y. pestis* during macrophage infections (37). Based on these observations and the high DNA sequence homology of *E. coli* and *Y. pestis ter* operons, we speculated that filamentous morphologic stress response of *Y. pestis* in macrophage infections may be a consequence of expression of *Y. pestis ter* operon. To better understand the possible association of *ter* expression and *Y. pestis* filamentous stress response, the relationship between *Y. pestis ter* operon expression, resistance to tellurite toxicity, and the bacterial morphological changes were studied. These experiments revealed that *Y. pestis ter* operon genes *terC*, *-D* and *-E* were upregulated 3 to 4-fold for mouse macrophage infection during the initial period of experiment, and thereafter, the expression levels returned to those of PBS treated control groups. Similar to this expression pattern, all these genes were induced by sodium tellurite to increase expression by 2 to 4-fold. In addition, *Y. pestis* cultured in the presence of sodium tellurite showed resistance upto

312.5 µg/mL and assumed filamentous cellular morphology similar to that observed during mouse macrophage infection. Overall, these experiments support a possible role for the proteins of the *Y. pestis ter* operon in a stress response of *Y. pestis* involving filamentous cellular morphology during the early stage of macrophage infection.

Introduction

The causative agent of plague, the Gram-negative bacterium *Y. pestis*, has evolved as a systemic pathogen from its close relative the enteric pathogen *Yersinia pseudotuberculosis* (1, 19, 31). *Y. pestis* causes severe disease in natural rodent hosts, in which outbreaks can cause the loss of entire local populations (3, 8, 13, 19). Transmission between rodents is primarily by fleas which act as biological vectors (3, 19). After inoculation of rodents by the bite of infected fleas, *Y. pestis* is phagocytized by both the local neutrophils and macrophages (14, 16, 19). Subsequently, neutrophils kill the bacteria; whereas, in contrast, *Y. pestis* survives and multiplies intracellularly in macrophages for a short period before disseminating to initiate severe systemic infection (7, 11, 19, 21-23, 28, 29). From our previous experiment, *Y. pestis* strain KIM6+ infection of mouse and dog primary and tissue culture macrophages showed the presence of intracellular stress induced filamentous *Y. pestis* in macrophages, especially during the initial stage of infection. These filaments were either partially or fully non-septated and confined within tight *Yersinia* containing vacuoles (YCV). Further, these filaments had multiple genomes per bacterium as evidenced by approximately 4-fold higher GE per CFU ratio in macrophages during the early stage of infection (Chapter 3).

In addition to the filamentous cellular morphology observed in mouse macrophage infections, *Y. pestis* proteins TerD and TerE from tellurite resistance *ter* operons *terZABCDE* were detected by proteomics in intracellular *Y. pestis* in RAW2647 cell infection but not in *Y. pestis* grown in extracellular culture at 8 h post infection (p.i.) (9, 18, 20). Similarly, the expression of *Y. pestis ter* operon genes *terZABC*, *terZAB*, or *terDE* was observed by others to be upregulated by exposure to stressors such as streptomycin, polymyxin or chloramphenicol, respectively (24, 25, 38). Intact *terZABCDE* gene cluster is also indispensable for the survival of uropathogenic *E. coli* in the presence of hydrogen peroxide in culture media and in mouse peritoneal macrophages (33). Exposure of *Proteus mirabilis* culture to hydrogen peroxide induced expression of the *terZABCDE* operon (32). Apart from these potential roles in bacterial stress regulation, *terZABCDE* operon has also been associated with bacterial resistance to certain phage attack and pore-forming colicins (37). It is noteworthy to mention here that the *ter* operons from *Y. pestis*, pathogenic *E. coli* and *P. mirabilis* exhibit significant sequence homology to one another (30). Interestingly, laboratory *E. coli* strain DH5α transformed with and actively expressing *ter* operon genes *terZ*, *-A*, *-B* and *-C* from pathogenic *E. coli* exhibited filamentous cellular morphology similar to that observed for *Y. pestis* in macrophage infections (37). Based on these observations, we speculate that filamentous cellular morphology of *Y. pestis* in macrophage infections may be associated with expression of proteins from *Y. pestis ter* operon which are induced by the intracellular stress. To investigate this possibility further, we examined the temporal expression profiles of *Y. pestis ter* operon genes *terC*, *-D* and *-E* during mouse macrophage infection and compared these expression profiles to those for *Y. pestis*

cultures exposed to tellurite or chloramphenicol. Also, we determined minimum inhibitory concentration (MIC) for and bacterial cellular morphology of *Y. pestis* to sodium tellurite exposure. The resulting experiment supports the proposed speculation, as *Y. pestis ter* operon expression was induced during the macrophage infections and the expression caused *Y. pestis* to exhibit filamentous cellular morphology.

Materials and methods

Bacterial strain and growth conditions

Y. pestis strain KIM62053.1+ reported in Chapter 3 was used for this study. Briefly, isolated colonies on Brain Heart Infusion (BHI) (Difco, Becton Dickinson Company, USA) agar plates were inoculated into BHI broth and cultured overnight at 26^{o}C with 160 rpm shaking.

Tissue culture cell and growth conditions

Mouse macrophage-like cell line RAW264.7 provided by Dr. Guolong Zhang, Department of Animal Science, Oklahoma State University was cultured in RPMI-1640 media containing 10% FBS at 37^{o}C with 5% CO_2 tension.

Light and electron microscopic examinations of *Y. pestis* infected RAW264.7 cells

Y. pestis strain KIM6+ infected RAW264.7 cells were sampled at 2.5 h p.i., processed and examined under light and transmission electron microscopes as mentioned in Chapter 3.

Preparation of *Y. pestis* infected RAW264.7 cell samples for quantification of *ter* operon expression in macrophage infections

RAW264.7 cells infected with *Y. pestis* strain KIM6+ as described in Chapter 3 were sampled at 0.5, 1.0, 2.0, 4.0 and 8.0 h p.i. At the time of sampling, 75 cm^2 tissue culture flasks having infected RAW264.7 cells were washed thrice with sterile PBS, 2 mL of RNA*later*® solution (Applied Biosystems, USA) was added to each flask, and finally, these infected cells were fixed in the same solution at 4^oC for overnight and stored at -20^oC. The stored samples were processed for RNA isolation as described below.

Induction of *Y. pestis ter* operon with sodium tellurite, chloramphenicol, or PBS

Y. pestis strain KIM6+ cultured in BHI broth at 26^oC for overnight was appropriately diluted in RPMI-1640 media with 10% FBS to yield 1 X 10^7 CFUs/mL. Subsequently, this inoculum was dispensed into three conical flasks at 30 mL/flask. To each of these flasks, an additional 30 mL of RPMI-1640 media with 10% FBS contained sodium tellurite, chloramphenicol or PBS (control) was added to the final concentrations of 3.125 µg/mL sodium tellurite, 320 µg/mL chloramphenicol, or equivalent volume of PBS, respectively. The flasks were incubated at 37^oC with 220 rpm shaking, and 10 mL

samples were collected at 0.5, 1.0, 2.0, 4.0, and 8.0 hours of culturing. From these samples, *Y. pestis* was pelleted at 1,500xg for 10 min at 4^{o}C, resuspended in 2 mL of RNA*later* and fixed at 4^{o}C for overnight and then stored at -20^{0}C. At the same time, uninfected RAW264.7 cells grown in 75 cm^2 flasks were washed thrice with and then released into sterile PBS. Subsequently, the cell concentration was measured, and cells were centrifuged at 250xg for 10 min and resuspended in RNA*later* solution such that every 2 mL containing 10^7 RAW264.7 cells. Finally, these cells were fixed at 4^{o}C for overnight and stored at -20^{0}C until processed further. At the time of RNA isolation, for every 2 mL of above fixed *Y. pestis* culture from tellurite, chloramphenicol or PBS treatment, 2 mL of RNA*later* fixed RAW264.7 cells was added, and then the cells were pelleted at 5,000xg for 10 min at 4^{o}C. Subsequently, these pellets were subjected sequentially to total RNA isolation, reverse transcription reaction and quantification of expressions of genes, *terC*, *-D* and *-E* as mentioned below.

Isolation of total RNA from *Y. pestis* infected RAW264.7 cells and *Y. pestis* cultures treated with sodium tellurite, chloramphenicol or PBS

For RNA isolation, the RNA*later* fixed infected RAW264.7 cells and *Y. pestis* pellets obtained from sodium tellurite, chloramphenicol or PBS treatment were thoroughly resuspended each in 1 mL of TRI reagent® (Applied Biosystems) by brief vertexing. Thereafter, bromochloropropane (BCP) (Sigma Aldrich) at $1/10^{th}$ volume of TRI reagent was added to the TRI reagent resuspensions, vertexed briefly, incubated at room temperature for 5 min, and then centrifuged at 12,000xg for 15 min at 4^{o}C. The resulting aqueous phase (top transparent layer) was transferred into new microcentrifuge

tube, mixed briefly with isoprophenol (Sigma Aldrich) at 1/2 volume of TRI reagent, incubated at room temperature for 10 min and finally centrifuging at 12,000xg for 10 min at 20^{o}C to pellet out the total RNA from the solution. Subsequently, the RNA pellets were washed once with 75% ethanol (Sigma Aldrich) at 12,000xg for 10 min at 4^{o}C, air dried completely, and resuspended in Tris-EDTA buffer pH8.0. From this preparation, 10 µg of total RNA was treated with 4 units of DNase-I (New England Biolabs Inc.) in 100 µL volume at 37^{o}C for 20 min, and by adding of EDTA to a final concentration of 5 mM, the DNase-I was inactivated at 75^{o}C for 10 min. From this preparation, 500 ng of total RNA was subjected to reverse transcription reaction in 20 µL volume by using the mixture of all the reverse primers noted in Table 1 at the final concentration of 10 pM of each primer. The reaction was performed using a DyNAmo^{TM} cDNA synthesis kit (Finnzymes, Thermo Fisher Scientific). Briefly, from the total RNA isolated, cDNA was synthesized at 37^{o}C for 60 min and the reaction was terminated by heating at 85^{o}C for 5 min. Then the samples were cooled at 4^{o}C and stored at -20^{o}C or processed further. These cDNA samples were subsequently used to quantify the relative mRNA concentrations of *Y. pestis* genes *terC*, *terD*, *terE* and *tmK*. The *Y. pestis* gene *tmK* was used as the reference gene. For the quantification, 2 µL of above synthesized cDNA was transferred into 20 µL of fast SYBR® green master mix (Applied Biosystems) contained 300 nM final concentrations of each forward and reverse primers of gene *terC*, *terD*, *terE*, or *tmK*. The reaction was performed in a 7500 Fast Real-Time PCR system (Applied Biosystem) with the following settings: one cycle of initial enzyme activation at 95^{o}C for 20 sec and then 40 cycles of denaturation at 95^{o}C for 3 sec and annealing/extension at 60^{o}C for 30 sec. The resulting ct-values obtained were used to calculate the relative expression rates

of *Y. pestis* genes *terC*, *-D* and *-E* in RAW264.7 cell infections or exposure to sodium tellurite or chloramphenicol compared to those of PBS treated control groups. Comparative ΔΔct method explained by Bustin (4-6) was used for the calculation as described below.

Δct(experimental *terC*, *-D* or *-E*) = ct(experimental *terC*, *-D* or *-E*) – ct(experimental *tmK*)

Δct(control *terC*, *-D* or *-E*) = ct(control *terC*, *-D* or *-E*) – ct(control *tmK*)

ΔΔct = Δct(experimental *terC*, *-D* or *-E*) – Δct(control *terC*, *-D* or *-E*)

Relative expression (fold change) of *Y. pestis* gene *terC*, *-D* or *-E* in test samples to that of control groups = $2^{-\Delta\Delta ct}$

Determination of minimum inhibitory concentration (MIC) of sodium tellurite for *Y. pestis*

For this experiment, BBL™ Prompt™ system (Becton, Dickinson and Company, NJ, USA) was used according to the manufacturer's instruction to prepare *Y. pestis* test inoculum of $1x10^8$ CFU/mL in saline. Subsequently, the stock inoculum was 50-fold diluted in Luria-Bertani (LB) (Sigma) broth to prepare the working inoculum, $2x10^6$ CFU/mL.

In a 96-well U-bottom plate, two-fold serially diluted sodium tellurite in LB broth contained maximum concentration of 10 mg/mL was dispensed at 50 µL/well in an orderly manner starting with column A1-G1 to down A12-G12. As a control, 50 µL normal LB broth contained PBS was added to each well in H1 to H12. Finally, 50 µL/well of *Y. pestis* working inoculum described above was added to all the wells on the plate, yielding $1x10^6$ CFUs/mL. The plate was incubated at 28°C for overnight and then

the minimum concentration of sodium tellurite at which no visible growth of *Y. pestis* observed was recorded as MIC.

Colony morphology of *Y. pestis* on tellurite agar plates

Isolated colonies from BHI agar plates were streaked directly on fresh LB agar plates containing 100 µg/mL of sodium tellurite or PBS as the replacement to sodium tellurite. These plates were incubated at 28^{o}C for 2 to 3 days, and the resulting colony morphologies were visualized.

Light microscopic examination of *Y. pestis* cultures treated with sodium tellurite, chloramphenicol or PBS

Y. pestis strain KIM6+ was cultured in RPMI -1640 media with 10% FBS containing 30 µg/mL sodium tellurite, 320 µg/mL chloramphenicol, or equivalent volume sterile PBS for 2.5 h at 37^{o}C with 220 rpm shaking. Subsequently, samples from each of these cultures were spun onto the microscopic slides at moderate speed for 5 min using a cytocentrifuge (Statspin Cytofuge, Norwood, MA, USA). Later, the slides were stained with Wright Giemsa stain and examined via light microscopy at 1,000x magnification.

Statistical analysis

Mean fold changes of expression of genes *terC, -D* and *-E* from the experimental groups were compared with their respective controls through two tailed student's t-test. The same analysis was made on the changes of expression of gene *terC, -D* or *-E* between different sampling intervals. Furthermore, in a given sampling interval, the

genes *terC*, *-D* and *-E*, expressions were compared with one another within them. Significant difference in the mean fold changes of expression of *terC*, *-D* and *-E* was reported at p-value < 0.01 or < 0.05 wherever appropriate.

Results

Cellular filamentous morphology of *Y. pestis* in mouse macrophage infections

Light and electron microscopic examinations of *Y. pestis* strain KIM6+ infected mouse macrophage cell line RAW264.7 revealed the presence of filamentous *Y. pestis* in tightly confining intracellular vacuoles at 2.5 h p.i. (Fig. 1). These filamentous *Y. pestis* were on an average 6.9 ± 1.9 µm long with the range from 5.2 to 11.1 µm and either partially or fully non-septated. Further, comparing the GEs with CFUs for intracellular *Y. pestis* in macrophage at 2.5 h p.i. indicated that the intracellular filamentous *Y. pestis* possessed multiple genomes per bacterium (data shown in Chapter 3).

Expression of *Y. pestis* genes *terC*, *terD* and *terE* during mouse macrophage infections and exposure to tellurite or chloramphenicol

Besides filamentous cellular morphology, *Y. pestis* residing in macrophages had increased levels of *ter* operon proteins TerD and TerE compared with culture grown *Y. pestis* at 8 h p.i. (20). In order to confirm the intracellular expression of *Y. pestis ter* operon during mouse macrophage infections and to examine further the temporal expression patterns of this operon during infection, the relative quantification of

transcripts of *Y. pestis* genes *terC, terD* and *terE* were measured. In addition, the same measurement was made for *Y. pestis* cultures exposed to tellurite or chloramphenicol for comparison of the magnitude of the response as well as to serve as positive controls. For the macrophage infection, *Y. pestis terC, terD,* and *terE* genes were 2.5 to 3-fold upregulated at 0.5 h p.i. with further modest increase at 1 h p.i. for *terD* and ter*E* to 3 to 3.5-fold compared with culture grown control groups (Fig. 2A, Table 2A). However, *terC* expression at 1 h p.i. dropped slightly from the level at 0.5 h p.i. and was significantly less than that of *terD* or *terE* expression. After 1 h p.i., the expression rates began to decrease; at 4 and 8 h p.i, the magnitudes of expressions either did not vary or was slightly down regulated from the respective negative controls. *Y. pestis* exposed to tellurite also upregulated the expression of all the three genes at varying levels similar to in macrophage infection (Fig. 2B, Table 2B). After 30 min post-exposure (p.e.), except for slight upregulation of *terD,* there were no noticeable changes with the expressions of genes *terC* and *terD.* But after 1 h p.e., all the three genes were significantly upregulated upto 3 to 4-fold (Fig. 2B). At 2 h p.e., the expression of *terC, terD* and *terE* was still above the control levels, but the fold changes were lower at 2 h than they were at 1 h p.e., especially concerning with *terD* and *terE* genes. At 4 and 8 h p.e., the genes either were down regulated slightly or did not vary from the respective control groups.

As a positive control, chloramphenicol at the concentration of 10 x MIC (320 µg/mL) was used as determined by Wendte *et al*. (2011), to induce *ter* operon of *Y. pestis* (25, 36). During the first 2 h p.e., upregulation of genes *terC, terD* and *terE* to various extent was noticed (Fig. 2C, Table 2C). Subsequently, the overall expressions dropped at 4 h p.e.; however, *terC* and *terD* mRNA concentrations were still marginally higher than

those of control groups. At 8 h p.e., *terC* and *terD* expressions did not vary from the respective controls, but *terE* was noticeably down regulated. As a whole, these results indicate that when *Y. pestis* resides inside the macrophages, the bacterial *ter* operon expression is likely induced by intracellular stress similar to stress elicited by exposure of *Y. pestis* to tellurite or chloramphenicol.

Y. pestis **resistance to sodium tellurite**

The experimental results for expression of *Y. pestis ter* operon in macrophage infections and various *in vitro* stimuli indicated that *Y. pestis* tellurite operon is intact as shown by genomic sequencing studies and is actively expressed (9, 18). To confirm that *Y. pestis* exhibits resistance to tellurite metal similar to *E. coli*, the minimum inhibitory concentration (MIC) for sodium tellurite for *Y. pestis* strain KIM6+ was determined. When *Y. pestis* was grown overnight at 28^{o}C in LB broth containing various concentration of sodium tellurite, no growth was observed at the tellurite concentration ≥ 312.5 µg/mL. Below this specific concentration, the bacterial growth associated with blackish precipitation at the bottom of 96-well plate was observed. Further, *Y. pestis* strain KIM6+ streaked on LB agar contained 100 µg/mL sodium tellurite also produced black colonies measuring 1 to 3 mm size (Fig. 3). These observations indicate that *Y. pestis* strain KIM6+ is capable of growing in the presence of tellurite metal and of converting soluble tellurite into insoluble tellurium.

Cellular filamentous morphology of *Y. pestis* to the exposure of tellurite or chloramphenicol

Presence of tellurite or chloramphenicol in the culture media upregulated the expression of *Y. pestis ter* operon genes. Hence, under the influence of *ter* operon expression, *Y. pestis* may assume the filamentous cellular morphology as noticed in laboratory *E. coli* expressing *ter* operon from pathogenic *E. coli*. To this end, morphological features of *Y. pestis* grown in RPMI-1640 media with 10% FBS containing sodium tellurite, chloramphenicol or PBS were observed under light microscopy. As with *E. coli*, *Y. pestis* exposed to sodium tellurite exhibited filamentous cellular morphology (Fig. 4B). Comparing with PBS treated cultures, tellurite exposed *Y. pestis* cultures were extensively filamentous in shape, and some of those filaments had multiple darkly stained probable nuclear materials (nucleoids) along the length (Inset from Fig. 4B). Interestingly, this filamentous morphology in *in vitro* culture is comparable to that of *Y. pestis* in macrophage infections. Chloramphenicol treated *Y. pestis* cultures were predominantly coccobacilli in form similar to PBS treated controls, but some filaments were also observed (Fig. 4C). Overall, the filamentous cellular morphology of *Y. pestis* in tellurite containing *in vitro* culture is compatible with that in mouse macrophage infections, which may be related to effects of the proteins from tellurite resistance operon induced to expression by the exposure of *Y. pestis* to tellurite metal.

Discussion

Y. pestis inoculated subcutaneously in rodent hosts is phagocytized by local macrophages, in which the bacterium survives and multiplies intracellularly before causing systemic infection (7, 11, 21-23, 28, 29). In our experiment, intracellular *Y. pestis* in infected mouse macrophages assumed filamentous cellular morphology at 2.5 h p.i. (Fig. 1), which later returned to normal coccobacillary form (Chapter 3). These filamentous *Y. pestis* had either partial or no septation and more than one genomic equivalence per bacterium. Appearance of this filamentous cellular morphology mirrored the filamentous structure of laboratory *E. coli* transformed with and actively expressing *ter* operon genes *terZ, -A, -B* and -*C* from pathogenic *E. coli* (37). Consistent with these observations in *E. coli*, *Y. pestis* residing in macrophages also expressed *ter* operon proteins TerD and TerE at 8 h p.i. (20). Further, the expression of genes from *Y. pestis ter* operon has been shown to be upregulated by various stressful stimuli including some which mimic the intracellular environment in macrophage infections (24, 25, 38). Therefore, it is plausible that the filamentous cellular morphology of intracellular *Y. pestis* in macrophage infections is associated with expression of *ter* operon proteins induced by bacterial stress. In support of this speculation, we observed that *Y. pestis ter* operon genes *terC, -D* and -*E* were upregulated upto 2.5 to 3.5 fold after 0.5 to 1 h p.i. in RAW264.7 cells as a response to the intracellular stress (Fig. 2A). Importantly, these changes in expression closely correlated with the presence of filamentous *Y. pestis* in macrophages. In addition, *Y. pestis* exposed to tellurite stress also showed upregulation of expression of all three genes at different levels from 0.5 to 2 h p.i. (Fig. 2B). These tellurite treated *Y. pestis* exhibited long filamentous forms similar to those observed

intracellularly in mouse macrophages (Fig. 4B). Close examination of each of these filaments revealed the presence of multiple nucleoid along the length of the filaments. Considering these observations together they support the potential role of *Y. pestis ter* operon in the intracellular environment as a part of *Y. pestis* stress regulation.

Although proteins from *ter* operon may be associated with the filamentous cellular morphology of intracellular *Y. pestis* in macrophages, the molecular mechanism involved in this filamentation process is not clear. Likely, proteins from *Y. pestis ter* operon may act as signal transducers connecting cell surface recognition of stress to the bacterial cell division machinery. In support of this hypothesis, TerD and TerE proteins have significant amino acid sequence homology to the C-terminus of cyclic AMP-binding protein-1 (CAMP-1) from *Dictyostelium discoideum* which is likely involved in cellular signaling mechanisms (30, 35). In addition, *Y. pestis ter* proteins TerA, TerD and TerE are, respectively, 34.2%, 87.9% and 64.5% homologous to *Klebsiella pneumoniae* protein TerD which belongs to von Willebrand factor domain-A (vWFA) super family which exhibits strong calcium binding capacity, providing a strong probability that the *ter* operon proteins may be signaling molecules for an unknown bacterial physiological process (17). Beyond these associations, none of *Y. pestis ter* operon proteins has striking amino acid homology to any bacterial protein known for involvement in the process of cell division (2, 10, 12, 15, 27).

Y. pestis ter operon gene map derived from genomic sequencing studies shows that genes *terZ, -A, -B, -C, -D* and *-E* are presumably transcribed in an unidirectional pattern from *terZ* to *terE* by promoter sequence located 5' to *terZ* gene. Thus, the mRNAs concentrations of the genes *terC, -D* and *-E* would be anticipated to be present at

nearly an equal proportion for any given sampling time. However, in our experiments, *Y. pestis* genes *terC, -D,* and *-E* were not expressed in proportion to one another; as the expression of gene *terC, -D,* or *-E* varied significantly from the other two at 1 h p.i. in macrophage infections (Fig 2A), at 2 and 8 h p.e. in tellurite exposure (Fig 2B), and all the time points in chloramphenicol exposure. This disproportional expression is possible if *Y. pestis ter* operon has more than one functional transcription start site. Using the 1999 Neural Network Promoter Prediction (NNPP) version 2.2 program from Berkeley Drosophila Genome Project (http://www.fruitfly.org/seq_tools/promoter.html) (26) to search for the possible prokaryotic RNA polymerase-II binding sites on the whole operon including 200bp upstream of 5' end of *terZ* translation start site revealed that there are twelve strong candidates for promoter sequences with probabilities of 95 to 100%. Of these twelve promoter sequences, six are clustered in front of *terZ* translation start site, and the remaining are scattered throughout the operon. Particularly, there are promoter sequences in front of genes *terC, -D* and *-E* with the probability of 98, 97 and 99%, respectively. In contrast to multiple promoter sequences, the entire operon has only one well recognizable intrinsic transcription terminator, positioning 18bp downstream to 3' end of *terE*. Thus, it is possible to have different lengths of transcripts from *Y. pestis ter* operon. Specifically, transcript *terCDE, terDE* or *terE* can be present in the test samples we measured.

Conversion of tellurite into black crystals by *Y. pestis* indicates that the bacterium is capable of reducing water soluble, toxic tellurite (TeO_3^{2-}) into water insoluble, non toxic tellurium (Te^0) (30, 34). Although precise mechanism by which tellurite detoxification occurs in *Y. pestis* is not known, for *E. coli*, *P. mirabilis*, *Pseudomonas*

pseudoalcaligenes, and *Xanthomonas campestris*, it is thought that tellurite likely enters into the bacterium through phosphate channels and is reduced to Te^0 by various cytoplasmic reductases (34). Subsequently, Te^0 is either deposited on the cytoplasmic membrane or effluxed into the media. Te^0 also has the capability to induce bacterial reactive oxygen species (ROS) production by reacting with molecular O_2, the induction of which can prepare the bacterium for various other external stresses (34). In this sequence of events, *ter* operon proteins are believed to be beneficial for the bacterium to replenish the cytoplasmic reductase enzymes concentration especially NADPH reductase (34).

Although *ter* operon confers resistance to tellurite ion, *Y. pestis* is not exposed to tellurite in its normal ecological niche. In the absence of selection pressure by tellurite, *Y. pestis ter* operon is more vulnerable to mutational changes, particularly when the plasticity of *Y. pestis* genome highly favors this change (9, 18). However, various strains of *Y. pestis* isolated from distant geographical locations and *Y. pseudotuberculosis* strain IP32953 share completely identical copies of *ter* operon with 100% sequence homology. This unexpected DNA homology suggests that the proteins from *Y. pestis ter* operon are not primarily involved in the process of conferring resistance against tellurite metal; whereas, this tellurite resistance property may be a secondary function or side effect to an unknown metabolic and/or regulatory function of *ter* operon.

In conclusion, the results of this study demonstrate that although *Y. pestis ter* operon confers resistance to tellurite metal when the metal is present, the proteins from this operon are induced by intracellular stress in macrophage infections and may cause *Y. pestis* to assume a filamentous cellular morphology as an adaptive cellular change to withstand the harsh intracellular environment.

References

1. **Achtman, M., K. Zurth, G. Morelli, G. Torrea, A. Guiyoule, and E. Carniel.** 1999. *Yersinia pestis*, the cause of plague, is a recently emerged clone of *Yersinia pseudotuberculosis*. Proc Natl Acad Sci USA **96:**14043-14048.
2. **Adams, D. W., and J. Errington.** 2009. Bacterial cell division: assembly, maintenance and disassembly of the Z-ring. Nat Rev Microbiol **7:**642-653.
3. **Anonymous.** 1999. Plague manual--epidemiology, distribution, surveillance and control. Wkly Epidemiol Rec **74:**447-481.
4. **Bustin, S. A.** 2000. Absolute quantification of mRNA using real-time reverse transcription polymerase chain reaction assays. J Mol Endocrinol **25:**169-193.
5. **Bustin, S. A.** 2002. Quantification of mRNA using real-time reverse transcription PCR (RT-PCR): trends and problems. J Mol Endocrinol **1:**23-39.
6. **Bustin, S. A., V. Benes, T. Nolan, and M. W. Pfaffl.** 2005. Quantitative real-time RT-PCR - a perspective. J Mol Endocrinol **34:**597-601.
7. **Cavanaugh, D. C., and R. Randall.** 1959. The role of multiplication of *Pasteurella pestis* in mononuclear phagocytes in the pathogenesis of flea-borne plague. J Immunol **83:**348-363.
8. **Cully, J. F., Jr., T. L. Johnson, S. K. Collinge, and C. Ray.** 2010. Disease limits populations: plague and black-tailed prairie dogs. Vector Borne Zoonotic Dis **10:**7-15.
9. **Deng, W., V. Burland, G. Plunkett, 3rd, A. Boutin, G. F. Mayhew, P. Liss, N. T. Perna, D. J. Rose, B. Mau, S. Zhou, D. C. Schwartz, J. D. Fetherston, L. E. Lindler, R. R. Brubaker, G. V. Plano, S. C. Straley, K. A. McDonough, M. L.**

Nilles, J. S. Matson, F. R. Blattner, and R. D. Perry. 2002. Genome sequence of *Yersinia pestis* KIM. J Bacteriol **184:**4601-4611.

10. **Gitai, Z.** 2005. The new bacterial cell biology: moving parts and subcellular architecture. Cell **120:**577-586.
11. **Grabenstein, J. P., H. S. Fukuto, L. E. Palmer, and J. B. Bliska.** 2006. Characterization of phagosome trafficking and identification of PhoP-regulated genes important for survival of *Yersinia pestis* in macrophages. Infect Immun **74:**3727-3741.
12. **Hett, E. C., and E. J. Rubin.** 2008. Bacterial growth and cell division: a mycobacterial perspective. Microbiol Mol Biol Rev **72:**126-156.
13. **Kartman, L., F. M. Prince, S. F. Quan, and H. E. Stark.** 1958. New knowledge on the ecology of sylvatic plague. Ann NY Acad Sci **70:**668-711.
14. **Laws, T. R., M. S. Davey, R. W. Titball, and R. Lukaszewski.** 2010. Neutrophils are important in early control of lung infection by *Yersinia pestis*. Microbes Infect **12:**331-335.
15. **Losick, R., and F. J. Gueiros.** 2002. A widely conserved bacterial cell division protein that promotes assembly of the tubulin-like protein FtsZ. Gene Dev **16:**2544-2556.
16. **Lukaszewski, R. A., D. J. Kenny, R. Taylor, D. G. Rees, M. G. Hartley, and P. C. Oyston.** 2005. Pathogenesis of *Yersinia pestis* infection in BALB/c mice: effects on host macrophages and neutrophils. Infect Immun **73:**7142-7150.

17. **Pan, Y. R., Y. C. Lou, A. B. Seven, J. Rizo, and C. Chen.** 2011. NMR structure and calcium-binding properties of the tellurite resistance protein TerD from *Klebsiella pneumoniae*. J Mol Biol **405:**1188-1201.

18. **Parkhill, J., B. W. Wren, N. R. Thomson, R. W. Titball, M. T. Holden, M. B. Prentice, M. Sebaihia, K. D. James, C. Churcher, K. L. Mungall, S. Baker, D. Basham, S. D. Bentley, K. Brooks, A. M. Cerdeno-Tarraga, T. Chillingworth, A. Cronin, R. M. Davies, P. Davis, G. Dougan, T. Feltwell, N. Hamlin, S. Holroyd, K. Jagels, A. V. Karlyshev, S. Leather, S. Moule, P. C. Oyston, M. Quail, K. Rutherford, M. Simmonds, J. Skelton, K. Stevens, S. Whitehead, and B. G. Barrell.** 2001. Genome sequence of *Yersinia pestis*, the causative agent of plague. Nature **413:**523-527.

19. **Perry, R. D., and J. D. Fetherston.** 1997. *Yersinia pestis*--etiologic agent of plague. Clin Microbiol Rev **10:**35-66.

20. **Ponnusamy, D., S. D. Hartson, and K. D. Clinkenbeard.** 2011. Intracellular *Yersinia pestis* expresses general stress response and tellurite resistance proteins in mouse macrophages. Vet Microbiol **150:**146-151.

21. **Pujol, C., and J. B. Bliska.** 2003. The ability to replicate in macrophages is conserved between *Yersinia pestis* and *Yersinia pseudotuberculosis*. Infect Immun **71:**5892-5899.

22. **Pujol, C., and J. B. Bliska.** 2005. Turning *Yersinia* pathogenesis outside in: subversion of macrophage function by intracellular *Yersiniae*. Clin Immunol **114:**216-226.

23. **Pujol, C., J. P. Grabenstein, R. D. Perry, and J. B. Bliska.** 2005. Replication of *Yersinia pestis* in interferon gamma-activated macrophages requires *ripA*, a gene encoded in the pigmentation locus. Proc Natl Acad Sci USA **102:**12909-12914.

24. **Qiu, J., D. Zhou, Y. Han, L. Zhang, Z. Tong, Y. Song, E. Dai, B. Li, J. Wang, Z. Guo, J. Zhai, Z. Du, X. Wang, and R. Yang.** 2005. Global gene expression profile of *Yersinia pestis* induced by streptomycin. FEMS Microbiol Lett **243:**489-496.

25. **Qiu, J., D. Zhou, L. Qin, Y. Han, X. Wang, Z. Du, Y. Song, and R. Yang.** 2006. Microarray expression profiling of *Yersinia pestis* in response to chloramphenicol. FEMS Microbiol Lett **263:**26-31.

26. **Reese, M. G.** 2001. Application of a time-delay neural network to promoter annotation in the *Drosophila melanogaster* genome. Comput Chem **26:**51-56.

27. **Romberg, L., and P. A. Levin.** 2003. Assembly dynamics of the bacterial cell division protein FtsZ: poised at the edge of stability. Annu Rev Microbiol **57:**125-154.

28. **Straley, S. C., and P. A. Harmon.** 1984. Growth in mouse peritoneal macrophages of *Yersinia pestis* lacking established virulence determinants. Infect Immun **45:**649-654.

29. **Straley, S. C., and P. A. Harmon.** 1984. *Yersinia pestis* grows within phagolysosomes in mouse peritoneal macrophages. Infect Immun **45:**655-659.

30. **Taylor, D. E.** 1999. Bacterial tellurite resistance. Trends Microbiol **7:**111-115.

31. **Toma, S.** 1986. Human and nonhuman infections caused by *Yersinia pseudotuberculosis* in Canada from 1962 to 1985. J Clin Microbiol **24:**465-466.

32. **Toptchieva, A., G. Sisson, L. J. Bryden, D. E. Taylor, and P. S. Hoffman.** 2003. An inducible tellurite-resistance operon in *Proteus mirabilis*. Microbiology **149:**1285-1295.

33. **Valkova, D., L. Valkovicova, S. Vavrova, E. Kovacova, J. Mravec, and J. Turna.** 2007. The contribution of tellurite resistance genes to the fitness of *Escherichia coli* uropathogenic strains. Cent Eur J Biol **2:**182-191.

34. **Vasquez, C. C., T. G. Chasteen, D. E. Fuentes, and J. C. Tantalean.** 2009. Tellurite: history, oxidative stress, and molecular mechanisms of resistance. FEMS Microbiol Rev **33:**820-832.

35. **Walter, E. G., and D. E. Taylor.** 1992. Plasmid-mediated resistance to tellurite: expressed and cryptic. Plasmid **27:**52-64.

36. **Wendte, J. M., D. Ponnusamy, D. Reiber, J. L. Blair, and K. D. Clinkenbeard.** 2011. *In vitro* efficacy of antibiotics commonly used to treat human plague against intracellular *Yersinia pestis*. Antimicrob Agents Chemother **55:**3752-3757.

37. **Whelan, K. F., R. K. Sherburne, and D. E. Taylor.** 1997. Characterization of a region of the *IncHI*2 plasmid R478 which protects *Escherichia coli* from toxic effects specified by components of the tellurite, phage, and colicin resistance cluster. J Bacteriol **179:**63-71.

38. **Zhou, D., Y. Han, J. Qiu, L. Qin, Z. Guo, X. Wang, Y. Song, Y. Tan, Z. Du, and R. Yang.** 2006. Genome-wide transcriptional response of *Yersinia pestis* to stressful conditions simulating phagolysosomal environments. Microbes Infect **8:**2669-2678.

Table 1. Sequence information of primers used in *Y. pestis ter* operon expression study

Gene targeted	Primer sequence
terC	Forward(F): 5'-TCCATCTCGAAAAAGCCGTT-3' Reverse(R): 5'-TCGCCAGTACACCAATGACC-3'
terD	F: 5'- TTCGAAAGGCGGTAATGTCTCC-3' R: 5'- GAAATCCTGACCATCTGTAGAACGG-3'
terE	F: 5'- GCTCCAACCATGAACATTGCTGTCG-3' R: 5'-CGTTTTCACCGACCATAAATACCGA-3'
tmK	F: 5'-ACGATATCGTTTTTACCCGTGAGCC-3' R: 5'-TTATCCGTCAGGACCTCACCGTCAA-3'

Table 2A. Comparative statistical analysis of *Y. pestis* genes *terC, -D* and *-E* expression levels for macrophage infection between sampling intervals

	Exp.	terC					terD					terE				
Exp.	p.i. (hr)	0.5	1.0	2.0	4.0	8.0	0.5	1.0	2.0	4.0	8.0	0.5	1.0	2.0	4.0	8.0
terC	0.5		-	-	*	**										
	1.0			-	-	-										
	2.0				-	*										
	4.0					-										
	8.0															
terD	0.5						-	-	*	**						
	1.0							*	*	**						
	2.0								-	*						
	4.0									-						
	8.0															
terE	0.5											-	-	*	**	
	1.0												*	*	**	
	2.0													-	-	
	4.0														-	
	8.0															

Note: *, $p < 0.05$; **, $p < 0.01$

Table 2B. Comparative statistical analysis of *Y. pestis* genes *terC, -D* and *-E* expression levels for sodium tellurite exposure between sampling intervals

	Exp.	terC					terD					terE				
Exp.	p.i. (hr)	0.5	1.0	2.0	4.0	8.0	0.5	1.0	2.0	4.0	8.0	0.5	1.0	2.0	4.0	8.0
terC	0.5		**	*	-	-										
	1.0			-	**	**										
	2.0				**	**										
	4.0					-										
	8.0															
terD	0.5						**	**	-	-						
	1.0							*	**	**						
	2.0								**	**						
	4.0									-						
	8.0															
terE	0.5											-	-	*	-	
	1.0												*	**	**	
	2.0													**	**	
	4.0														-	
	8.0															

Note: *, $p < 0.05$; **, $p < 0.01$

Table 2C. Comparative statistical analysis of *Y. pestis* genes *terC, -D* and *-E* expression levels for chloramphenicol exposure between sampling intervals.

	Exp.	terC					terD					terE				
Exp.	p.i. (hr)	0.5	1.0	2.0	4.0	8.0	0.5	1.0	2.0	4.0	8.0	0.5	1.0	2.0	4.0	8.0
terC	0.5		**	**	-	*										
	1.0			-	**	**										
	2.0				**	**										
	4.0					**										
	8.0															
terD	0.5							**	**	-	**					
	1.0								**	**	**					
	2.0									**	**					
	4.0										**					
	8.0															
terE	0.5												-	-	**	**
	1.0													**	**	**
	2.0														**	**
	4.0															**
	8.0															

Note: *, $p < 0.05$; **, $p < 0.01$

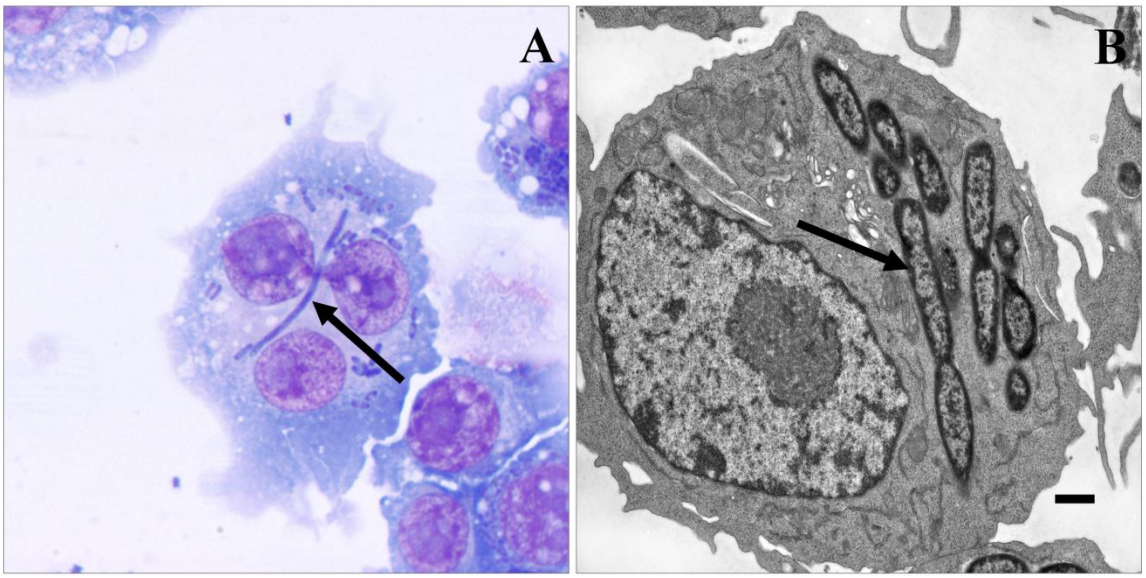

Fig. 1. Filamentous *Y. pestis* in mouse macrophage infection. Mouse macrophage-like cell line RAW264.7 was infected with *Y. pestis* strain KIM6+ for 30 min and subsequently the extracellular bacteria were killed by 50 µg/mL gentamicin for 2 hrs. The infected macrophages were affixed onto slides using a cytospin centrifuge and stained with Wright Giemsa for light microscopic examination (A). At the same time, replica samples were fixed in 2.5% (v/v) glutaraldehyde in PBS for 1 h and processed for transmission electron microscopic examination (B). Arrows indicate filamentous *Y. pestis*. Images A and B are at 1,000 and 6,000x magnification, respectively, and measuring bar on image B is 1µm long.

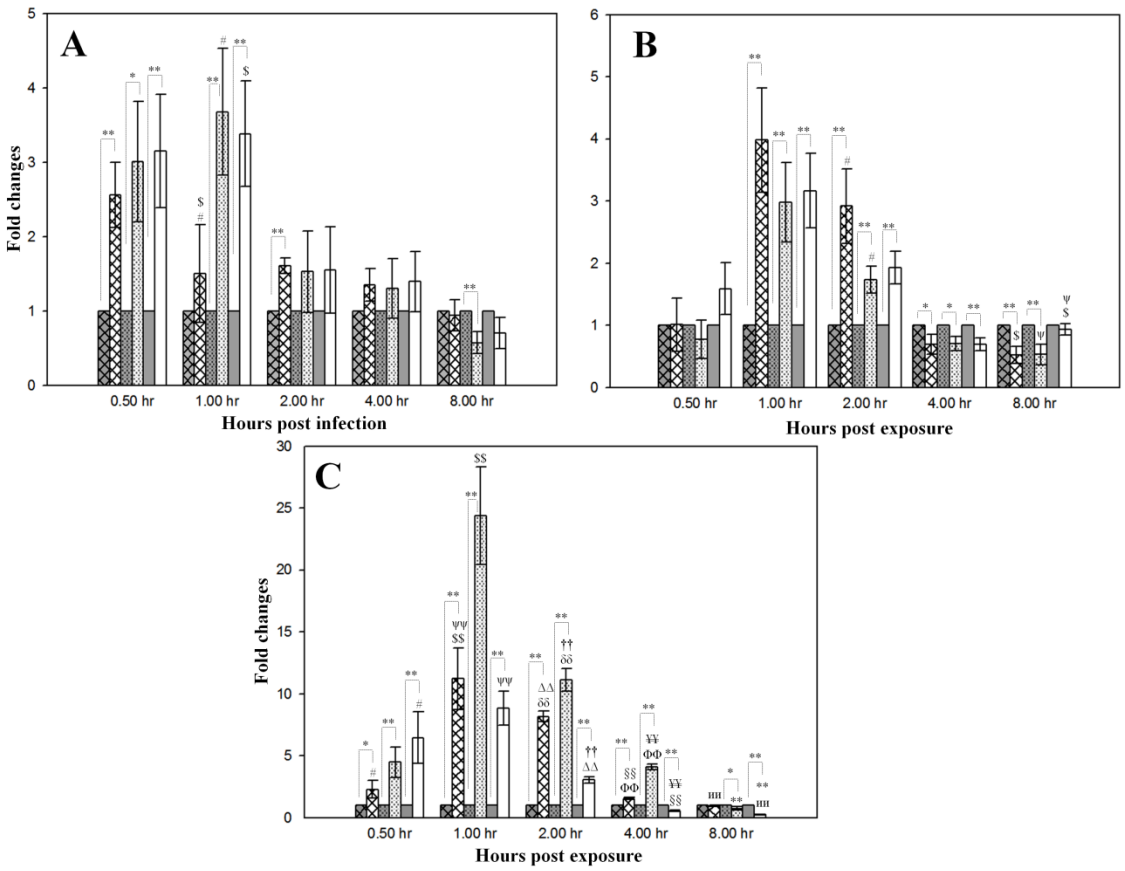

Fig. 2. Expression patterns of *Y. pestis* genes *terC*, *terD* and *terE*. Graphs represent expression profiles of *Y. pestis* strain KIM6+ *ter* operon genes *terC*, *terD* and *terE* for mouse macrophage infection (A) and exposure to sodium tellurite (B) or chloramphenicol (C). Shaded and white bars are, respectively, control and experimental groups (n=3). Genes *terC*, *terD* and *terE* are represented by bars filled with cross lines, dots or nothing, respectively. The results are expressed as means ± SEM. For the experimental samples, in a given sampling interval the genes *terC*, *-D* and *-E*, expressions were compared one another within them and the resulting statistical difference between the two measurements was marked by a symbol in pair as following: #, $, ψ, $p<0.05$; $$, ψψ, δδ, ΔΔ, ††, §§, ΦΦ, ¥¥, ии, **, $p<0.01$. Significant difference between the experimental

terC, *-D* or *-E* and the respective control was noted by dashed line and asterisk (*, $p < 0.05$; **, $p < 0.01$).

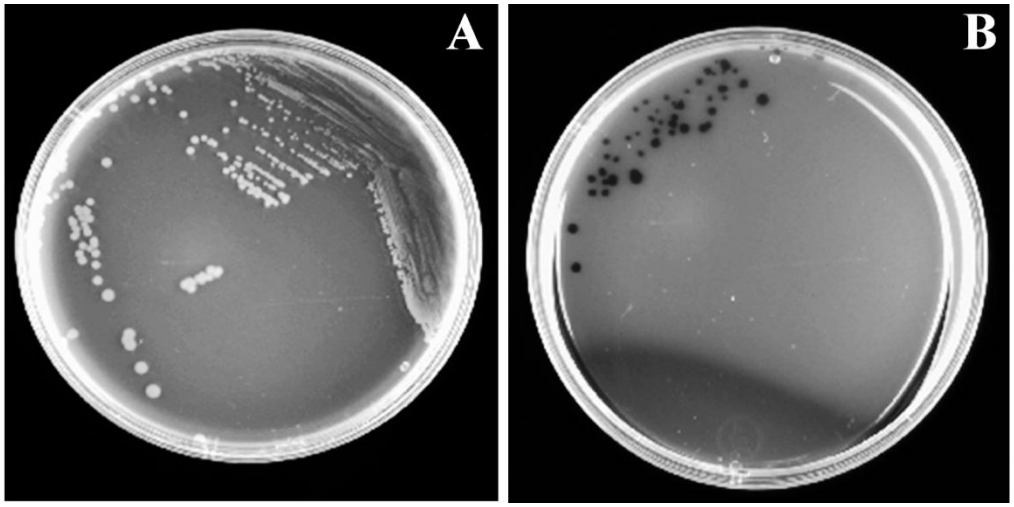

Fig. 3. *Y. pestis* colonies on sodium tellurite agar plates. *Y. pestis* strain KIM6+ was streaked on LB-agar plates containing PBS (A) or 100 µg/mL of sodium tellurite (B) and incubated at 37^{o}C for 3 days.

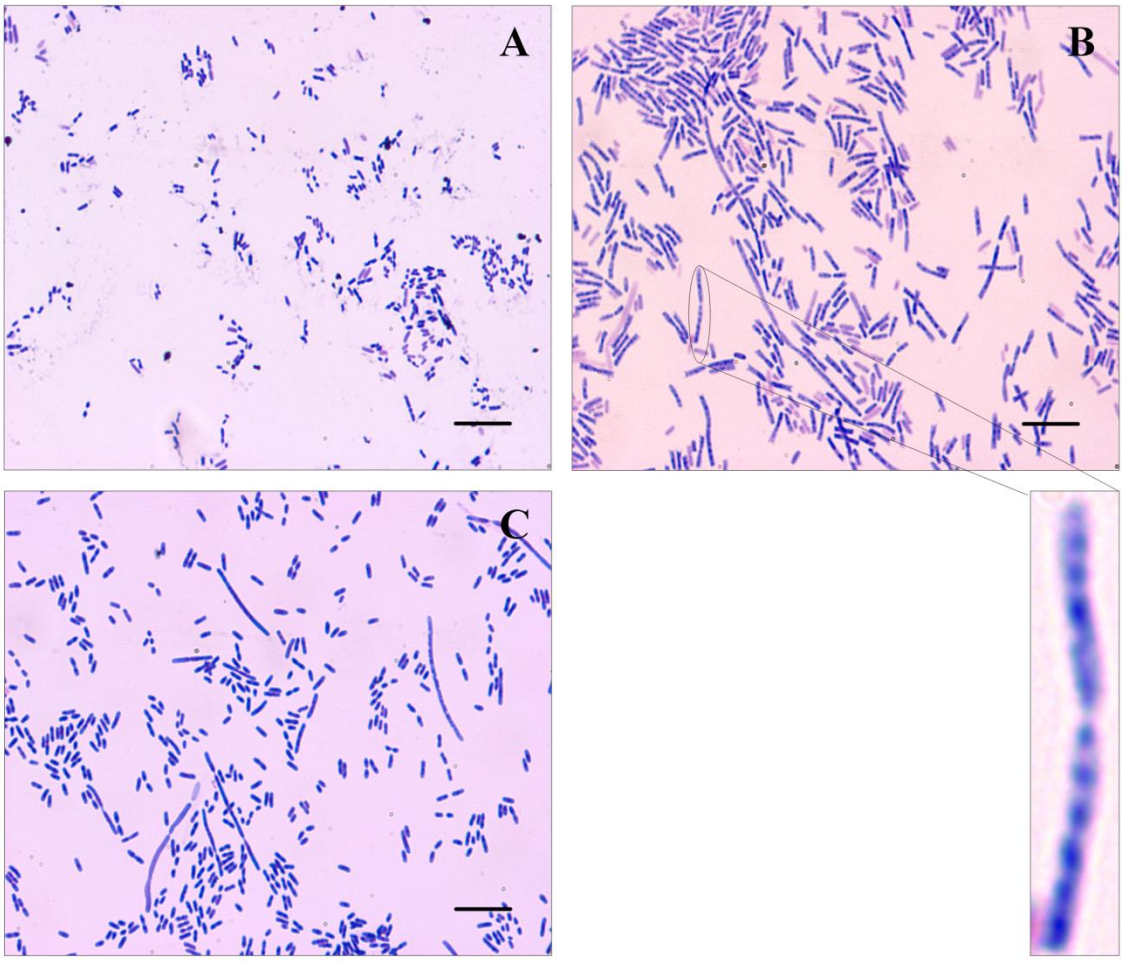

Fig. 4. Filamentous *Y. pestis* in *in vitro* cultures. *Y. pestis* strain KIM6+ was cultured at 37^{o}C in RPMI-1640 media with 10% FBS containing PBS (A), 30 µg/mL sodium tellurite (B), or 320 µg/mL chloramphenicol (C). After 2.5 h of culture, samples were prepared by staining with Wright Giemsa stain for light microscopic examination. Inset from image B represents multi-nucleoids appearance of a filamentous *Y. pestis*. Images are presented at 1,000x magnification.

CHAPTER VI

CONCLUSIONS

Y. pestis infection of macrophages and disease severity

Y. pestis, an obligatory intracellular pathogen during the initial stage of infection, causes severe disease plague in natural rodent hosts (1, 32). Rodents are highly susceptible to plague and suffer severe disease with high mortality as demonstrated by *Y. pestis* infected mice and rats which die within 3 to 15 days post-infection in experimental infections (46, 47, 50). Infected animals show enlargement of local lymph nodes as the initial clinical sign which is followed by septicemia, disseminated intravascular coagulation and death of the animals (46). Under natural conditions, *Y. pestis* is transmitted among susceptible rodent hosts by feeding fleas (1, 32). Before being transmitted to a new host, *Y. pestis* multiplies in the flea mid-gut region and forms a biofilm, which maximizes the efficiency of vector mediated plague transmission (32).

In this rodent-flea-rodent plague infection cycle, rodent predators such as dogs, coyotes, ferrets and cats occasionally intrude and extend the rodent epizootic foci, as these predators can carry the infected rodent carcasses and infected rodent fleas from place to place (54). During this intrusion, rodent predators can also contract the infection mainly by ingestion of infected carcasses or occasionally by bite of *Y. pestis* infected rodent fleas (27, 28). For the *Y. pestis* infection, unlike rodents, some rodent predators such as dogs and coyotes exhibit only mild or inapparent clinical disease. In an experimental exposure, dogs fed *Y. pestis* infected guinea pig carcasses were anorectic and lethargic for few days post-exposure, and thereafter, all of the exposed dogs recovered completely without succumbed to severe disease or mortalities (27, 42).

During flea bite infection in rodents, *Y. pestis* inoculated into subcutaneous tissues are mainly killed by the neutrophils present in the subcutis (32). At the same time, the

macrophages also phagocytize *Y. pestis*; but in contrast to neutrophils, *Y. pestis* taken up by macrophages survive and multiply intracellularly for 24 to 36 h during the initial stage of infection (15, 37). Later, these intracellular *Y. pestis* are released from the macrophages probably by cell lysis and initiate the septicemic infection (52). Therefore, it is possible that *Y. pestis* infection dynamics in host macrophages may determine the subsequent disease progression and severity. In particular, *Y. pestis* in macrophages from host suffering severe disease may overcome macrophage induced stress, whereas *Y. pestis* may not escape host antimicrobial activity of macrophages from hosts with less severe disease.

Y. pestis filamentous cellular morphology during macrophage infections

In an *in vitro* experimental model, we compared *Y. pestis* infection progress in mouse and dog macrophages which represent the hosts experiencing severe and less severe disease, respectively. In primary macrophages from mouse spleen and dog peripheral blood and tissue culture cells RAW264.7 from mouse and DH82 from dog, *Y. pestis* assumed filamentous cellular morphology, especially at the early stage of infection. These filamentous *Y. pestis* had multiple genomes per bacterium, as shown by genomic equivalences (GEs) per colony forming unit (CFU), which was approximately 4-fold high during the initial phase of infection in RAW264.7 cells and throughout the experiment in DH82 cells. These filaments were twice or greater the maximum length of normal *Y. pestis* bacilli and were confined within tight *Yersinia* containing vacuoles (YCV). These intracellular filamentous *Y. pestis* appeared similar to the filamentous forms of uropathogenic *E. coli* in mouse urinary bladder epithelial cells, *Legionella* spp. in Vero

cell line, *Mycobacterium tuberculosis* in human macrophage cell line THP-1, and *Salmonella enterica* serovar Typhimurium in mouse bone marrow and RAW264.7 macrophages (5, 18, 21, 26, 40, 41).

Although the exact beneficial nature of filamentous cellular morphology for intracellular *Y. pestis* is not known, this morphologic change is considered to be a bacterial adaptive strategy to cope with the harsh intracellular environment (61). Assumption of a filamentous cellular morphology may provide sufficient time for the *Y. pestis* DNA repair system to restore the damage done to its genome by various phagolysosomal stressors such as nitric oxide, reactive oxygen species, proteases and cationic antimicrobial peptides (19, 20, 40, 41, 43). In addition to these intracellular stressors, low calcium concentration in the phagolysosomal niche may also trigger the filamentation process in *Y. pestis* (17, 35). Further, *Y. pestis* had filamentous structure in all macrophages irrespective of host origin, indicating that a conserved macrophage lineage specific stressor may exert this intracellular filamentation process in *Y. pestis*. Although the assertion is made herein that intracellular filamentous *Y. pestis* is due to the macrophage associated stress, the molecular pathway which communicates this stressor cue to the bacterial cell division machinery is yet to be identified. In addition, studies focusing on the role of filamentous *Y. pestis* in mitigating intracellular stress need to be addressed to better understand the early pathodynamics of *Y. pestis* infection in macrophages.

Liberation of *Y. pestis* from stress in mouse and dog macrophages

During progress of the infection, the filamentous *Y. pestis* reverted to normal coccobacillary form both in primary and tissue culture macrophages from mouse, and later these intracellular coccobacilli were released from the macrophages by cell lysis. However, in dog peripheral blood derived macrophages, *Y. pestis* return to coccobacilli at 7.5 h p.i., but towards end of the experiment, these coccobacilli were killed by the macrophages. In dog tissue culture macrophages, the filamentous *Y. pestis* formed during the early stage of infection was continuously retained in the same adaptive cellular morphology for the entire experiment of 27.5 h as evidenced by 4-fold higher GEs per CFU ratio and the presence of filamentous *Y. pestis* in DH82 cells throughout the experiment. Overall, these findings clearly support the hypothesis that *Y. pestis* in mouse macrophages can successfully overcome the intracellular stresses, resulting in survival and multiplication of *Y. pestis* in these macrophages. But in dog macrophages, *Y. pestis* may not overcome the macrophage associates stress and thus are killed by the macrophages. A predicted outcome of this conclusion is that failure to control *Y. pestis* infection progress at the macrophage infection stage in mice or in other similarly highly susceptible rodents leads to acute, severe disease with high mortality (1, 32, 46, 47, 50). Whereas, restriction of *Y. pestis* growth by dog macrophages limits the disease to either mild or inapparent form (42). To advance this area of research, an animal study using mouse models having normal levels or depletion of macrophages is necessary to confirm the role the host macrophages play on *Y. pestis* infection severity and the resulting outcome of the disease. Particularly, the mice which lack any mononuclear phagocytic system might be expected to develop less severe disease through flea bite infection but

may be fully vulnerable for intravenous route of injection of or aerosolized exposure to *Y. pestis* which have been cultured at mammalian body temperature. Similarly, dogs injected intravenously with *Y. pestis* culture grown at 37^{o}C might be expected to succumb to severe disease. Experiments of these types may further our understanding of the contributions of host macrophages for *Y. pestis* infection progression during the early stage of the disease.

Intracellular *Y. pestis* in mouse macrophages causes spacious extension of YCV

During the conversion of filamentous *Y. pestis* to normal coccobacilli in mouse primary and tissue culture macrophages, the YCV were remodelled into spacious vacuoles. In contrast, such changes were not noticed in either primary or tissue culture macrophages from dog. These spacious YCV in mouse macrophages appeared similar to those in *Y. pestis* strain KIM6 infected mouse macrophage-like cell line J774A.1 (15). Inactivation of *Y. pestis* transcriptional regulator PhoP-PhoQ led to a failure to form any such vacuoles (15), indicating that genes under the control of PhoP-PhoQ regulator are involved in this YCV extension process. In addition, we propose that *Y. pestis* enzyme urease may also play a role in YCV remodelling, which is further explained in the intracellular stress response proteins section.

Macrophage cell lysis from *Y. pestis* infections

In addition to differences in vacuolar extension of YCV, mouse and dog tissue culture macrophages also varied between *Y. pestis* induced cell lysis of macrophages. RAW264.7 cells showed upto 45% cell lysis to *Y. pestis* infection in contrast to

approximately 10% cell lysis in DH82 cells, which did not differ significantly from the uninfected control cells. This high percentage of macrophage cell lysis in mouse macrophages indicates the nature of vulnerability of these macrophages to *Y. pestis* infection as previously reported for mouse J774A.1 cell line infections (51). This *Y. pestis* infection mediated macrophage cell lysis was comparable with that observed in *E. coli* infection of RAW264.7 cells or mouse bone marrow derived macrophages, and in *Salmonella typhi* infection of RAW264.7 cells (13, 16). Likely, restriction of intracellular *Y. pestis* to its stress-responsive filamentous cellular morphology throughout the experiment by dog macrophages results in negligible cell lysis as observed in antibiotic-induced *Burkholderia pseudomallei* filament infection of THP-1 cells (7). However, failure to limit the intracellular growth and modulation of YCV by *Y. pestis* in mouse macrophages may cause extensive cell lysis.

Intracellular *Y. pestis* expresses general stress response proteins

For successful survival during the initial macrophage parasitism phase, *Y. pestis* has to adapt to or overcome the various intracellular antimicrobial defense mechanisms such as acidic pH; hydrolytic enzymes such as lipase, nuclease, glycosidase; reactive oxygen species; oxidizing agent; cationic peptides; nitric oxide and reactive nitric oxide intermediates (11, 56). Further, phagolysosomal compartments contain very low concentration of calcium, iron, magnesium and manganese; these ions are essential for many intracellular pathogens including *Y. pestis* (11, 32). In order to survive in this hostile environment *Y. pestis* can employ a wide spectrum of stress responders; many of these have been reported, but some have to be identified. In particular, *Y. pestis* virulence

factors *ripA* and *ripB* genes from pigmentation locus help *Y. pestis* to reduce nitric oxide concentration during macrophage infections (37). Similarly, genes associated with metal ion transportation systems such as *mgtC* for magnesium; and *yfeABC* and *yfeD*, and *feoABC* for iron are also indispensable for the macrophage infection of *Y. pestis* (15, 33). Other *Y. pestis* virulence factors for which a clear role in macrophage infection have not yet been confirmed are Hfq chaperon and Braun's lipoprotein synthesizing gene *lpp* (14, 49). Under these circumstances, as an effort to search for additional *Y. pestis* virulence factors involved in the macrophage life cycle, a proteomic study was carried out to explore the *Y. pestis* proteins which are expressed in the intracellular environment but not in extracellular culture condition. The resulting study revealed that in the intracellular environment, *Y. pestis* expressed proteins such as superoxide dismutase-A, inorganic diphosphatase, autonomous glycycl radical cofactor GrcA, molecular chaperone DnaK, serine endoprotease GsrA, global DNA-binding transcriptional dual regulator H-NS, urease gamma subunit, and tellurite resistance protein-D and -E.

Y. pestis superoxide dismutase, a metalloenzyme which detoxifies macrophage respiratory burst superoxides into less harmful hydrogen peroxide and molecular oxygen, has previously been implicated for intracellular survival of *Bordetella pertussis* Tohama I and *E. coli* GC4468 in J774A.1 macrophages and *E. coli* GC4468, *S. typhimurium* ATCC 14028s, *S. flexneri* M90T and *Mycobacterium tuberculosis* in mouse peritoneal macrophages (4, 9, 12, 22, 25, 34). Two other enzymatic proteins inorganic pyrophosphatase and GrcA may be important for the metabolic activities of intracellular *Y. pestis*. Inorganic pyrophosphatase hydrolyses pyrophosphate to monophosphate to recycle phosphate and to avoid accumulation of pyrophosphates (6). GrcA is likely

involved in pyruvate metabolism and is expressed under acidic and anaerobic conditions such as those present in phagolysosomes (8, 30).

DnaK chaperone of *Y. pestis* is a critical stress responsive protein supporting proper folding of misfolded proteins which accumulate when *Y. pestis* resides in the hostile macrophage phagolysosomal compartments. Further, DnaK also functions to facilitate degradation of abnormally folded proteins (24, 31). Similarly, GsrA, a periplasmic-serine protease, protects the periplasmic space from the accumulation of abnormally folded proteins during the stress conditions (60).

DNA binding protein H-NS is a negative transcriptional regulator of various genes which recognizes environmental cues and is highly conserved in the *Enterobacteriaceae* family (2, 3). H-NS expression by intracellular *Y. pestis* may repress genes which might interfere with intracellular life phase of *Y. pestis* (2, 23).

Urease gamma subunit (UreA) is a part of tri-heterotrimeric $(UreABC)_3$ functional urease, which may play an important role in the spacious extension of YCV (45, 48). From studies on *Helicobacter pylori* urease, it is conceivable that *Y. pestis* urease may increase the osmotic concentration of YCV, and thus causes water influx and swelling of YCV (44). As support for this contention, during *Y. pestis* infection of RAW264.7 cells, a functional subunit of active urease UreA is expressed exclusively in the intracellular niche (36). However, the role of *Y. pestis* urease in the spacious remodelling of YCV is in question because the *Y. pestis* gene *ureD* which encodes an accessory protein needed for active urease assembly carries an insertion mutation (45). Therefore, *Y. pestis* urease may not be active. However, if urease were inactive and not necessary for intracellular survival of *Y. pestis*, then it would be expected to accumulate mutations in the *Y. pestis*

urease enzyme encoding locus. But in contrast to this assumption, *Y. pestis ure* locus including adjacent nickel transporters is highly conserved among various strains of *Y. pestis* from distant geographical origins (45), suggesting high level of selection pressure on this locus likely due to dependency of *Y. pestis* on this locus for an unknown but an essential bacterial physiological activity. Furthermore, there is also a possibility that *Y. pestis* can revert between non-urolytic and urolytic status at high frequency rate (45). These latter observations support the potential role of *Y. pestis* urease in the process of spacious extension of YCV. To prove this assumption, the relationship between *Y. pestis* urease and YCV extension will need to be further explored.

Finally, the possible role of *Y. pestis* protein TerD and TerE from the *terZABCDE* operon are further examined in the context of macrophage stress mediated *Y. pestis* filamentous structure formation in the following section.

Expression of tellurite resistance operon causes filamentous cellular morphology of *Y. pestis* in mouse macrophage infections

The filamentous cellular morphology of intracellular *Y. pestis* in macrophages resembled laboratory *E. coli* strain DH5α expressing genes *terZ*, *-A*, *-B*, and *-C* from pathogenic *E. coli* tellulrite resistance operon *terZABCDEF*. Expression of the *ter* operon has been purposed to be beneficial for *E. coli* to survive inside the mouse peritoneal macrophages and to resist hydrogen peroxide mediated stress (57, 59). Further, *Y. pestis ter* operon proteins TerD and TerE were observed in protein samples prepared from intracellular *Y. pestis* in macrophages but not in culture grown *Y. pestis* (36). Various genes from *Y. pestis ter* operon were noticed to be upregulated by various *in vitro* stimuli

which may mimic the intracellular environmental stresses in macrophage infections (38, 39, 62). All these findings strongly indicate the possible association between macrophage induced stress, *ter* operon expression, and *Y. pestis* filamentous cellular morphology in macrophage infections.

Quantification of mRNA concentration of *Y. pestis* genes *terC*, *-D* and *-E* during RAW264.7 cell infections agreed with proteomics data for expression of TerD and TerE proteins in macrophages. These studies revealed upregulation of expressions of all these genes upto 2.5 to 3.5 fold at 1 h p.i. as a response to intracellular stress. Further, similar type of upregulations was noticed in *Y. pestis* culture exposed to sodium tellurite or chloramphenicol. Notably, the upregulations of expression of *terC, -D* and *-E* in macrophages closely correlated with the time of presence of intracellular filamentous *Y. pestis*. In addition to this correlation, *Y. pestis* culture exposed to sodium tellurite exhibited bacterial filamentous cellular morphology similar to those presented in RAW264.7 cell infections. Considering these observations together, there are two possible conclusions which can be made. First, *Y. pestis ter* operon expression is induced as a part of bacterial intracellular stress regulatory mechanism. Second, the resulting expression leads *Y. pestis* to assume filamentous cellular morphology as a morphologic adaptation to manage the hostile intracellular environment in macrophages. Likely, *Y. pestis ter* operon proteins function as a signal transducer to communicate the macrophage associated stresses to the bacterial cell division machinery. A growing body of evidence supports this conjecture. Proteins TerD and TerE share high percentage of amino acid homology to a cyclic AMP-binding protein of *Dictyostelium discoideum* slime mold (53, 58), indicating the possibility that the proteins TerD and TerE may be involved in a

bacterial cell signaling process. This conjecture is further supported by observations that *Y. pestis* proteins TerA, TerD, and TerE are also highly homologous to *Klebsiella pneumoniae ter* operon protein TerD which exhibits a strong calcium binding property (29). To better understand the role *Y. pestis ter* operon proteins may play during macrophage infection, it will be necessary to observe the infection progress of *Y. pestis* strains which are mutated for the various *ter* operon genes. In particular, *Y. pestis ter* gene mutants are anticipated to be less competent for responding to the macrophage associated stress, such as filamentation process and survivability of intracellular stress.

Y. pestis tellurite resistance and *ter* operon DNA sequence homology

Apart from playing a role in the filamentation process, *Y. pestis ter* operon provides the capability for the bacteria to grow in the presence of < 312.5µg/ mL of sodium tellurite in the culture media, showing that the tellurite resistance property of *Y. pestis* is similar to that exhibited by *Proteus mirabilis* (55). However, although *Y. pestis* showed tellurite resistance, in its ecological niche the bacterium is not exposed to toxic tellurite metal. In the absence of selection pressure, it is expected that mutations would be accumulated in the *Y. pestis ter* operon locus. However, in contrast to this expectation, sequence comparison of various *Y. pestis* strains from different geographic origins and *Yersinia pseudotuberculosis* strain IP32953 showed identical *ter* operons (10, 30). This unexpected observation suggests that *Y. pestis ter* operon proteins are likely involved in an unknown bacterial physiological process, to which the tellurite resistance properties are a secondary enzymatic activity. The role of the *Y. pestis ter* operon proteins in stress

related cell signaling mechanisms may be explored by identifying other proteins with which these proteins interact.

Summary

Overall, the results of our study indicate that *Y. pestis* in macrophages from mouse or from other similarly high susceptible hosts can overcome the initial macrophage induced stress during the flea bite infection and resulting in subsequent severe systemic disease. But in dog or other low susceptible hosts, macrophages likely restrict the infection progress at the intracellular parasitism phase, and thus *Y. pestis* infections are mild to inapparent. During the intracellular parasitism phase, *Y. pestis* applies various general stress regulatory mechanisms to better adapt the harsh macrophage phagolysosomal environment. As a part of this stress regulation, *Y. pestis ter* operon expression which is induced likely results in adaptation to a filamentous cellular morphology in macrophages as a response to the stress stimuli.

References

1. **Anonymous.** 1999. Plague manual--epidemiology, distribution, surveillance and control. Wkly Epidemiol Rec **74:**447-481.
2. **Atlung, T., and H. Ingmer.** 1997. H-NS: a modulator of environmentally regulated gene expression. Mol Microbiol **24:**7-17.
3. **Barth, M., C. Marschall, A. Muffler, D. Fischer, and R. Hengge-Aronis.** 1995. Role for the histone-like protein H-NS in growth phase-dependent and osmotic regulation of sigma S and many sigma S-dependent genes in *Escherichia coli*. J Bacteriol **177:**3455-3464.
4. **Battistoni, A., G. Donnarumma, R. Greco, P. Valenti, and G. Rotilio.** 1998. Overexpression of a hydrogen peroxide-resistant periplasmic Cu, Zn superoxide dismutase protects *Escherichia coli* from macrophage killing. Biochem Biophys Res Commun **243:**804-807.
5. **Chauhan, A., M. V. Madiraju, M. Fol, H. Lofton, E. Maloney, R. Reynolds, and M. Rajagopalan.** 2006. *Mycobacterium tuberculosis* cells growing in macrophages are filamentous and deficient in FtsZ rings. J Bacteriol **188:**1856-1865.
6. **Chen, J., A. Brevet, M. Fromant, F. Leveque, J. M. Schmitter, S. Blanquet, and P. Plateau.** 1990. Pyrophosphatase is essential for growth of *Escherichia coli*. J Bacteriol **172:**5686-5689.
7. **Chen, K., G. W. Sun, K. L. Chua, and Y. H. Gan.** 2005. Modified virulence of antibiotic-induced *Burkholderia pseudomallei* filaments. Antimicrob Agents Chemother **49:**1002-1009.

8. **ChenWyborn, N. R., S. L. Messenger, R. A. Henderson, G. Sawers, R. E. Roberts, M. M. Attwood, and J. Green.** 2002. Expression of the *Escherichia coli yfiD* gene responds to intracellular pH and reduces the accumulation of acidic metabolic end products. Microbiology **148:**1015-1026.

9. **De Groote, M. A., U. A. Ochsner, M. U. Shiloh, C. Nathan, J. M. McCord, M. C. Dinauer, S. J. Libby, A. Vazquez-Torres, Y. Xu, and F. C. Fang.** 1997. Periplasmic superoxide dismutase protects *Salmonella* from products of phagocyte NADPH-oxidase and nitric oxide synthase. Proc Natl Acad Sci USA **94:**13997-14001.

10. **Deng, W., V. Burland, G. Plunkett, 3rd, A. Boutin, G. F. Mayhew, P. Liss, N. T. Perna, D. J. Rose, B. Mau, S. Zhou, D. C. Schwartz, J. D. Fetherston, L. E. Lindler, R. R. Brubaker, G. V. Plano, S. C. Straley, K. A. McDonough, M. L. Nilles, J. S. Matson, F. R. Blattner, and R. D. Perry.** 2002. Genome sequence of *Yersinia pestis* KIM. J Bacteriol **184:**4601-4611.

11. **Flannagan, R. S., V. Jaumouille, and S. Grinstein.** 2011. The cell biology of phagocytosis. Annu Rev Pathol **7:**49-86.

12. **Franzon, V. L., J. Arondel, and P. J. Sansonetti.** 1990. Contribution of superoxide dismutase and catalase activities to *Shigella flexneri* pathogenesis. Infect Immun **58:**529-535.

13. **Fu, W., J. Wei, and J. Gu.** 2006. MEF2C mediates the activation induced cell death (AICD) of macrophages. Cell Res **16:**559-565.

14. **Geng, J., Y. Song, L. Yang, Y. Feng, Y. Qiu, G. Li, J. Guo, Y. Bi, Y. Qu, W. Wang, X. Wang, Z. Guo, R. Yang, and Y. Han.** 2009. Involvement of the post-transcriptional regulator Hfq in *Yersinia pestis* virulence. PLoS One **4:**6213-6223.

15. **Grabenstein, J. P., H. S. Fukuto, L. E. Palmer, and J. B. Bliska.** 2006. Characterization of phagosome trafficking and identification of PhoP-regulated genes important for survival of *Yersinia pestis* in macrophages. Infect Immun **74:**3727-3741.

16. **Groesdonk, H. V., S. Schlottmann, F. Richter, M. Georgieff, and U. Senftleben.** 2006. *Escherichia coli* prevents phagocytosis-induced death of macrophages via classical NF-kappaB signaling, a link to T-cell activation. Infect Immun **74:**5989-6000.

17. **Hall, P. J., G. C. Yang, R. V. Little, and R. R. Brubaker.** 1974. Effect of Ca^{2+} on morphology and division of *Yersinia pestis*. Infect Immun **9:**1105-1113.

18. **Henry, T., F. Garcia-del Portillo, and J. P. Gorvel.** 2005. Identification of *Salmonella* functions critical for bacterial cell division within eukaryotic cells. Mol Microbiol **56:**252-267.

19. **Imlay, J. A., and S. Linn.** 1987. Mutagenesis and stress responses induced in *Escherichia coli* by hydrogen peroxide. J Bacteriol **169:**2967-2976.

20. **Justice, S. S., D. A. Hunstad, L. Cegelski, and S. J. Hultgren.** 2008. Morphological plasticity as a bacterial survival strategy. Nat Rev Microbiol **6:**162-168.

21. **Justice, S. S., D. A. Hunstad, P. C. Seed, and S. J. Hultgren.** 2006. Filamentation by *Escherichia coli* subverts innate defenses during urinary tract infection. Proc Natl Acad Sci USA **103:**19884-19889.

22. **Khelef, N., D. DeShazer, R. L. Friedman, and N. Guiso.** 1996. *In vivo* and *in vitro* analysis of *Bordetella pertussis* catalase and Fe-superoxide dismutase mutants. FEMS Microbiol Lett **142:**231-235.

23. **Landini, P., and A. J. Zehnder.** 2002. The global regulatory *hns* gene negatively affects adhesion to solid surfaces by anaerobically grown *Escherichia coli* by modulating expression of flagellar genes and lipopolysaccharide production. J Bacteriol **184:**1522-1529.

24. **Lindquist, S., and E. A. Craig.** 1988. The heat-shock proteins. Annu Rev Genet **22:**631-677.

25. **Nunoshiba, T., T. deRojas-Walker, J. S. Wishnok, S. R. Tannenbaum, and B. Demple.** 1993. Activation by nitric oxide of an oxidative-stress response that defends *Escherichia coli* against activated macrophages. Proc Natl Acad Sci USA **90:**9993-9997.

26. **Ogawa, M., A. Takade, H. Miyamoto, H. Taniguchi, and S. Yoshida.** 2001. Morphological variety of intracellular microcolonies of *Legionella* species in Vero cells. Microbiol Immunol **45:**557-562.

27. **Orloski, K. A., and M. Eidson.** 1995. *Yersinia pestis* infection in three dogs. J Am Vet Med Assoc **207:**316-318.

28. **Orloski, K. A., and S. L. Lathrop.** 2003. Plague: a veterinary perspective. J Am Vet Med Assoc **222:**444-448.

29. **Pan, Y. R., Y. C. Lou, A. B. Seven, J. Rizo, and C. Chen.** 2011. NMR structure and calcium-binding properties of the tellurite resistance protein TerD from *Klebsiella pneumoniae*. J Mol Biol **405:**1188-1201.

30. **Parkhill, J., B. W. Wren, N. R. Thomson, R. W. Titball, M. T. Holden, M. B. Prentice, M. Sebaihia, K. D. James, C. Churcher, K. L. Mungall, S. Baker, D. Basham, S. D. Bentley, K. Brooks, A. M. Cerdeno-Tarraga, T. Chillingworth, A. Cronin, R. M. Davies, P. Davis, G. Dougan, T. Feltwell, N. Hamlin, S. Holroyd, K. Jagels, A. V. Karlyshev, S. Leather, S. Moule, P. C. Oyston, M. Quail, K. Rutherford, M. Simmonds, J. Skelton, K. Stevens, S. Whitehead, and B. G. Barrell.** 2001. Genome sequence of *Yersinia pestis*, the causative agent of plague. Nature **413:**523-527.

31. **Parsell, D. A., and S. Lindquist.** 1993. The function of heat-shock proteins in stress tolerance: degradation and reactivation of damaged proteins. Annu Rev Genet **27:**437-496.

32. **Perry, R. D., and J. D. Fetherston.** 1997. *Yersinia pestis*--etiologic agent of plague. Clin Microbiol Rev **10:**35-66.

33. **Perry, R. D., I. Mier, Jr., and J. D. Fetherston.** 2007. Roles of the Yfe and Feo transporters of *Yersinia pestis* in iron uptake and intracellular growth. Biometals **20:**699-703.

34. **Piddington, D. L., F. C. Fang, T. Laessig, A. M. Cooper, I. M. Orme, and N. A. Buchmeier.** 2001. Cu,Zn superoxide dismutase of *Mycobacterium tuberculosis* contributes to survival in activated macrophages that are generating an oxidative burst. Infect Immun **69:**4980-4987.

35. **Pollack, C., S. C. Straley, and M. S. Klempner.** 1986. Probing the phagolysosomal environment of human macrophages with a Ca^{2+}-responsive operon fusion in *Yersinia pestis*. Nature **322:**834-836.

36. **Ponnusamy, D., S. D. Hartson, and K. D. Clinkenbeard.** 2011. Intracellular *Yersinia pestis* expresses general stress response and tellurite resistance proteins in mouse macrophages. Vet Microbiol **150:**146-151.

37. **Pujol, C., J. P. Grabenstein, R. D. Perry, and J. B. Bliska.** 2005. Replication of *Yersinia pestis* in interferon gamma-activated macrophages requires *ripA*, a gene encoded in the pigmentation locus. Proc Natl Acad Sci USA **102:**12909-12914.

38. **Qiu, J., D. Zhou, Y. Han, L. Zhang, Z. Tong, Y. Song, E. Dai, B. Li, J. Wang, Z. Guo, J. Zhai, Z. Du, X. Wang, and R. Yang.** 2005. Global gene expression profile of *Yersinia pestis* induced by streptomycin. FEMS Microbiol Lett **243:**489-496.

39. **Qiu, J., D. Zhou, L. Qin, Y. Han, X. Wang, Z. Du, Y. Song, and R. Yang.** 2006. Microarray expression profiling of *Yersinia pestis* in response to chloramphenicol. FEMS Microbiol Lett **263:**26-31.

40. **Rosenberger, C. M., and B. B. Finlay.** 2002. Macrophages inhibit *Salmonella typhimurium* replication through MEK/ERK kinase and phagocyte NADPH oxidase activities. J Biol Chem **277:**18753-18762.

41. **Rosenberger, C. M., R. L. Gallo, and B. B. Finlay.** 2004. Interplay between antibacterial effectors: A macrophage antimicrobial peptide impairs intracellular *Salmonella* replication. Proc Natl Acad Sci USA **101:**2422-2427.

42. **Rust, J. H., Jr., D. C. Cavanaugh, R. O'Shita, and J. D. Marshall, Jr.** 1971. The role of domestic animals in the epidemiology of plague. I. Experimental infection of dogs and cats. J Infect Dis **124:**522-526.

43. **Schapiro, J. M., S. J. Libby, and F. C. Fang.** 2003. Inhibition of bacterial DNA replication by zinc mobilization during nitrosative stress. Proc Natl Acad Sci USA **100:**8496-8501.

44. **Schwartz, J. T., and L. A. Allen.** 2006. Role of urease in megasome formation and *Helicobacter pylori* survival in macrophages. J Leukoc Biol **79:**1214-1225.

45. **Sebbane, F., A. Devalckenaere, J. Foulon, E. Carniel, and M. Simonet.** 2001. Silencing and reactivation of urease in *Yersinia pestis* is determined by one G residue at a specific position in the *ureD* gene. Infect Immun **69:**170-176.

46. **Sebbane, F., D. Gardner, D. Long, B. B. Gowen, and B. J. Hinnebusch.** 2005. Kinetics of disease progression and host response in a rat model of bubonic plague. Am J Pathol **166:**1427-1439.

47. **Sebbane, F., C. O. Jarrett, D. Gardner, D. Long, and B. J. Hinnebusch.** 2006. Role of the *Yersinia pestis* plasminogen activator in the incidence of distinct septicemic and bubonic forms of flea-borne plague. Proc Natl Acad Sci USA **103:**5526-5530.

48. **Sebbane, F., M. A. Mandrand-Berthelot, and M. Simonet.** 2002. Genes encoding specific nickel transport systems flank the chromosomal urease locus of pathogenic *Yersiniae*. J Bacteriol **184:**5706-5713.

49. **Sha, J., S. L. Agar, W. B. Baze, J. P. Olano, A. A. Fadl, T. E. Erova, S. Wang, S. M. Foltz, G. Suarez, V. L. Motin, S. Chauhan, G. R. Klimpel, J. W.**

Peterson, and A. K. Chopra. 2008. Braun lipoprotein (Lpp) contributes to virulence of *Yersiniae*: potential role of Lpp in inducing bubonic and pneumonic plague. Infect Immun **76:**1390-1409.

50. **Sha, J., J. J. Endsley, M. L. Kirtley, S. M. Foltz, M. B. Huante, T. E. Erova, E. V. Kozlova, V. L. Popov, L. A. Yeager, I. V. Zudina, V. L. Motin, J. W. Peterson, K. L. DeBord, and A. K. Chopra.** 2011. Characterization of an F1 deletion mutant of *Yersinia pestis* CO92, pathogenic role of F1 antigen in bubonic and pneumonic plague, and evaluation of sensitivity and specificity of F1 antigen capture-based dipsticks. J Clin Microbiol **49:**1708-1715.

51. **Spinner, J. L., K. S. Seo, J. L. O'Loughlin, J. A. Cundiff, S. A. Minnich, G. A. Bohach, and S. D. Kobayashi.** 2010. Neutrophils are resistant to *Yersinia* YopJ/P-induced apoptosis and are protected from ROS-mediated cell death by the type III secretion system. PLoS One **5:**9279-9288.

52. **Straley, S. C., and P. A. Harmon.** 1984. *Yersinia pestis* grows within phagolysosomes in mouse peritoneal macrophages. Infect Immun **45:**655-659.

53. **Taylor, D. E.** 1999. Bacterial tellurite resistance. Trends Microbiol **7:**111-115.

54. **Thomas, C. U., and P. E. Hughes.** 1992. Plague surveillance by serological testing of Coyotes (*Canis latrans*) in Los-Angeles county, California. J Wildlife Dis **28:**610-613.

55. **Toptchieva, A., G. Sisson, L. J. Bryden, D. E. Taylor, and P. S. Hoffman.** 2003. An inducible tellurite-resistance operon in *Proteus mirabilis*. Microbiology **149:**1285-1295.

56. **Underhill, D. M., and A. Ozinsky.** 2002. Phagocytosis of microbes: complexity in action. Annu Rev Immunol **20:**825-852.

57. **Valkova, D., L. Valkovicova, S. Vavrova, E. Kovacova, J. Mravec, and J. Turna.** 2007. The contribution of tellurite resistance genes to the fitness of *Escherichia coli* uropathogenic strains. Cent Eur J Biol **2:**182-191.

58. **Walter, E. G., and D. E. Taylor.** 1992. Plasmid-mediated resistance to tellurite: expressed and cryptic. Plasmid **27:**52-64.

59. **Whelan, K. F., R. K. Sherburne, and D. E. Taylor.** 1997. Characterization of a region of the *IncHI*2 plasmid R478 which protects *Escherichia coli* from toxic effects specified by components of the tellurite, phage, and colicin resistance cluster. J Bacteriol **179:**63-71.

60. **Yamamoto, T., T. Hanawa, S. Ogata, and S. Kamiya.** 1996. Identification and characterization of the *Yersinia enterocolitica gsrA* gene, which protectively responds to intracellular stress induced by macrophage phagocytosis and to extracellular environmental stress. Infect Immun **64:**2980-2987.

61. **Young, K. D.** 2006. The selective value of bacterial shape. Microbiol Mol Biol Rev **70:**660-703.

62. **Zhou, D., Y. Han, J. Qiu, L. Qin, Z. Guo, X. Wang, Y. Song, Y. Tan, Z. Du, and R. Yang.** 2006. Genome-wide transcriptional response of *Yersinia pestis* to stressful conditions simulating phagolysosomal environments. Microbes Infect **8:**2669-2678.

APPENDIX

COPYRIGHT AGREEMENT

ELSEVIER LICENSE
TERMS AND CONDITIONS

Oct 20, 2011

This is a License Agreement between Duraisamy Ponnusamy ("You") and Elsevier ("Elsevier") provided by Copyright Clearance Center ("CCC"). The license consists of your order details, the terms and conditions provided by Elsevier, and the payment terms and conditions.

All payments must be made in full to CCC. For payment instructions, please see information listed at the bottom of this form.

Supplier	Elsevier Limited The Boulevard,Langford Lane Kidlington,Oxford,OX5 1GB,UK
Registered Company Number	1982084
Customer name	Duraisamy Ponnusamy
Customer address	76S, Apt#3, University place Stillwater, OK 74075
License number	2772780322203
License date	Oct 19, 2011
Licensed content publisher	Elsevier
Licensed content publication	Veterinary Microbiology
Licensed content title	Intracellular*Yersinia pestis*expresses general stress response and tellurite resistance proteins in mouse macrophages
Licensed content author	Duraisamy Ponnusamy,Steven D. Hartson,Kenneth D. Clinkenbeard
Licensed content date	12 May 2011

Licensed content volume number	150
Licensed content issue number	1-2
Number of pages	6
Start Page	146
End Page	151
Type of Use	reuse in a thesis/dissertation
Portion	full article
Format	electronic
Are you the author of this Elsevier article?	Yes
Will you be translating?	No
Order reference number	
Title of your thesis/dissertation	*Yersinia pestis* response to macrophage-induced stress from hosts with high and low susceptibility to plague
Expected completion date	Dec 2011
Estimated size (number of pages)	180
Elsevier VAT number	GB 494 6272 12
Permissions price	0.00 USD
VAT/Local Sales Tax	0.0 USD / 0.0 GBP
Total	0.00 USD
Terms and Conditions	

INTRODUCTION

1. The publisher for this copyrighted material is Elsevier. By clicking "accept" in connection with completing this licensing transaction, you agree that the following terms and conditions apply to this transaction (along with the Billing and Payment terms and conditions established by Copyright Clearance Center, Inc. ("CCC"), at the time that you opened your Rightslink account and that are available at any time at http://myaccount.copyright.com).

GENERAL TERMS

2. Elsevier hereby grants you permission to reproduce the aforementioned material subject to the terms and conditions indicated.

3. Acknowledgement: If any part of the material to be used (for example, figures) has appeared in our publication with credit or acknowledgement to another source, permission must also be sought from that source. If such permission is not obtained then that material may not be included in your publication/copies. Suitable acknowledgement to the source must be made, either as a footnote or in a reference list at the end of your publication, as

follows:

"Reprinted from Publication title, Vol /edition number, Author(s), Title of article / title of chapter, Pages No., Copyright (Year), with permission from Elsevier [OR APPLICABLE SOCIETY COPYRIGHT OWNER]." Also Lancet special credit - "Reprinted from The Lancet, Vol. number, Author(s), Title of article, Pages No., Copyright (Year), with permission from Elsevier."

4. Reproduction of this material is confined to the purpose and/or media for which permission is hereby given.

5. Altering/Modifying Material: Not Permitted. However figures and illustrations may be altered/adapted minimally to serve your work. Any other abbreviations, additions, deletions and/or any other alterations shall be made only with prior written authorization of Elsevier Ltd. (Please contact Elsevier at permissions@elsevier.com)

6. If the permission fee for the requested use of our material is waived in this instance, please be advised that your future requests for Elsevier materials may attract a fee.

7. Reservation of Rights: Publisher reserves all rights not specifically granted in the combination of (i) the license details provided by you and accepted in the course of this licensing transaction, (ii) these terms and conditions and (iii) CCC's Billing and Payment terms and conditions.

8. License Contingent Upon Payment: While you may exercise the rights licensed immediately upon issuance of the license at the end of the licensing process for the transaction, provided that you have disclosed complete and accurate details of your proposed use, no license is finally effective unless and until full payment is received from you (either by publisher or by CCC) as provided in CCC's Billing and Payment terms and conditions. If full payment is not received on a timely basis, then any license preliminarily granted shall be deemed automatically revoked and shall be void as if never granted. Further, in the event that you breach any of these terms and conditions or any of CCC's Billing and Payment terms and conditions, the license is automatically revoked and shall be void as if never granted. Use of materials as described in a revoked license, as well as any use of the materials beyond the scope of an unrevoked license, may constitute copyright infringement and publisher reserves the right to take any and all action to protect its copyright in the materials.

9. Warranties: Publisher makes no representations or warranties with respect to the licensed material.

10. Indemnity: You hereby indemnify and agree to hold harmless publisher and CCC, and their respective officers, directors, employees and agents, from and against any and all claims arising out of your use of the licensed material other than as specifically authorized pursuant to this license.

11. No Transfer of License: This license is personal to you and may not be sublicensed, assigned, or transferred by you to any other person without publisher's written permission.

12. No Amendment Except in Writing: This license may not be amended except in a writing signed by both parties (or, in the case of publisher, by CCC on publisher's behalf).

13. Objection to Contrary Terms: Publisher hereby objects to any terms contained in any purchase order, acknowledgment, check endorsement or other writing prepared by you, which terms are inconsistent with these terms and conditions or CCC's Billing and Payment terms and conditions. These terms and conditions, together with CCC's Billing and Payment terms and conditions (which are incorporated herein), comprise the entire agreement between you and publisher (and CCC) concerning this licensing transaction. In the event of any conflict between your obligations established by these terms and conditions and those established by CCC's Billing and Payment terms and conditions, these terms and conditions shall control.

14. Revocation: Elsevier or Copyright Clearance Center may deny the permissions described in this License at their sole discretion, for any reason or no reason, with a full refund payable to you. Notice of such denial will be made using the contact information provided by you. Failure to receive such notice will not alter or invalidate the denial. In no event will Elsevier or Copyright Clearance Center be responsible or liable for any costs, expenses or damage incurred by you as a result of a denial of your permission request, other than a refund of the amount(s) paid by you to Elsevier and/or Copyright Clearance Center for denied permissions.

LIMITED LICENSE

The following terms and conditions apply only to specific license types:

15. **Translation**: This permission is granted for non-exclusive world **English** rights only unless your license was granted for translation rights. If you licensed translation rights you may only translate this content into the languages you requested. A professional translator must perform all translations and reproduce the content word for word preserving the integrity of the article. If this license is to re-use 1 or 2 figures then permission is granted for non-exclusive world rights in all languages.

16. **Website**: The following terms and conditions apply to electronic reserve and author websites:
Electronic reserve: If licensed material is to be posted to website, the web site is to be password-protected and made available only to bona fide students registered on a relevant course if:
This license was made in connection with a course,
This permission is granted for 1 year only. You may obtain a license for future website posting,
All content posted to the web site must maintain the copyright information line on the bottom of each image,

A hyper-text must be included to the Homepage of the journal from which you are licensing athttp://www.sciencedirect.com/science/journal/xxxxx or the Elsevier homepage for books athttp://www.elsevier.com , and
Central Storage: This license does not include permission for a scanned version of the material to be stored in a central repository such as that provided by Heron/XanEdu.

17. **Author website** for journals with the following additional clauses:

All content posted to the web site must maintain the copyright information line on the bottom of each image, and
he permission granted is limited to the personal version of your paper. You are not allowed to download and post the published electronic version of your article (whether PDF or HTML, proof or final version), nor may you scan the printed edition to create an electronic version,
A hyper-text must be included to the Homepage of the journal from which you are licensing athttp://www.sciencedirect.com/science/journal/xxxxx , As part of our normal production process, you will receive an e-mail notice when your article appears on Elsevier's online service ScienceDirect (www.sciencedirect.com). That e-mail will include the article's Digital Object Identifier (DOI). This number provides the electronic link to the published article and should be included in the posting of your personal version. We ask that you wait until you receive this e-mail and have the DOI to do any posting.
Central Storage: This license does not include permission for a scanned version of the material to be stored in a central repository such as that provided by Heron/XanEdu.

18. **Author website** for books with the following additional clauses:
Authors are permitted to place a brief summary of their work online only.
A hyper-text must be included to the Elsevier homepage at http://www.elsevier.com

All content posted to the web site must maintain the copyright information line on the bottom of each image
You are not allowed to download and post the published electronic version of your chapter, nor may you scan the printed edition to create an electronic version.
Central Storage: This license does not include permission for a scanned version of the material to be stored in a central repository such as that provided by Heron/XanEdu.

19. **Website** (regular and for author): A hyper-text must be included to the Homepage of the journal from which you are licensing
at http://www.sciencedirect.com/science/journal/xxxxx. or for books to the Elsevier homepage at http://www.elsevier.com

20. **Thesis/Dissertation**: If your license is for use in a thesis/dissertation your thesis may be submitted to your institution in either print or electronic form. Should your thesis be published commercially, please reapply for permission. These requirements include permission for the Library and Archives of Canada to supply single copies, on demand, of

the complete thesis and include permission for UMI to supply single copies, on demand, of the complete thesis. Should your thesis be published commercially, please reapply for permission.

21. **Other Conditions**:

v1.6

If you would like to pay for this license now, please remit this license along with your payment made payable to "COPYRIGHT CLEARANCE CENTER" otherwise you will be invoiced within 48 hours of the license date. Payment should be in the form of a check or money order referencing your account number and this invoice number RLNK500649049.
Once you receive your invoice for this order, you may pay your invoice by credit card. Please follow instructions provided at that time.

Make Payment To:
Copyright Clearance Center
Dept 001
P.O. Box 843006
Boston, MA 02284-3006

For suggestions or comments regarding this order, contact RightsLink Customer Support:customercare@copyright.com or +1-877-622-5543 (toll free in the US) or +1-978-646-2777.

Gratis licenses (referencing $0 in the Total field) are free. Please retain this printable license for your reference. No payment is required.

VITA

Duraisamy Ponnusamy

Candidate for the Degree of

Doctor of Philosophy

Thesis: *YERSINIA PESTIS* RESPONSE TO MACROPHAGE-INDUCED STRESS FROM HOSTS WITH HIGH AND LOW SUSCEPTIBILITY TO PLAGUE

Major Field: Veterinary Biomedical Sciences

Biographical:

Education:

Completed the requirements for the Doctor of Philosophy in Veterinary Biomedical Sciences at Oklahoma State University, Stillwater, Oklahoma in December, 2011.

Completed the Master of Veterinary Science in Veterinary Pathology at Indian Veterinary Research Institute Deemed University, Bareilly, Uttar Pradesh, India in 2006.

Completed the Bachelor of Veterinary Science in Veterinary and Animal Sciences at Tamil Nadu Veterinary and Animal Sciences University, Chennai, Tamil Nadu, India in 2003.

Experience: Teaching Assistant, Infectious Diseases and Immunology, Department of Veterinary Pathobiology, Center for Veterinary Health Sciences, Oklahoma State University, Oklahoma, from 2006 to 2011.

Professional Memberships:
Tamil Nadu Veterinary Council, Tamil Nadu, India.

Name: Duraisamy Ponnusamy Date of Degree: December, 2011

Institution: Oklahoma State University Location: Stillwater, Oklahoma

Title of Study: *YERSINIA PESTIS* RESPONSE TO MACROPHAGE-INDUCED STRESS FROM HOSTS WITH HIGH AND LOW SUSCEPTIBILITY TO PLAGUE

Pages in Study: 187 Candidate for the Degree of Doctor of Philosophy

Major Field: Veterinary Biomedical Sciences

Yersinia pestis causes severe disease in natural rodent hosts but mild to inapparent disease in rodent predators such as dogs. *Y. pestis* initiates infection in susceptible hosts by parasitizing and multiplying intracellularly in local macrophages during the early stage of infection. Thus, we hypothesized that *Y. pestis* infection severity may depend on how well the intracellular bacterium overcomes the initial host macrophage associated stress. To test this hypothesis, *Y. pestis* infection progress was studied in mouse splenic and dog peripheral blood macrophages, and various parameters of this infection were measured in mouse and dog tissue culture macrophages RAW264.7 and DH82, respectively. The study showed that during the early stage of infection, intracellular *Y. pestis* assumed filamentous cellular morphology with multiple genomes per bacterium in both mouse and dog macrophages. Later, in mouse macrophages, these filamentous *Y. pestis* returned to coccobacilli with spacious vacuolar extension of *Yersinia* containing vacuoles (YCV) and extensive macrophage lysis. However, in dog macrophages, intracellular *Y. pestis* were either retained in the same filamentous cellular morphology for the entire experiment in tissue culture cells or killed eventually in blood macrophages. In addition, *Y. pestis* infected dog macrophages did not show noticeable extension of YCV and macrophage lysis. To further understand the *Y. pestis* virulence factors in macrophage parasitism, protein profiles of *Y. pestis* residing in RAW264.7 cells were compared with those of culture grown *Y. pestis*. The experiment showed the expression of various general stress response and tellurite resistance proteins of *Y. pestis*. Tellurite resistance genes were analyzed for their possible role in *Y. pestis* intracellular stress regulation. This analysis indicated that *Y. pestis* tellurite resistance (*ter*) operon expression was induced as a response to the macrophage stress and expression of these proteins associated with conversion to a filamentous cellular morphology by *Y. pestis* similar to that observed in macrophage infections. These studies indicate that *Y. pestis* in mouse macrophages can overcome the initial intracellular stress and cause systemic infection. But failure to overcome the dog macrophage induced stress by *Y. pestis* may result in mild disease in these animals. During this intracellular parasitism, *Y. pestis* employs various general stress regulatory mechanisms to survive in macrophages. As a part of this stress response, expression of *Y. pestis ter* operon likely causes filamentous cellular morphology response in order to adapt to the macrophage associated stress.

ADVISER'S APPROVAL: Dr. Kenneth D. Clinkenbeard